Faculty of Mathematics and Natural Sciences
Leiden University, Leiden

Performance of Networks and Systems
TNO, Delft

Damage Reduction of Cascade Tripping in High Voltage Power Grids by means of Intentional Islanding

Bart Kamphorst
Student number: 0832995

Study: Mathematics
Specialization: Applied mathematics

Master's thesis defended on August 23rd, 2013

Committee members:

Supervisor university:	Dr. F. M. (Floske) Spieksma
Supervisor TNO:	Dr. S. (Bas) Marban
	Prof. dr. ir. R. E. (Robert) Kooij

Abstract

Modern society greatly relies on a secure energy supply for communication, security, health care and many more applications. Just rarely do we experience blackouts that make us aware of our dependence on the various components of the power network. However, the power network was not designed to supply the ever-increasing demand that it faces today and without changes this will lead to more blackouts in the future. This thesis focusses on reducing the damage caused by cascading failures – failures that induce new failures and ultimately lead to a blackout.

Concretely, we zoom in on a part of the power network – the high voltage power grid – and study intentional islanding, a mechanism that reduces the damage done by cascading failures. Intentional islanding separates the network in two or more components in order to isolate a cascading failure. This should protect the rest of the network from serious damage, although islanding by itself may also cause a wide disturbance. In this thesis, intentional islands are designed by formulating a MILP optimization problem that takes into consideration various trade-offs in islands design such as stability and load shed.

To test the islanding mechanism introduced in this thesis, we want to create instances with cascading failures. For this, it is essential to know which transmission lines are most important to the power grid's robustness. The relative importance of individual transmission lines to the power grid is calculated and used to simulate cascading failures. Both damage done by the cascading failures and general grid safety are analyzed with and without the implementation of islanding. Our results show that intentional islanding can be a very effective mechanism to protect the grid if implemented correctly.

Preface

At this moment, you hold the result of eight months research. Research that has been carried out at the TNO department Performance of Networks and Systems (PoNS) in Delft. Research that concludes the master specialization Applied Mathematics at Leiden University. Research that helped me develop as a mathematician, a researcher and a person. But most of all, research that was made possible with the help of many people.

I would like to start with my TNO supervisor Bas Marban. You counselled me in our weekly meetings and gave guidance on both the content and the structure of my work. I always found your door open and – provided I would carefully announce my presence – you would help me any time. Your virtually everlasting good mood made it a pleasure both to work and to grab snacks with you. Thank you for that.

My other TNO supervisor Rob Kooij and the word 'inspiration' have to be mentioned in the same breath. I have never met a person who can talk about research and limitless opportunities with the sincere passion that you share. Illustratively, you sent me to the other side of the world. Thank you for that.

Some of these opportunities – travelling to Cambridge, UK and Manhattan, Kansas – would not have been possible without the help of my university supervisor Floske Spieksma. Your support in expanding my world and your help with mathematical issues along the way are well appreciated. Also, you connected me to the mathematical community which led to a Ph.D. position. Thank you for that.

From the other side of the world, I would also like to mention Caterina Scoglio and Sakshi Pahwa. Not only did you make my trip possible – you made it a visit to never forget. I had a great time in your rather small and quiet city and I learned a lot. Two weeks of collaboration easily resulted in a complete chapter and an appendix for my thesis and I feel like I can always come back. I came to you as a stranger, yet I left as a friend. Thank you for that.

Impossible to forget is my manager, Dick van Smirren. Dick educated me in subjects where my background was lacking. Our daily meetings took quite some time, but I can faithfully say that these lessons will be useful to me for the rest of my life. More precisely, you are amazing. Thank you for that.

Of course there are others that have contributed to this work in their own ways. Without going into further detail, I thank the professionals at PoNS, the researchers in the Sunflower Networking Group, Yakup Koç from the Technical University Delft and Paul van den Heuvel from TenneT for providing wonderful experiences.

Contents

List of Figures

Chapter 1

Introduction

1.1 Motivation for studying power grids

Assume a world where humanity has no control over electrical energy. Try to imagine how this would affect a regular working day. You would not go to work by an electricity-driven train or car, have no computer to work on and no cell phone for quick correspondence with clients. Back home you would have no fridge to conserve vegetables, not the luxury of many kitchen tools to help you prepare your food and no microwave to heat up leftovers. Instead you would go out in the cold to get wood or some other fuel that you need to get the stove working. You would light some candles that hardly emit enough light to read the books that you never get to with television. Life would be a lot different in this world, not to mention issues like security, quality of medical care and the response times of emergency services.

The importance and relevance of power grid reliability is one of the motivations to write this thesis. Motivation for the reader to continue beyond this chapter. Power networks are part of our everyday lives although we usually don't think about it. For most of the time we just take it for granted; pressing a power button or plugging in some device is all it takes to get going. Just for a couple of minutes every year some of us are confronted with the undeniable truth that we are dependent: during blackouts. Blackouts seem to occur frequently and before starting this research I wondered why this is. It doesn't seem to hard to provide electrical energy via transmission lines – especially with nowadays technologies – does it?

Apparently there are a lot of problems to face when it comes to operating and managing the grid. Many researchers have contributed to the field of power networks and there are still a lot of open questions. The future power grid combines decentralized power generation, time-shifting of demand and technologies to keep the network stable. Where problems in the traditional power networks domain were physics-orientated (e.g. stability issues), it is now no longer possible to limit research to one field. Researchers of natural, social and behavioural sciences need to collaborate with economists, jurists and politicians to tackle the multidisciplinary challenges that lie ahead.

So what more motivates a student in Mathematics to study the complex power grid? As a student in Mathematics, especially the more theoretical branch, it is not always clear how the obtained knowledge can be put to practice. Surely mathematics plays a major role in the world around us, but how can one contribute to this if not via a university? TNO gave me the opportunity to create a possible answer to this question. Not only did they allow me to apply mathematics to the power grid and to look inside an applied research

institute, they rather provided a way to do research in a multidisciplinary field. During my research I have talked with professionals in the power grid industry (TenneT, NL), professionals and researchers from various industries and fields at the Energy Systems Week 2013 (Cambridge, UK) and collaborated with researches from across the world (Manhattan, Kansas). The next two subsections will introduce the central questions that shaped my research, and the structure of the thesis.

1.2 Research questions

In this thesis we are looking for a way to reduce the damage done by cascading failures in high voltage power grids. Cascading failures are failures that weaken the network and in turn induce new failures. It is easy to imagine how the domino-like behaviour of failures can bring down a big part of the network and ultimately lead to a blackout. One way to stop the cascade is to isolate it. In this way, only a small part of the network can go down whereas the major part is (almost) unaffected. Additionally, restoration of the network is easier when just a small part is down. Isolating a part of the network on purpose is called *intentional islanding* and we formulate the following research question:

Primary research question:

How can the damage caused by cascading failures in a power grid be reduced by means of intentional islanding?

This question is hard to answer in one go, especially without a solid background in power grids and their dynamics. It is essential to understand more about the power grid, to know how it can be modelled and to find a way to construct good islands. Concretely, the following research questions have to be answered:

Secondary research questions:

- *What is the power grid and how does it work?*
- *What kind of power grid models have been studied in literature?*
- *Can we propose a power grid model that is reasonably accurate and yet fast enough to run many simulations?*
- *How can we determine topological islands for a certain power grid that are optimal in some sense?*
- *Which transmission lines are most important to the power grid's robustness?*

The last research question requires a short explanation. By 'most important to the power grid's robustness', we aim at those transmission lines that upon failure are most likely to cause a cascading failure. That is, if failure of line A is likely to cause a cascading failure and failure of line B is not likely to cause any disturbance, then line A is more important to the robustness than line B. The relative importance of generators (also: buses, nodes) is not studied in this thesis.

1.3 Thesis outline

Basically, every secondary research question will be answered in its own chapter. Chapter 2 introduces the reader to the power grid and some of the terminology used throughout the rest of the thesis. From Section 2.1 to Section 2.4, the reader is led from the generation of electrical energy to the consumption of electrical energy and from safety measures to actual blackouts.

After the reader is somewhat familiar with the power grid, Chapter 3 provides an overview of relevant literature. The presented literature verifies the importance of research in this field, includes examples of the many different models that have been used to simulate cascading failures and proposes various methods to make the grid more reliable. After this chapter, the reader knows more about the motivation for, possibilities in and results of cascade failure modeling.

Chapter 4 formulates the model that will be used for all simulations in this thesis. All aspects of the model are explained into detail in Section 4.1. Based on the previous chapter, the reader is able to understand and judge the choices that have been made in the model. Section 4.2 focusses entirely on an approximation of the power flow dynamics through transmission lines; the DC power flows.

Chapter 5 introduces the reader to intentional islanding. Motivation for islanding and difficulties in finding an optimal island are explained in Section 5.1. Following this discussion, a mixed integer linear programming (MILP) formulation for intentional islanding is presented in Section 5.2. This formulation will be used to construct optimal islands that isolate cascading failures. Section 5.3 provides the reader with results from solving the MILP formulation and discusses the impact of islanding.

After all fundamentals have been laid down, Chapter 6 shows the results of cascading failure simulations and the effect of islanding. A brief introduction to the simulation outputs is given in Section 6.1, followed by the actual analysis of important lines in Section 6.2. The most important lines are then used to initiate cascading failures in Section 6.3, where the effect of intentional islanding is analyzed. Section 6.4 shortly discusses the sensitivity of the model to the various input parameters.

Finally, Chapter 7 summarizes everything that has been done in this thesis. Answers to all research questions will be presented and discussed in Section 7.1. Section 7.2 thoroughly analyzes the proposed model and lists possibilities for future research.

We would also like to mention Appendix A, where two theorems are stated and proved. Theorem 1 states a novel method to update the so-called PTDF matrix. A more general result on the invertibility of a special class of matrices is presented in Theorem 2. This result may also be useful in applications other then power grid modeling.

Chapter 2

The power grid

At the beginning of Chapter 1 we gave some thoughts on how much modern day society relies on electrical energy. Only seldom do we experience a power blackout, and if so, it usually does not last for a long time. The power network we use every day is a complex network of generators, transmission lines and distribution facilities. It has evolved so that minor deficiencies have little to no impact on the consumers. Unfortunately, multiple deficiencies may cause a large part of the power network to fail; especially if those deficiencies occur in the high voltage parts of the power network. The high voltage part of the power network is the stem of the power network tree that will be described later in this chapter. When multiple deficiencies occur, other transmission lines may experience overload and subsequently fail too, causing more overload on the remaining part of the network and more failures. Real life examples of these *cascading failures*[1] are given by the U.S.-Canada Power System Outage Task Force [80], FERC/NERC staff [32] and the Ministry of Power Enquiry Committee [56]. They describe and analyze cascading failures in Northeast America-Canada (2003, 50 million consumers affected, 61,800 MW lost), Arizona-Southern California (2011, 2.7 million, 7,835 MW) and India (2012, 630 million, 32,000 MW), respectively. In this thesis, we propose a mathematical model for these kind of cascading failures and evaluate a technique that aims to reduce the damage done by them. The remainder of this chapter will explain some of the basics of the power network and cascading failures in particular.

2.1 Generation of electrical power

There are many ways to generate electrical power. A simple yet crucial division between those many ways is the level of centralization of the generation of power. *Decentralized generation* is generation from small energy sources such as solar panels and wind turbines. This makes it relatively easy to distribute electricity over a geographical area, which is an important financial benefit. A downside is that most small energy sources depend on external (and uncertain) 'fuels' like wind or sunlight. The power generation from those sources is therefore unpredictable and this leads to one of the major challenges in matching energy supply and demand.

Centralized generation is generation from large (centralized) facilities such as power plants, nuclear plants and hydro power plants. These kind of generators allow extensive control on the amount of power produced and they benefit from economies of scale, which

[1] *Cascading*: "The uncontrolled successive loss of system elements triggered by an incident. Cascading results in widespread service interruption, which cannot be restrained from sequentially spreading beyond an area predetermined by appropriate studies." [80].

makes the produced power relatively cheap. A downside is that those generators can not be placed everywhere for reasons of facility size (power plant), environmental security (nuclear plant) and environmental properties (hydro power plant). In this thesis, we will only consider centralized generation to avoid the computational complexity of decentralized generation. No distinction is made between the different kinds of plants from this point on. The reason for this is that facility output properties are relevant for our model, but the fuels that they use are not.

Virtually all plants use some kind of fuel to set a spinning electrical generator into motion (often by means of a steam turbine). The spinning of this generator produces *Alternating Current (AC)* power. When one would monitor this on an oscillator one would see that the power behaves like a sine wave with rate 50 to 60 Hertz, depending on country regulations. Three of those sine waves are combined at the plant into 3-phase AC power, which is then sent into the power network. Due to the 120 degree phase differences, the 3-phase AC power is always close to the maximum output of some wave. This is a necessary property for powering heavy machinery like induction motors. It is also possible to convert Alternating Current power to *Direct Current (DC)* power. DC power is a constant power flow in one direction. For example, batteries always output DC power that flows from the plus to the minus terminal. DC power is also used for long-distance transmission. It is cheap to convert AC power to DC power, but relatively expensive to convert DC power to AC power. AC power is the natural output of spinning generators.

2.2 From power plant to consumer

Once the power has been generated at the generation facility as discussed above, there are five more steps to get the power to your home (see Figure 2.1). Every step decreases the number of consumers served per unit.

Step 1. 3-Phase AC power is generated at the *generation facility*.

Step 2. For a fixed amount of power, the transportation losses of electrical energy are inversely proportional to the squared voltage[2]. For this reason it is efficient to transport power at a high voltage. A *step-up transformer* ramps up the power from the generation facility to high voltage transmission for long-distance transmission.

Step 3. From the step-up transformer, the power is transported via *transmission lines*. Transmission lines distribute the electricity to 'transmission customers' and substations. They usually transport power at 110 kiloVolts (kV) or above.

Step 4. *Substations step-down transformers* convert the voltage from high to medium voltage, which is ranged from 10kV to 110kV[3]. This voltage is more suitable for use in businesses and homes.

[2]For power P, element resistance R and voltage V, the transportation loss L is given by $L = P^2R/V^2$. Note that some European countries (including the Netherlands) use U for voltage. In this thesis, we adopt the more conventional notation V.

[3]To the author's knowledge, there are no universal upper and lower voltage limits that define high, medium and low voltage. Many operators, countries and other parties state different limits. The values given in this chapter are for illustrative purposes only and should be treated as such.

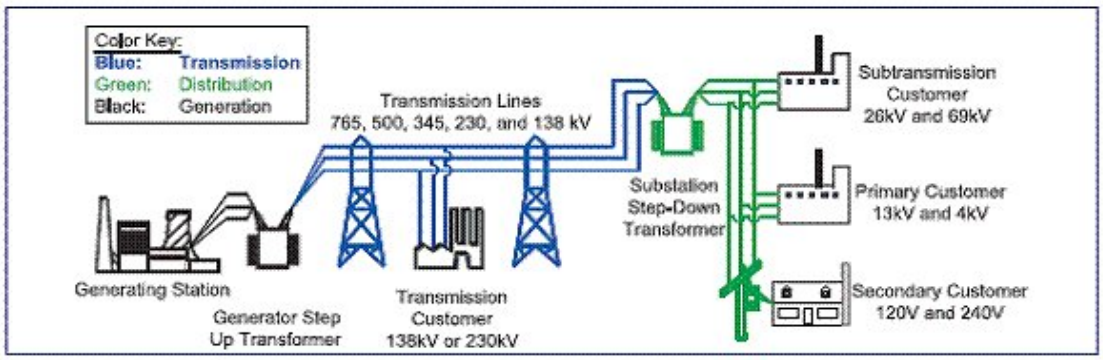

Figure 2.1: From power plant to consumer – a graphical representation [62].

Step 5. *Distribution lines* transport the power from substations to 'subtransmission customers', 'primary customers' and 'secondary customers'. Regular households belong to this latter category. The distribution lines branch multiple times and pass some switches along the way. 3-phase AC power lines may be branched to 2- and 1-phase AC power lines at branching points and at substations. Also, for some branches the voltage is transformed to below 10kV for secondary customers. These lines are known as tap lines.

Step 6. *Tap lines* come in your neighborhood and branch multiple times to reach all homes. A tap line may branch into multiple tap lines by sending some of the initial phases along new lines. For example, a 2-phase current tap line may branch into two 1-phase current tap lines. Ultimately, the tap lines deliver one phase of AC power at your home.

The first three steps – generation facilities, transmission lines, substations – are together referred to as the transmission grid or *power grid*.

The electrical devices in your home use energy in different ways. Roughly, devices can use power or store it (e.g. as a magnetic field) and return it to the power network later. When power is used directly, it is called *real*, *resistive* or *active* power. Circuits that rely completely on real power are recognizable by the fact that there is no phase shift between voltage and current oscillations (see Figure 2.2(a)). If energy is stored and returned later, it is called *imaginary* or *reactive* power. One device that does this, is a coil. Coils convert increasing supply of electrical energy to a magnetic field, and convert the magnetic field back to electrical energy when the supply decreases. Thus, coils oppose the change in electrical energy supply that is characteristic for AC power. A perfect circuit with a coil and no resistance would have a 90 degree ($= \pi/2$ radians) phase difference between voltage and current oscillations (see Figure 2.2(b)). Since power $P(t)$ equals voltage $V(t)$ times current $I(t)$, it follows that the power consumption of the coil equals

$$\int_0^{2\pi} P(t)\,dt = A\int_0^{2\pi} V(t)\cdot I(t)\,dt = A\int_0^{2\pi} \sin(t)\cdot\sin\left(t-\frac{\pi}{2}\right)\,dt = -A\int_0^{2\pi}\frac{1}{2}\sin(2t)\,dt = 0,$$

where A is the amplitude of the voltage times the amplitude of the current oscillation. Indeed it can be seen that reactive energy does not consume power. In practice, power

consumption is a combination of both types and no device consumes purely reactive power (see Figure 2.2(c)). Power companies can charge active power only, which can be calculated from the phase difference between voltage and current[4]. This makes reactive power expensive for power companies because transmission costs are for them.

2.3 Safety first

The power grid is monitored 24/7 by operators in control centers all over the world. Operators use history records and demand statements from companies to predict and plan the demand and supply of every day. During the day, they watch grid information and take actions to keep the grid in a secure state if necessary. Tools used by operators acquire data from the grid, visualize this data and provide analysis software. In particular, control centers collect data by System Control and Data Acquisition (SCADA) systems. This data is communicated with State Estimation software to visualize the condition of the network on regular intervals. Among others it estimates bus[5] voltages and active and reactive power flows. The state estimation can then be used in Contingency Analysis software[6]. Contingency Analysis software can be used for reliability analysis of future system states or for following significant system events. So why do operators need all these protective software tools?

Besides being very complex, the power grid is also subject to many natural and artificial environmental elements and one can be expect to encounter problems at some point in time. Weather conditions force brutal environments on transmission lines like cold, heat, rain, lightning and storms. Alternatively, vegetation under the transmission line may grow too high and make contact with the line[7] [82]. Human errors in maintenance work or during construction activities also cause problems. Any of these and other events [70] may cause a *short circuit* in the network. A short circuit is a low resistance connection between two points of an electrical circuit that may result in abnormally high current flow. For instance, when a transmission line makes contact with a tree, the electrical power goes into the ground at high speed instead of along the line at relatively low speed.

To prevent damage to equipment or surroundings, protection devices are implemented into the network. *Breakers* are switching devices at the end of transmission lines capable of opening (out-of-service) and closing (back into service) the line. They are commonly controlled by *relays*. Relays monitor the impedance of a line, which depends on (abnormalities in) voltage and current[8]. When the impedance is too high for a certain length of time, relays send a signal to the corresponding breaker to open the line [69]. This is also known as the *tripping* of a transmission line.

[4] Actions can be taken against excessive 'borrowers' of reactive power, but that is beyond the scope of this thesis.

[5] *Buses* are the technical term for certain communicating components in electronic circuits. In this setting, buses refer to generator, distribution and load points. We will also use the mathematical term *nodes* later in this thesis.

[6] A contingency is the event where a transmission line fails due to some fault.

[7] In this context, contact is not necessarily physical. If vegetation is close enough to a transmission line, it is also possible that an electric arc jumps from the line.

[8] Given the resistance R (opposition to passage of current) and the reactance X (opposition to change of current) of a circuit element, the impedance Z is given by $Z = R + iX$ where i is the imaginary unit.

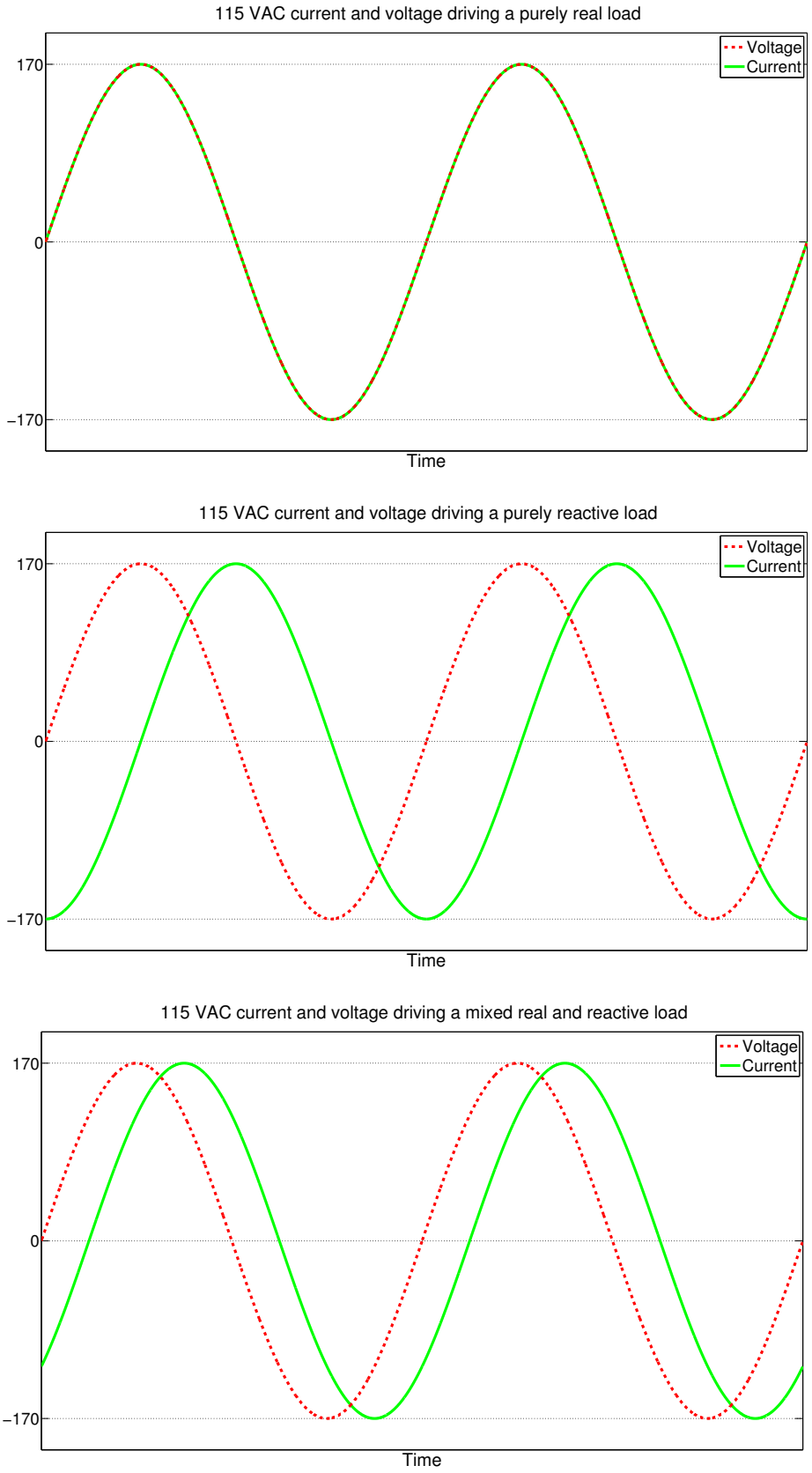

Figure 2.2: Voltage versus current for active, reactive and mixed loads, respectively. Theoretically perfect reactive load has a phase shift of 90 degrees between voltage and current (b). In practice, the phase shift rarely exceeds 45 degrees (c). Figures based on [74].

The tripping of a line may cause system instability, as we will discuss shortly. In case this happens, the system operators can physically disconnect load points in the network to return the grid to the secure state. Disconnecting load points relieves some of the stress on transmission lines and the generators, and is known as *load shedding*. When this is not sufficient, they can also split the network in several pre-engineered self-sustaining islands (*islanding*). By disconnecting parts of the network, the failures are hopefully isolated to only one island so that the rest of the network may survive. Islanding may also facilitate the restoration processes afterwards. We will now discuss the progression of system instability that may lead to these actions.

2.4 Why do we experience blackouts?

Most blackouts are small and only apply to a limited number of households. This is the effect of a local disruption in the network such as a broken tap pole. These kind of disruptions can often be solved in a few hours. More serious blackouts find their cause in disruptions in the transmission grid. The transmission grid transports the power from the plants to substations that may be hundreds of kilometers away and ultimately serve tens or even hundreds of thousands of people. It has been designed in such way that tripping of a single transmission line has no big consequences. However, multiple contingencies in a short time frame may have a huge impact. Regulations[9] therefore require that the power grid must be capable of accommodating any situation with a single contingency without exceeding operational security limits. That is, for any single contingency the power grid must be able to serve power to all its customers in a justified manner. This is called the $N-1$ *criterion* [35].

Large blackouts are often caused by a series of events, a *cascade failure*. Cascade failures are initiated by a disturbance of the energy flow in the grid (*trigger event*), followed by redistribution of the energy flows that may cause new disturbances. The initial trigger is the combination of failing components from the grid such as transmission lines, distribution points and generator points. Failure of any such component puts additional stress on the working part of the grid and thus weakens the system. Additionally, the trigger event may cause voltage or frequency swings. Increased stress on the network may cause relays to trip other lines in the grid, which in turn can be considered as a new trigger event. Voltage and frequency swings are dangerous for generator equipment and may cause protection devices to shut down generation. Both types of events cause further instability. Once these failures follow up rapidly after one other, one speaks of a cascading failure. Cascading failures can last for seconds up to minutes.

Although relays are implemented to protect the system, they sometimes worsen its condition. It is possible for relays to act when this is not desired, especially when facing abnormal conditions. Roughly, there are three ways in which relays may worsen the system condition. The first one is known as a *hidden failure* and is defined as "a permanent defect that will cause a relay or relay system to incorrectly and inappropriately remove a circuit element(s) as a direct consequence of another switching event" [73]. That is, the physical condition of the relay is not correct, meaning that the relay activates the breaker when the transmission conditions are within safety limits. Hidden failures may accelerate the

[9]Enforced by the North American Electric Reliability Corporation (NERC) in Northern America, the European Network of Transmission System Operators for Electricity (ENTSO-E) in Europe, etc..

cascading process instead of stopping it by tripping lines that do not exceed operational limits [5, 18, 19, 29, 52, 55]. Other components in the system can also be subject to hidden failures, but these can be detected during regular inspections. The second way in which relays may worsen the condition is by installing the wrong type of relay or having incorrect relay settings. In this case the relay operates according to its settings, yet the settings are not optimal for the situation. Thirdly, a correct relay may act according to its settings, but this may put undesired additional stress on other parts of the system. In this case it may be better to temporarily allow transmission line overload while relieving the system stress by other means.

There usually are some minutes between the trigger events, the first failures that follow and the cascading failures. Within this time interval, automatic protection devices and operators can take actions in an attempt to stabilize the grid. Both can take the same actions: shed load (decrease demand) or initiate intentional islanding; the electrical separation of the network by disconnecting transmission lines in order to isolate the cascade. The most common automatic protection mechanisms are Under-Voltage Load Shedding (UVLS) and Under-Frequency Load Shedding (UFLS). UVLS intends to restore the power grid and prevent islanding. UVLS sheds several hundred megawatts (MW) of load within urban load centers to prevent voltage collapse or to meet reactive power demand. If this is not sufficient to restore system balance, islanding can be initiated. Islanding has a lot of impact, so UFLS sheds load after islanding to stabilize the islands. Both UVLS and UVLS shed load in steps of a few hundred MW. This gives the grid a short time to restore by itself.

More information on protection devices and the working of the power grid can be found in [32].

Chapter 3

Related work

Over the last decade, an increasing amount of research has been spent on cascade failure problems, especially in the domain of energy grids. This section will summarize the results of some of this research in order to show both the relevance and the variety of the subject. The literature that will be mentioned also motivates the direction of our own research.

First of all, it is important to understand the impact that failures in electrical transmission and/or distribution networks may have upon everyday life. For many infrastructures, failures affect only the infrastructure itself. Energy grids on the other hand, tend to affect not only the energy grid itself but also other infrastructures. Effects of an energy blackout include degradation of traffic infrastructures and telecommunications systems, defrost of foods in supermarkets and generator needs for hospitals [72]. Economical impact can be vast as many factories and businesses are unable to operate without a decent energy supply. It is for those and many more reasons [13, 38] that failures in an energy grid can have serious impact.

Although it is obvious that cascading failures in the power grid can have huge consequences, it is difficult to state the damage of a cascade in financial measures. For example, it is difficult to quantify the health risk of persons walking through subway tunnels in financial terms. Instead the damage can be measured by the amount of power lost (in MW) or the number of customers affected [38]. Knowing what impact an energy failure can have, one may reasonably ask what the risk of such a failure is. Carreras et al. [15, 16] and Chen et al. [20] have statistically shown that the probability of a cascading failure follows a power law distribution as function of the amount of power lost. This implies that the risk of heavy damage caused by cascade failure is quite high, and thus damage by such failure can be considered as a genuine threat. Acknowledging this fact motivates the need for mathematical models that simulate cascade failures. A better understanding of global high voltage energy grid dynamics is essential in the process of reducing the number of, and damage done by, cascade failures in these grids.

Researchers have proposed a vast amount of different models to simulate cascade failures. We will mention several distinguishing aspects of these models. The first and most self-evident aspect is the goal of the model. The goal of the simulation may be to predict damage done by a cascade (e.g. power lost, unserved energy, unserved customers), to determine the cascading sequence (e.g. first line 4, then generator 2, etc.), or to analyze the effect of long term dynamics (e.g. amount of stress due to increasing demand and expansion of the grid in order to meet this demand) [25, 26] or of defensive measures on cascades. A second aspect is the accuracy of the model. As the model aims for more accurate results, it is often required to make the model more realistic. Making the model more realistic can range from more detailed physical constraints (e.g. how power redistributes)

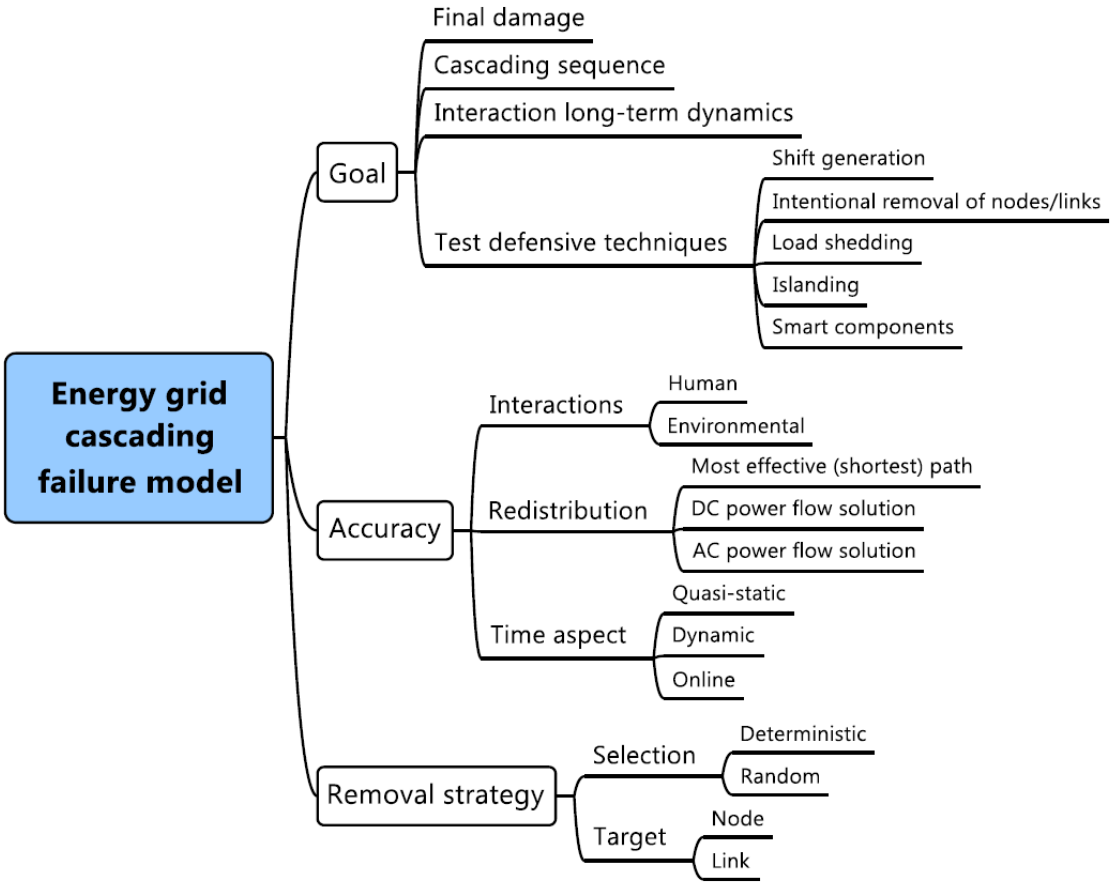

Figure 3.1: Overview of relevant aspects for modeling cascading failures in high voltage power grids.

to the involvement of weather conditions [70] or the implementation of automatic/human operator actions [2, 11]. Especially the redistribution of flow can be done in different - and computing time related - ways. One way to control the accuracy of the model is by using approximations or not, and if so, by deciding on the type of approximation used. Also, the time component of the model ranges from steady state to online. A third aspect is the event that triggers the cascade. Cascades start with the failure of one or more nodes (generators), links (transmission lines) or both. Which components fail, and whether the components are chosen deterministically or probabilistically, can be modeled in various ways. We refer to this part of the model as the removal strategy. An overview is given in Figure 3.1.

Concerning the first aspect, the goal of the model, we will specifically discuss research on defensive measures since this is closely related to the subject of this thesis. An increasing amount of research is spent on techniques to reduce the damage done by a cascade failure in the event that it occurs. Interesting results have been found by the intentional (partial) shut down of distribution points (load shedding) [11, 18, 28, 59, 85] or even isolating parts of the network (islanding) [1, 3, 23, 28, 63, 78, 83] so that the cascade is contained

and cannot continue[10]. Research on islanding can focus on the timing of islanding, the formation of islands and the stability issues after islanding. For example, Diao et al. [23] study real-time monitoring of the network to determine the optimal time to start islanding. Ahmed et al. [1] and You et al. [83] use slow coherency theory to form stable islands. Slow coherency is used to determine groups of generators that are well synchronized in terms of their slowest modes (eigenvalues of eigensubspace matrix of generators). The general approach of mixed integer linear programming has been explored by Pahwa et al. [63] and Trodden et al. [78]. Dola and Chowdhury [28] integrate islanding with automated post-islanding load shedding to deal with system stability. Finally, Aponte and Nelson [3] focus on stability issues and present an optimal load shedding time algorithm that minimizes deviations of voltage and frequency trajectories after islanding by applying optimal corrective load shedding at the optimal time. Opposed to removing part of the network, Hayashi and Miyazaki [37] examined the effect of emergency rewiring close to attacked nodes. The results indicate that emergency rewiring may boost the system, yet one may question the application of this technique in high voltage power grids due to the short time frame in which cascades develop. As mentioned in Section 1, this thesis will focus on the formation of islands by a mixed integer linear programming approach.

Possibilities in making the grid 'smarter' are also studied. Such possibilities include decentralized control and improvement of communication of protection devices. A certain kind of relays, zone 3 distance relays, in the grid sometimes tend to worsen the cascade by operating in a non-optimal way [32, 56, 69, 80]. Zhang et al. [84] propose new relays that incorporate a machine learning approach. Also, Hines et al. [39] and Hopkinson et al. [43] have obtained interesting results by intensifying and improving communications between various components in the grid. Both papers consider relays to be autonomous, cooperating agents in order to make load shedding and islanding more efficient. This is achieved by enhancing communication between the various components and decision-making on real-time data. By autonomous agents, the authors refer to individual relays that make their own decisions based on information that is provided by other relays. All papers that describe a smarter grid show promising results.

Concerning the second aspect, the redistribution of flow was initially modeled by quasi-steady models [11, 17, 19, 22, 37, 59, 60, 85]. Quasi-steady models were proposed in order to take the underlying dynamics of the network into account while keeping computing requirements low. In these models, the redistribution of flow is done in several steps. Components are checked for failure after each step and labeled out-of-service if necessary. Quasi-steady models already illustrate the damage that may follow from a single failure. Following steady-state models, dynamic models started to get used more and more often since the 00s. Dynamic models use differential equations and are capable of generating accurate results. However, these models are generally time consuming and high performance computing is required [27, 46, 64]. Finally, McCalley et al. [54] developed online tools that can be used by system operators to monitor system performance and enhance reliability. In this thesis, we will focus on quasi-steady state models. Dynamic and online models are very accurate yet they require too much computing time. A model that requires less computing time is more useful for processing the many runs that are necessary for the validation of results and the testing of our intentional islanding mechanism.

[10]Technically, an island is an electrical circuit that is disjoint from the rest of the network. All connecting lines to other parts of the network are disconnected so that no energy flows are possible. More information on islanding can be found in Chapter 5.

All power grid models need a method to recalculate the power flows. The method that is used greatly affects the accuracy of the model. A fast and relatively simple method is to use shortest paths to redistribute flow [22, 49, 59, 60]. However, energy flows along many paths and therefore a more sophisticated approach is required to approximate real flow. One such approach is to use Alternating Current (AC) power flow solutions [10, 61]. The AC power flow equations are a non-linear system of equations that take the most important dynamics into account. They are often solved via the Newton-Raphson method [77]. Although this approach yields accurate results, the computing time can be disadvantageous. Additionally, the AC power flow solution may not converge after some contingencies in the power grid. These problems can be overcome by using a suitable approximation.

Peterson et al. [66] obtained good results with their non-linear approximation of the AC equations. The approximation is faster than solving the AC power flow equations and the loss in accuracy relatively cheap compared to the gain in computing time. This makes approximations better suited for most models. More recently, a linear programming approximation to the AC power flow has been proposed by Coffrin and Van Hentenryck [21]. Their method approximates both active and reactive AC power flows by means of solving a linear program. However, even less computation time is required when reactive power is neglected. This is done in another – less accurate, yet far faster – approximation used widely throughout literature.

This widely used linear approximation of the AC power flow is the Direct Current (DC) power flow. The DC power flow is shown to give reasonable results under conditions that will be discussed in Section 4.2. These conditions are generally met in high voltage power grids, as studied in this thesis. Many papers [8, 11, 17–19, 25] that aim for a better understanding of the global dynamics of a cascade failure use this method. Purchala et al. [68] found that the DC method has an 5% error bound on almost the entire network when the aforementioned conditions are met. More significant errors may occur on lightly loaded links. In this thesis, we will also make use of DC power flow solutions to reduce the computing time of simulations.

The last considered aspect that sets models apart is the way in which the trigger events are modeled. Initial removal of a generator or distribution point as trigger event is done by Holme and Kim [41]. This event simulates the effect of some calamity at a generator where all transmission lines are assumed to be invulnerable. Initial removal of a single transmission line as trigger event generally does not have a big impact on the network[11], yet as more lines are removed sequentially they can trigger a cascade [2, 40, 51]. This type of removal corresponds to cascade failure in transmission lines, which is often the case in practice [32, 56, 80]. Consider, for example, a transmission line that is hit by lightning or that makes contact with a tree, both causing safety relays to shut the line down.

Also, the initial removal as trigger event can be chosen deterministically or probabilistically. Deterministic selection of the initial removal is mainly done for removal of distribution and generator points [37, 41, 42, 57, 85]. When considering worst-case scenarios, it is common practice to determine the target according to some measure (often from complex network theory) that indicates the importance of the node. One such measure is the number of transmission lines that are adjacent to a node (node degree). Other importance measures will be explained in more detail in Chapter 4. Deterministic removal

[11] See also Section 2.4 about the $N-1$ rule.

of lines [40, 42, 58] is slightly less common in literature, although Arianos et al. [4] and Bompard et al. [14] published interesting research on the net-ability performance measure.

Probabilistic selection of removals is practiced for both line removals [2, 19, 51] and node removals, where the latter case is often in combination with deterministic selection [18, 22, 51, 60]. This choice is motivated by the fact that a cascade may be caused by unpredictable causes such as damaged or obsolete equipment, lightning, extreme temperatures, wind or any form of precipitation [38]. During the cascade, unpredictable behaviour can also be caused by relays, as described in Section 2.4. The tripping of lines due to short circuits or unintended relay actions motivates a probabilistic line failure approach for models that do not incorporate very accurate physical calculations. In particular, these models are unable to predict relay actions and can only incorporate these events in a probabilistic way. Relay actions due to hidden failures can never be predicted and motivate a probabilistic element in all models. More advanced models usually incorporate both deterministic and probabilistic disturbances in any component or in the voltage or frequency profile. This thesis will focus on random line failures, hidden failures and random node failures to simulate voltage and frequency disturbances.

The interested reader may also have a look at Baldick et al. [6, 7] for a more elaborated review on power grid models that range from real-time grid monitoring to simulating cascading failures. Boccaletti et al. [12] and Mei et al. [55] give a more detailed introduction to the topic of energy grid modeling.

Chapter 4

Modeling

The previous chapter gave an overview of the relevant aspects for modeling cascading failures in high voltage power grids. This chapter will first explain the translation from the real world problem to a mathematical model. Then, the choices and assumptions for our own model will be introduced and motivated. Fundamentals of our model have been based on the model in Anghel et al. [2]. When relevant, we will state the similarities and the differences between the model by Anghel et al. and our own.

In many aspects of the model that will be described below, assumptions are made for lack of actual data. Without data it is hard to make a realistic model or to verify results (e.g. in Chapter 6). This problem has also been mentioned during the Energy Systems Week 2013 (Appendix C) and is acknowledged as one of the biggest obstacles in energy grid modeling. If data were available, a lot of assumptions would not have been necessary.

4.1 Real world to mathematical model

4.1.1 Overview

A high voltage energy grid is assumed to consist of generator, distribution and load (demand) points that are interconnected by transmission links. This can be modeled in a very natural way as an undirected[12] graph G where every generator, distribution and load point is represented by a *node* and the transmission links are represented by *links* or *edges*, as can be seen in Figure 4.1. Thus, some nodes produce energy and some nodes require energy. The sets of nodes and edges are denoted by V and E, respectively. Also, G is in general not a simple graph. That is, there may be edges that share both endpoints. Multiple transmission lines are expensive, but also make the network more robust.

Electrical energy automatically flows from the generation nodes to the load nodes via the links. The flow of electrical energy is comparable to the flow of water; it does not take a single path but may flow among many paths to reach its destination. Also, some paths carry less flow than others. Specifically, the flow on a path is dependent on a physical property called electrical impedance. Paths that have low impedance will carry more flow than paths that have high impedance. As mentioned in the previous chapter, one way to approximate the flow in the network is by determining the DC power flow solution. Our model uses this method to approximate the flow. The DC method is described in Section 4.2.

[12]Technically, the edges of the graph are directed to indicate the direction of flow. However, flow can travel in both directions and for this reason we refer to the graph as undirected.

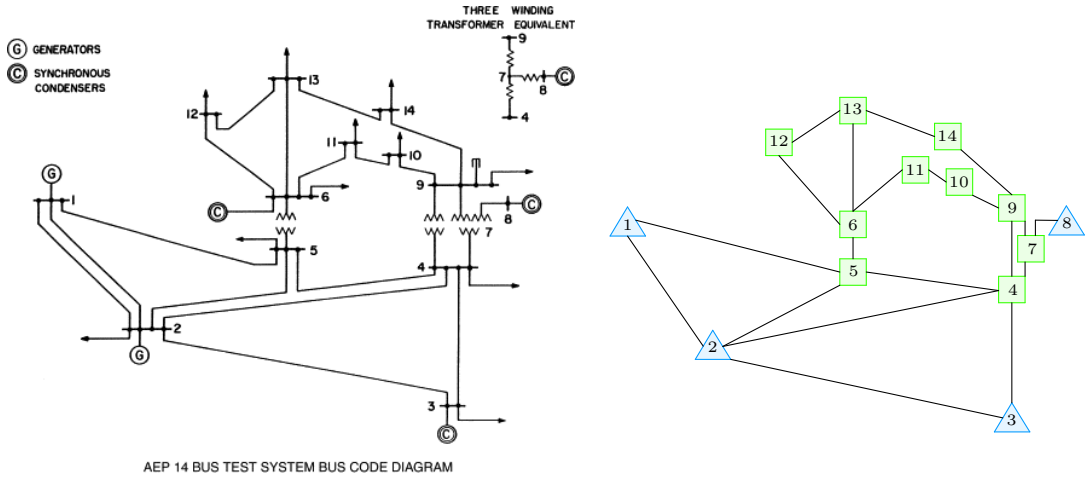

(a) (b)

Figure 4.1: Technical, single line diagram (a) and graph-theoretical (b) visualizations of the IEEE 14 bus network. Blue triangles correspond to generators, green squares to distribution and load points. Technical representation from [24].

4.1.2 Network

Data on both artificial and real world energy grids is available on the internet. Well-known artificial networks include the Barabási-Albert (BA) [9] scale-free model and the Erdös-Rényi (ER) [31] random graph model. The BA model uses a power law distribution for both the node degree and load distribution, whereas the ER model uses a binomial distribution for the node degree and an exponential distribution for the load. Both networks have been used with complex network theoretic approaches. Networks with more realistic electrical properties can be obtained via the Institute of Electrical and Electronics Engineers (IEEE 14, 30 , 57 and 188 bus test systems, obtained from [79]). Real world networks should be obtained via the European Network of Transmission System Operators for Electricity (ENTSO-E) or North American Electric Reliability Corporation (NERC). Our simulations have been performed on the IEEE test systems and the European power grid by UCTE, the former name of ENTSO-E. The networks will be referred to as *IEEE* $<number>$ *bus network* and *UCTE network*, respectively. The UCTE network has 1254 buses (nodes).

4.1.3 Line capacity

There often is no known value for the capacity of links due to lack of data. This is a key problem in making high energy grid modeling realistic. In general it can be noted that the capacity P_l^c of a link l is directly related to its initial load $P_l(0)$ as

$$P_l^c = \alpha_l \cdot P_l(0) \tag{4.1}$$

where α_l is some scalar bigger than one. The initial load $P_l(0)$ equals the solution of the DC power flows at $t = 0$. Energy grids are often operating near their operating limits, so

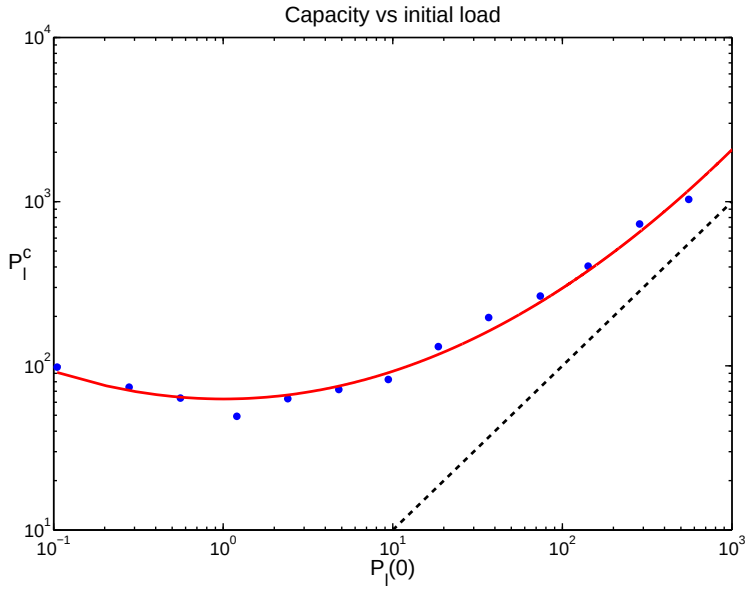

Figure 4.2: Log-log plot of line capacity P_{cl} versus initial line load $P_l(0)$. Blue dots represent the data points provided by Kim and Motter [48]. The red line represents approximation (4.2).

α_l can be expected to be close to one. In many papers, including the paper by Anghel et al. [2], the loading of links is even assumed to be homogeneous, i.e., $\alpha_l \equiv \alpha$ for some $\alpha > 1$. However, it has been argued by Kim and Motter [48] that this is unrealistic and that another relationship is more appropriate.

Historical data suggests that the relationship between capacity and load of transmission lines is non-linear; heavily loaded lines usually have a lower tolerance parameter than lightly loaded lines. With permission from Kim and Motter, the relation between initial load L and capacity C has been plotted in Figure 4.2. Using standard regression analysis tools, we found the relation

$$P_l^c = 60.34 \cdot \exp(0.08 \cdot \log^2 P_l(0)) \tag{4.2}$$

which is represented by the red curve in the figure. The dashed line represents the equality $P_l^c = P_l(0)$. Clearly, the heavily loaded lines are close to their capacities whereas lightly loaded lines have a relatively large margin. Line capacities in the proposed model have been assigned according to (4.2), hereby deviating from Anghel et al. [2].

4.1.4 Generator output

In daily power grid management, power is bought via an auction process. This implies that not every generator will produce equally much power, and daily deviations are likely to occur. Also, the output of various generators can in general not be shifted to the most secure system state. By random nature of the auction process, generation is more likely to be distributed in a financially beneficial manner. In both cases, it is hard to predict the actual generator outputs.

Anghel et al. [2] formulated an optimization problem similar to the one by Carreras et al. [17] to compute generator outputs. Solving this problem for many iterations is expensive and therefore this approach has not been followed in this thesis. Instead, we assume that all generators (the subset $gen \subset V$) have the same weighted output. That is, if the total demand of the network equals D and generators $i \in gen$ have maximum generator outputs P_i^{max}, then generator g is assumed to deliver an output P_g of

$$P_g = \frac{P_g^{max}}{\sum_{i \in gen} P_i^{max}} \cdot D. \tag{4.3}$$

This assumption is based on intuition rather than data.

4.1.5 Load Shed

When the combined maximum output of the generators is not sufficient to serve all load, some load must be shed. In line with the information from TenneT (see Appendix B), we assume three load shed levels: 15%, 30% and 50%. If a 15% reduction of demand is sufficient to match generation and demand, every load is dropped by 15% and generator outputs are assigned by (4.3) for the new demand $D_{reduced} = 0.85 \cdot D$. When 15% reduction is not sufficient, another 15% load is shed and possibly the remaining 20% too. In extreme cases where even 50% load shed is not enough to match generation and load, load is shed completely and the system can not sustain itself. It will remain non-sustaining until the time where generators or transmission lines are repaired (see Subsections 4.1.12 and 4.1.13) and at least 50% of the total load can be satisfied. It is also possible that the line failures have caused the network to electrically disintegrate into two or more components. In this case, the above load shed procedure is followed in every component individually.

4.1.6 Random line failures

As mentioned in Chapter 3, we assume that cascades in the network are triggered by both line and generator failures. This section focusses on the former kind. Two probabilistic approaches are modeled: random and biased random. The *random* approach follows Anghel et al. [2] where it is assumed that lines fail independently of each other at random times. Assuming that failure times are random and independent of other (past) events, it is natural to assume that the number of failure events for any line l follows a Poisson distribution with parameter $\lambda_{FD,l}$. That is, the number of failures of line l up to time t, $N_l(t)$, has the following probability distribution:

$$P_l(N_l(t) = n) = \frac{(\lambda_{FD,l} \cdot t)^n}{n!} e^{-\lambda_{FD,l} \cdot t}, \qquad n \geq 0, \tag{4.4}$$

with mean $E[N_l(t)] = \lambda_{FD,l} \cdot t$. This can be interpreted as $\lambda_{FD,l}$ being the average number of failures in line l during one time unit; the failure density. Failures are often caused by weather conditions or contact with vegetation [38], so it is reasonable to assume a direct relation between the failure density $\lambda_{FD,l}$ and line length L_l; $\lambda_{FD,l} = \lambda_{FR} \cdot L_l$. Here λ_{FR} is the failure rate per unit length. Every line has a non-zero probability to fail in the probabilistic approach.

A useful property of the Poisson distribution is the fact that the *interfailure* times $x = t_{i+1} - t_i$ between two consecutive failures in a line l follow an exponential distribution with parameter $\lambda_{FD,l}$;

$$F_l(t) = 1 - e^{-\lambda_{FD,l} \cdot t}. \tag{4.5}$$

Let X_i be independent random samples from distribution (4.5). Then the times $t_n = \sum_{i=1}^{n} X_i$ for $n \geq 1$ are a realization of (4.4) and can thus be used as failure times. An additional benefit of this approach is that sampling from an exponential distribution is numerically efficient [67].

The *biased random* approach prefers tripping of certain links above others based on an importance measure. For example, we may artificially increase the trip probability of links that carry much flow. Doing this may increase the number of cascades, which is useful when testing defensive methods (e.g. the effect of islanding). Other importance measures are described in the next subsection.

Let $\bar{E}$ be the list of links, sorted according to some rule. For biased random sampling, if link l is the i-th element in $\bar{E}$ then the probability p_l to trip line l is defined as

$$p_l = \mathbb{P}[\text{line } l \text{ fails}] = C \cdot \beta^i, \tag{4.6}$$

where $0 < \beta \leq 1$ is a parameter and C is the normalization factor. The parameter β controls the degree of bias; for $\beta = 1$, (4.6) is the same as the uniform random distribution; for $\beta \downarrow 0$, (4.6) will assign probability 1 to the first link in $\bar{E}$ and 0 to all others (deterministic selection). All simulations in this thesis where β is not mentioned explicitly assume $\beta = 0.8$. This implies reasonable probabilities for lower entries in $\bar{E}$ but already incorporates a strong bias. The effect of β will be studied in more detail in Section 6.2.

The biased random approach assigns failure probabilities to the links, but says nothing about the time at which the failures happen. Recall that the interfailure time of a line l is assumed exponentially distributed with parameter $\lambda_{FD,l}$. The interfailure time over all lines is then exponentially distributed with parameter $\Lambda_{FD} = \sum_{l \in E} \lambda_{FD,l}$;

$$F_E(t) = 1 - e^{-\Lambda_{FD} t}. \tag{4.7}$$

This distribution can be used to sample interfailure times over *all* links instead of individual links. At every failure time, an active (non-tripped) link is sampled according to the biased random probabilities and this will trip.

One can see that Λ_{FD} is the mean failure density over all lines. By changing the value of Λ_{FD} it is possible to simulate many (extreme operating conditions) or few (normal operating conditions) random line failures per time unit. In particular we may choose Λ_{FD} and set $\lambda_{FD} = \Lambda_{FD} / [\sum_{l \in E} L_l]$ so that both the random and the biased random approach have the same overall failure density Λ_{FD}. The values of Λ_{FD} and β completely determine the distribution and location of biased random line failures. Unless mentioned otherwise, we always assume $\Lambda_{FD} = 1/(24 \cdot 7)$ (one failure per week) and $\beta = 0.8$. The model of Anghel et al. [2] does not incorporate biased random failures and the corresponding importance measures.

4.1.7 Importance measures

The list of links $\bar{E}$ is determined according to an importance measure. Importance measures are functions that indicate the (relative) importance of lines or nodes. $\bar{E}$ is sorted from the most important to the least important line. In this context, importance is a very broad concept. For instance, the measure may be purely topological so that 'importance' relates to properties like node/edge degree, distance or centrality. Measures can also be based on a physical property such as initial flow through a node or a statistical property such as correlation similarity. From the wide range of measures, we have implemented the following:

- *Edge betweenness* is a centrality measure that was introduced by Girvan and Newman [34]. For every line l, the edge betweenness $\delta(l)$ is defined as the fraction of shortest paths between any two nodes that walk along l. If $\sigma(u, v)$ is the number of shortest paths between nodes u and v and $\sigma_l(u, v)$ is the number of such paths along l, then

$$\delta(l) = \sum_{\substack{u,v \in V, \\ u \neq v}} \frac{\sigma_l(u, v)}{\sigma(u, v)}. \tag{4.8}$$

  Note that our graph is undirected and thus $\sigma(u, v) = \sigma(v, u)$ and $\sigma_l(u, v) = \sigma_l(v, u)$ for all $u, v \in V, l \in E$. This measure can also be used for general graphs.

- *Edge degree* is a topological measure. The edge degree $d(l)$ equals the number of unique links that share at least one endpoint with l. It is equivalent to the node degree of node l in the line graph $L(G)$ of G. Intuitively, it also is a measure that relates to (but is not equal to) the number of times that edge l is on a (non-shortest) path when compared to other edges. Since power flows generally use all paths between two points, edge degree could be a good indicator of important links.

- *Initial flow* is a physical measure. This measure assumes that a line that carries a lot of flow is important. In power networks this is often true. If a heavily loaded line trips, the flow has to be redistributed. This puts stress on the remainder of the network and causes a disturbance in the voltage profile. A line that is not heavily loaded is expected to have less impact.

- *Node significance* is a measure that considers both the topological and the physical properties of the network. It has been proposed by Koç et al. [50] as (part of) a robustness measure for power networks. Basically, the distribution of flow from a node's perspective over its adjacent links (entropy) is combined with the importance of the node itself in terms of outgoing flow (amount of flow to be redistributed after failure of the node). This index is then related to the robustness of the network and yields a good correlation with experimental results.

  Unfortunately, this measure can not be used directly to compare individual links. In collaboration with the first author of [50] the following classification has been used as an importance measure. Initially, nodes are sorted according to outgoing flow. Then for the most important node, sort the adjacent links according to the amount of outgoing power carried. These links are on top of the list $\bar{E}$. Repeat this procedure for the second most important node and place the links after the previous links, etc. If a link adjacent to the current node is already in the list, the link will keep its original listing. This procedure adds every link exactly once to the list.

- *Empirical data* bases the importance of a link on the number of times that is has been involved in a cascade. This measure is explained in more detail in Chapter 6.2.

These importance measures will be compared to one other in Chapter 6.

4.1.8 Overloaded lines

Next to random line failures, lines can also fail because they experience overload for too long. Relays will then trigger the breaker to protect the transmission line by electrically removing it from the network. Specifically, when some lines have been removed from the network, then the loads on other lines have increased. This may cause overload on the working lines, followed by tripping of some of these lines due to relay actions causing an increase of load on the remaining working lines. Modeling this interaction is essential in the study of cascading failures.

Most relays in high voltage power grids are so-called impedance relays. Impedance relays roughly monitor the imaginary ratio between current and voltage and require precise information about real and reactive power flows. When the impedance has been too high for too long, the relay activates the breaker to disconnect the transmission line. Models that compute the AC power flows accurately are able to use this information to predict relay behaviour. However, this is not possible for models that use DC power flow equations. In particular, we are not able to model relay actions accurately. Instead, we follow the approach used by Anghel et al. [2]. Anghel et al. assume that heat conduction in transmission lines is a crucial factor in the tripping of lines. In the case of increased power flow through a transmission line, the line heats up till some critical tolerated temperature where it automatically trips. The line is then out of service until it is repaired manually. There are two reasons for this particular choice of relay replacement in the model. First, the line temperature depends on the current, which is also important for impedance relays. Second, the time until disconnection depends on the degree of overload; small overload can be sustained longer than big overload. This too is in agreement with the workings of impedance relays.

Modeling the temperature development in the lines can be done by solving the heat equation, where it is assumed that the temperature in the entire cross-section of the line is the same (heat equation for small rods). A number of line properties is required in order to specify the heat equation to this particular situation. The cross-section area ω, perimeter p, thermal conductivity K, electrical conductivity σ, density ρ, specific heat c and diffusivity κ are all assumed to be constant and known. Furthermore, the heat flux across the surface of the line is assumed to be proportional to the temperature difference between the rod and the surrounding medium. This flux is then given by $H \cdot (T - T_0)$ where T is the line temperature, T_0 is the temperature of the medium and H is the surface conductance. For air with velocity u perpendicular to a circular cylinder of diameter d, $H = 8 \cdot 10^{-5}(u/d)^{\frac{1}{2}}\ cal/(cm^2 s\, K)$.

For a specified time t and position x in a transmission line with current $I = P/V$, the heat equation is now given by

$$\frac{\partial T(x,t)}{\partial t} = \kappa \frac{\partial^2 T(x,t)}{\partial x^2} + \alpha I^2 - \nu(T - T_0), \tag{4.9}$$

where $\kappa = K/(\rho c), \alpha = 0.239/(\rho c \omega^2 \sigma)$ and $\nu = Hp/(\rho c \omega)$. Assuming that fluctuations in power flows dominate heat flow transients, the spatial variation in temperature can be neglected. For an initial line temperature $T(0)$, it is shown by Anghel et al. that (4.9) becomes

$$T(t) = e^{-\nu t}(T(0) - T_e(P)) + T_e(P) \tag{4.10}$$

where

$$T_e(P) = \frac{\alpha}{\nu}\frac{P^2}{I^2} + T_0 \tag{4.11}$$

is the equilibrium temperature of the line when a constant power flow of P is maintained as $t \to \infty$. When the power flow P changes at some point in time, the temperature at that moment is set as $T(0)$. This allows us to use (4.10) in determining further temperature development of the transmission line.

Equation (4.10) makes it possible to monitor the temperature of a line. We assume that a line l trips when its temperature exceeds its critical temperature T_l^c. This critical temperature can be initialized directly as T_l^c, or indirectly by letting P_l^c be capacity of line l and setting $T_l^c = T_e(P_l^c)$. With a fixed critical temperature it is straightforward to determine overload failure times of lines. Solving $T(t) = T_l^c$ yields

$$t_l^c = \frac{1}{\nu} \ln \frac{T_l^c - T_e(P_l)}{T(0) - T_e(P_l)}. \tag{4.12}$$

Thus, a transmission line with temperature $T(0)$ and critical temperature T_l^c, subject to a constant flow of $P_l > P_l^c$ will trip at time t_l^c due to excessive heating.

4.1.9 Hidden failures

Hidden failures have shortly been described in the previous section. Hidden failures are deficiencies in relays that do not show under normal operating conditions. However, under extreme operating conditions such relays may cause more lines to trip than required. In particular, all links that share at least one endpoint of a tripping link may be disconnected by the relay due to a hidden failure [18, 65]. This behaviour may also happen because of incorrect relay settings. Technically this is not a hidden failure, yet the direct consequences are the same. Regular maintenance as well as timely purchase of new equipment reduce chances on hidden failures.

To simulate hidden failures and incorrect relay actions, all links adjacent to a tripping link have a 0.001 probability of tripping as well. That is, when link $(1, 2)$ fails all links that have node 1 and/or node 2 as an endpoint are vulnerable to a hidden failure. Every such link has a 0.001 probability of tripping, independent of other links. This behaviour may accidentally speed up the cascading process. The 0.001 probability is not based on any data. Hidden failures have not been modeled by Anghel et al. [2].

4.1.10 Random generator failures

Generator failures are modeled in the same way as random line failures; interfailure times are exponentially distributed, the overall failure density is given by Λ_{FD} and at every failure time a random available generator trips. Random failures of lines and generators

are independent of each other. Biased random failures of generators are not considered in this thesis. It is important to note that a tripped generator is still capable of transferring power since the generation and the transportation of power are physically separated. This thesis only considers failure of generator nodes (random and stability failures) and not of other nodes. Failure of generators – both random and induced by protection devices – has not been modeled in [2].

4.1.11 Generators stability failures

Generators have protection systems that shut the generator down when frequency or voltage swings that may damage the machinery are measured. To model this behaviour in a probabilistic way, every generator is given a tripping probability that depends on the change in generation at this generator. In particular, for an absolute generation shift S_g at generator g, the probability of failure is given by

$$\mathbb{P}\left[\text{generator } g \text{ fails}\right] = 0.8 \cdot \left(\frac{S_g}{P_g^{max}}\right)^2. \tag{4.13}$$

The given distribution is not based on any data. It is chosen so that nodes are likely to trip during relatively large swings, as is observed in real world cascades. Intuitively, we assume that there is always at least a 20% chance that the generator keeps working correctly and safely. Also, a quadratic relation is more realistic than a linear relation since small swings happen frequently and generators should be constructed to cope with such swings, whereas big swings are far more likely to activate protection systems. As can be seen from Figure 4.3, a relative generation shift of 0.5 relates to a 20% probability to trip whereas a 0.75 relative generation shift relates to a probability of 45% to trip. Generators that have been repaired and return to service are assumed to be unaffected by swings during start-up.

4.1.12 Line restoration

Similarly to Anghel et al. [2], maintenance teams are sent to overloaded transmission lines to repair the lines and get them back into service. Some hours are needed to register and identify the failure, call for a maintenance team and wait for the team to arrive at the concerning line. After that, the line has to be repaired. According to the website of TenneT [75] the total repair time of overhead transmission lines takes 8 to 48 hours. We therefore assume that the repair time is normally distributed with a mean of 15 hours, a standard deviation of 7.5 hours and a minimum of 8 hours. If data is available, the correct times and possibly a different distribution can be implemented easily. As soon as the line is repaired, the maintenance team will notify the operator and the line is put back into service.

4.1.13 Generator restoration

Generators that are out-of service will be also be repaired as soon as possible. We have assumed a normally distributed maintenance period with mean 16 hours, standard deviation 4 hours and a minimum repair time of 5 hours. Again, the given distribution

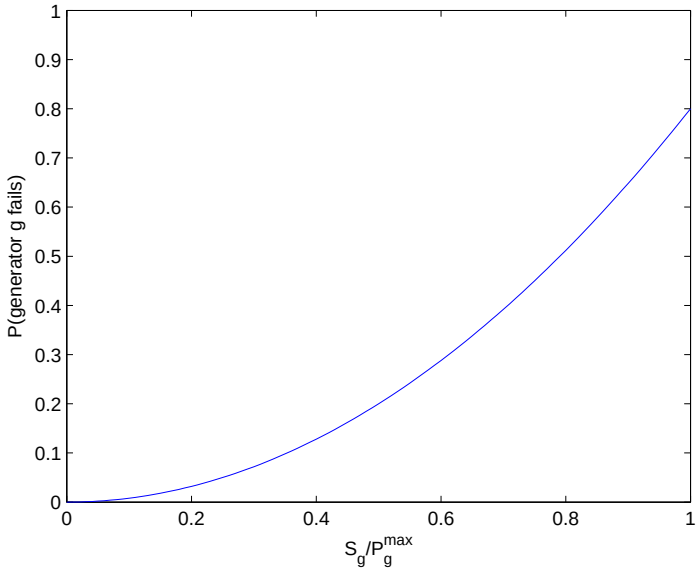

Figure 4.3: Probability of a generator to fail due to frequency and voltage swings. Depends on relative generation shift S_g/P_g^{max}.

and parameters have not been based on any data. When the repairs are finished, the generators are put back to service and are assumed to instantly produce their share of generation (according to the Generator Loading assumption). Since generator failures are not considered in Anghel et al. [2], this restoration process is no part of their model.

4.2 DC power flow

The redistribution of flow – e.g. due to failure of a link or shift in generation – will be done according to DC power flow solutions. The DC power flow equations are a linear approximation of the AC power flow equations. This method is reasonably accurate and faster than more accurate alternative methods as discussed in Chapter 3. However, the DC power flow equations discard frequencies, voltage magnitudes and reactive flows and only approximate real flows. The important manipulations in the derivation of the DC power flow equations depend on the following three assumptions:

- Line resistance is negligible compared to line reactance, i.e. $R << X$. Recall that the impedance Z of a line is given by $Z = R + \imath X$, where $\imath$ is the imaginary unit.
- Voltage angle differences over the network must be small, i.e. $\sin(\delta_i - \delta_j) \approx \delta_i - \delta_j$.
- The network has a flat voltage profile, i.e. all voltage magnitudes are considered to be 1 per unit (p.u.). Voltages in p.u. have been normalized by the base voltage of the network.

Different kinds of DC power flow equations and algorithms are compared by Stott et al. [71]. Stott et al. also argue that the DC power flow equations may not be as accurate as

claimed. Hereby they oppose common practice by other researchers and the papers by Liu and Gross [53] and Purchala et al. [68] that present justification and sensitivity analyzes of the assumptions in high voltage power grids. As the presented model simulates a high voltage power grid, the assumptions can be made and the DC power flow solutions can be used in the calculation of power flows. Besides the question marks that have been raised at the DC power flow equations, the model still benefits from a computational speed and simplicity that outperforms the AC power flow equations. Both this advantage and the general believe in good accuracy may contribute to the fact that DC power flow models are still widely used throughout literature and also in this thesis.

The classical derivation from AC power flow equations to DC power flow equations will now be presented. Consider the AC power flow equation for real power p_{ij} through link (i, j):

$$p_{ij} = |V_i||V_j| \left(g_{ij} \cos(\delta_i - \delta_j) + b_{ij} \sin(\delta_i - \delta_j)\right). \tag{4.14}$$

Here, $|V_i|$ and $|V_j|$ are the voltages per unit and δ_i and δ_j are voltage angles at nodes i and j. The complex *admittance* $Y = G + \imath B$ of the lines is given by $Y = 1/Z$. The units G and B are called *conductance* and *susceptance*, respectively. From $1/z_{ij} = 1/(r_{ij} + \imath x_{ij}) = (r_{ij} - \imath x_{ij})/(r_{ij}^2 + x_{ij}^2)$ it follows that

$$g_{ij} = \frac{r_{ij}}{x_{ij}^2 + r_{ij}^2} \quad \text{and} \quad b_{ij} = -\frac{x_{ij}}{x_{ij}^2 + r_{ij}^2}. \tag{4.15}$$

The first assumption, i.e. $R << X$, now implies that g_{ij} is negligible and $b_{ij} \approx -1/x_{ij}$. Substituting this into (4.14) yields

$$p_{ij} \approx |V_i||V_j| b_{ij} \sin(\delta_i - \delta_j). \tag{4.16}$$

The second assumption implies that the first order Taylor approximation of $\sin(\delta_i - \delta_j)$ is an accurate approximation, so we substitute $\sin(\delta_i - \delta_j) = \delta_i - \delta_j$ into (4.16) to obtain

$$p_{ij} \approx |V_i||V_j| b_{ij} (\delta_i - \delta_j). \tag{4.17}$$

Finally the assumption $|V_i||V_j| \approx 1$ reduces (4.17) to

$$p_{ij} \approx b_{ij} (\delta_i - \delta_j), \tag{4.18}$$

which is the DC power flow approximation of (4.14). Zimmerman et al. [86] developed a free to use Matlab package named Matpower[13]. This package is able to do AC and DC power flow computations and it is used for DC power flow computations in our algorithm.

Instead of calculating the DC power flow for every change in the network, there are also some useful tools to update the flows of the perturbed system. One of these is the *Power Transfer Distribution Factor (PTDF)* matrix. The entries of this matrix can be used to find the shift in power flows for a given shift in generation and/or load. In particular, it can be used to find the change in all links when some amount of power is injected in one node and rejected at another node. One example would be a 50 MW shift in generation from generator A to generator B; the PTDF matrix indicates the corresponding change in the network links.

Another tool is the *Line Outage Distribution Factor (LODF)* vector, which can be easily derived from the PTDF matrix. The LODF vector can be computed for a given

[13] More information and download at `http://www.pserc.cornell.edu/matpower/`.

link l and corresponds to the change in all links when link l is removed from the network. For example, it shows the impact on the network when link l experiences a failure. This information can be used to analyze the system and to check whether the $N-1$ criterion is respected. Güler et al. [36] developed a generalized method to find the LODF for the removal of multiple links at once.

A more detailed explanation of the PTDF matrix and derivation of LODF vectors can be found in Appendix A. Also, a novel method to update the PTDF matrix for small changes in the network topology is presented. The new method updates the PTDF matrix of the current network to the PTDF matrix for a reduced network. The reduced network is predominantly identical to the current network, but one or more links have been removed. Although the method is presented to update the PTDF matrix for the removal of one node and its adjacent links, it is not restricted to this kind of removal. Both the PTDF matrix and LODF vectors are not used in the remainder of this thesis.

As a last remark, the author would like to mention that Appendix A also states a theorem on the invertibility of a special kind of matrix. To the author's knowledge, the given theorem has not shown up in literature before and it may very well be useful in applications other than power grid modeling. The theorem can be found on page 70.

Chapter 5

Islanding

5.1 Introduction

Chapter 4 introduced a model to simulate several kinds of failures in the power grid. Transmission lines and generators are subject to random failures, stability failures, hidden failures and overloads. Repair actions are executed within two days of the initial failure. Unfortunately, as will be shown in Chapter 6, this does not make the power grid completely secure. The combination of the complex dynamics in the power system and the physical (safety) limits on lines and generators make that certain failures induce a cascading failure. Multiple protection mechanisms – e.g. Under-Frequency Load Shedding, see Section 2 – have been integrated to the real world power grid in order to keep the damage to a minimum. This section introduces an optimization problem for intentional islanding; the last defence for halting cascading failures.

Intentional islanding is the most rigorous radical defensive technique in power grids. Technically, an island is an electrical circuit that is disjoint from the rest of the network. All connecting lines to other parts of the network are opened so that no energy flows are possible[14]. Once islands have been formed, it takes a long time to synchronize them and put them back together. For this reason it is used only in extreme situations (e.g. during the India blackout [56]). Also, the designing of islands is a difficult task that concerns many different issues. Those issues include – but are not limited to –

- minimal load shed; serve as many consumers as possible,
- load versus generation capacities of each island, including the amount of reserves of generators,
- availability of black-start equipment (equipment that can be activated without energy supply from the grid) in case that a blackout can not be avoided,
- importance of loads; e.g. hospitals versus households,
- redistribution of flow, since changing the network topology also changes the flows,
- line overload; do the new flows respect line capacities,
- stability issues during island formation; disconnecting links may cause voltage or frequency swings,

[14] Terminology by electrical engineers. When an electrical circuit is *closed*, it means that their is a path from the source of energy to the load. This allows energy to travel along this path. Removing links in the path *opens* the circuit and prevents flow of energy.

- stability issues after island formation; islands should remain stable until they are merged again,
- size of islands; big islands allow the cascading failures to cause a lot of damage, whereas small islands isolate the cascade but deal with more stability issues.

It is difficult to optimize the island design for several issues at the same time. Trade-offs between different objectives make that the optimal island is hard to define. For example, increased stability may only be possible by means of more load shedding. At what point in this trade-off do we consider the island to be optimal?

Before addressing this question, the general idea of islanding will be made more specific. Recall that a given power grid can be represented as a graph $G(V, E)$ where V is the set of nodes, corresponding to generators and loads, and E is the set of links, corresponding to transmission lines. The set of nodes V is the union of two sets *gen* and *load*, containing all generator nodes and load nodes respectively. Note that a node can be both a generator and a load point, similarly to the real network. The cardinalities (number of elements in a set) of V, gen and $load$ are given by N, n_{gens} and n_{loads}, respectively. Since nodes can be both generators and loads, it follows that $n_{gens} + n_{loads} \geq N$. An islanding scheme is a partitioning over the nodes V such that one partition represents an island and the other partition represents the complement. Both the island and the complement have to be connected components and the power flows have to respect both DC power flow equations and line capacities. A more detailed explanation of the constraints is given in the next section. The challenge is to find a partitioning such that a majority of the issues above are taken into account, i.e., to find the 'optimal' island. It is also possible to split the network into more than two components. However, this will give more stability issues and synchronizing the islands afterwards will require more time. Since we isolate failures in one island, it is not beneficial to make other islands at the same time.

As a result of the trade-offs listed before, an island can only be optimal under certain assumptions. Which issues are more important than others? And how can one compare island schemes against one other? This first question will be addressed in the next paragraph. Concerning the second question, we make use of the fact that under some assumptions it is possible to formulate the 'optimal' islanding problem as a *mixed integer linear program (MILP)*. A MILP is a problem where decision variables (e.g. partitioning) have to be assigned such values that a given cost linear function is minimized (or maximized). This cost function is the clue in comparing different islanding schemes. Decision variables are also subject to a set of linear constraints that are defined beforehand (e.g. connectivity). The term 'mixed integer' in MILP comes from the fact that some decision variables are real and some are integer valued. An optimal solution returns the values of the decision variables as well as the corresponding optimal value of the cost function. Thus, assuming a linear cost function and linear constraints, it is possible to formulate the islanding problem as a MILP formulation. The solution to this formulation is an optimal island in the sense that it has minimum cost over all islands that satisfy the constraints. Finding a solution is not simple[15] in general and thus may take a long time.

Ahead of defining the cost function for the MILP, some assumptions have to be made. First, it is assumed that the stability of the island is directly related to the shift in flow

[15]Binary or 0-1 integer linear programming is a special case of MILP. Since binary linear programming is NP-complete [45], MILP is NP-complete as well.

before islanding versus the flow after. This means that a large shift in the flow is penalized harder (costs more) than a small shift. Secondly, it is assumed that all loads are equally important in the sense that all nodes are equally likely to be in the island. However, we do assume that nodes in the island are less important to serve. More specifically we say that load shed in the island is preferred to load shed in the complement. The reason for this is that consumers who live far from the failures should experience less of the problems than consumers who live near to the failures. It makes more sense to spare those far away and isolate the consequences of the failures as much as possible. For the same reason, the load nodes outside the island are required to receive at least a fraction α of their initial load whereas the load of nodes in the island may be shed completely. Thirdly, energy flows have to respect the DC power flow equations (4.18) and the line capacities given by (4.2). Finally, both the island and the complement must have at least one generator.

Under the listed assumptions, we propose the following cost function:

$$\text{Minimize } A\sum_{i=1}^{N}\sum_{j=i+1}^{N}|power_{ij}-f_{ij}|+B\sum_{l=1}^{n_{load}}p_{load(l)}^{s=2}+C\sum_{l=1}^{n_{load}}p_{load(l)}^{s=1}. \tag{5.1}$$

The first term equals the net shift in power flows from before ($power_{ij}$) and after (f_{ij}) islanding. The double summation is adjusted so that the power shift at every link is counted once with factor A. That is, the total shift in power is accounted for with factor A. The second and third term penalize load shed in the complement and the island, respectively. The variable $p_{load(l)}^{s=2}$ equals the load shed in node $load(l)$ when this load is in the complement, and equals zero otherwise. On the other hand, $p_{load(l)}^{s=1}$ equals the load shed if $load(l)$ is in the island and zero else. Load shed in the complement is accounted for with factor B and load shed in the island is accounted for with factor C. Since all these terms have to be minimized, the factors A, B and C are non-negative. Also, because load shed in the complement is considered worse than load shed in the island, we require $B \geq C$. The relative values of A, B and C will decide whether more importance is given to reducing load shift or load shed. For $A > B \geq C$, load shed is preferred over load shift since load shift is more expensive (A) than load shed (B, C). On the other hand, $B > A \geq C$ prefers load shift (cost A) above load shed in the complement (cost $B > A$), and considers load shed in the island as least important ($C \leq A$). The condition $B \geq C > A$ is also possible, implying that every kind of load shed is considered worse than load shift. One can see this by the fact that load shift only costs A per unit whereas load shed costs $B > A$ or $C > A$ per unit. Choosing suitable values for the parameters depends very much on the user's preferred importance of every term, and there are no perfect values in general. In this thesis we take $A = B = 10$ and $C = 1$, which considers load shed in the island unimportant and the other two factors about equally important.

Cost function (5.1) and the fundamentals for the formulation in the next section have been derived from a paper by Pahwa et al. [63]. Pahwa et al. made a formulation that forms multiple islands at the same time, where islands are defined by assigning links to either the island or the complement. Computational test cases showed good results for the MILP, although the method would not converge for test cases over 30 nodes. Therefore, Pahwa et al. presented two heuristic methods. The heuristics worked for larger cases as well and showed reasonable results compared to the MILP. A discussion on the paper with three of the corresponding authors and dr. S. Starrett can be found in Appendix D. The appendix also provides alternative formulations for some constraints in the original paper. These lead to improvements, because the total number of constraints is reduced and possibly

less binary decision variables are required (depending on software implementation). Both of these aspects reduce computational complexity. The main differences from the MILP formulation by Pahwa et al. and the formulation in the next section is that islands are now implied by assigning nodes, and that most improvements from the discussion in Appendix D.1 have been implemented.

5.2 MILP formulation

In this section, we will introduce and explain all variables and constraints for the MILP formulation. The main objective is to minimize the cost function (5.1) by assigning nodes to the island or the complement. Classification of node i is done by assigning a value σ_i; the decision variable σ_i equals one (zero) if node i has been assigned the the island (complement). The optimal island I can be extracted from the solution as $I = \{i \in V : \sigma_i = 1\}$. Other decision variables can be found in Table 5.3 at the end of this chapter. Note that the σ_i have a one-to-one relation with the assignment of links. If $\sigma_i = \sigma_j = 1$, then link (i, j) is part of the island. If $\sigma_i = \sigma_j = 0$ then link (i, j) is part of the complement, and if $\sigma_i \neq \sigma_j$ then the link will be opened in forming the island. Such links will also be referred to as *interconnecting links*. A useful way to identify interconnecting links is to consider the absolute difference between nodes, $|\sigma_i - \sigma_j|$. If $|\sigma_i - \sigma_j| = 1$, the link (i, j) is interconnecting whereas $|\sigma_i - \sigma_j| = 0$ implies that the link is either in the island or in the complement.

5.2.1 Topological constraints

$$\sum_{i=1}^{N} \sigma_i \geq 0.1 \cdot N \tag{5.2}$$

$$\sum_{i=1}^{N} (1 - \sigma_i) \geq 0.5 \cdot N. \tag{5.3}$$

These two constraints force a minimum size on the island and its complement so that there are always two non-empty components. Without these constraints, the algorithm returns the optimal island $I = V$ which is the original network. In particular, (5.2) ensures a minimum island size of 10% the network size to prevent very small islands. Constraint (5.3) makes sure that the complement contains at least half the network so that the island is always smaller than the complement. Without this constraint, the island and complement can be 'switched' to obtain a lower value of the cost function since load shed in the complement is cheaper. Originally, there were also constraints to ensure at least one generator in the island and its complement. However, these constraints are implied by the set of constraints that ensure connectivity of the island and its complement. The connectivity constraints are listed below:

$$|z_{ij}| \leq a_{ij}(1 - |\sigma_i - \sigma_j|)N \qquad \forall i, j = 1, \ldots, N \tag{5.4}$$

$$\sum_{i=1}^{N} z_{ij} = -1 \qquad \forall j = 1, \ldots, N \tag{5.5}$$

$$\sum_{g=1}^{n_{gens}} z_{gen(g),T} = N \tag{5.6}$$

$$z_{gen(g),T} \leq \xi_{gen(g)} N \qquad \forall g = 1, \ldots, n_{gens} \tag{5.7}$$

$$\sum_{g=1}^{n_{gens}} \xi_{gen(g)} = 2 \tag{5.8}$$

$$z_{ij} = -z_{ji} \qquad \forall i, j = 1, \ldots, N \tag{5.9}$$

$$z_{gen(g),T} = -z_{T,gen(g)} \qquad \forall g = 1, \ldots, n_{gens}. \tag{5.10}$$

These constraints can be considered as an imaginary flow z_{ij} over the network that is only possible when the components are connected. The imaginary flow z_{ij} is not in the cost function (5.1) and is only needed to ensure connectivity.

One may recognize these constraints as a variation on the (minimum cost) flow problem on an undirected graph. Basically, one supersink T is added to the network and it is connected to all generator nodes. Then, every node is assumed to generate one unit of energy (total of $N \times 1 = N$ units generation) (5.5) and this energy has to be transported to the supersink T with a demand of N (5.6). The transport of energy is restricted to the existing links assigned to the island (both ends in the island) and the complement (both ends in the complement) (5.4). Transport between the island and its complement is not allowed. Also, transport to T is restricted to exactly two links (5.7), (5.8). This implies that in the island/complement, all generation is transported to one generator and then to T. If the island/complement is not connected, it will need more than one connection to T and the above constraints can not be satisfied. Note that this formulation also forces the island and its complement to have at least one generator each, since only generators are connected to T. Constraints (5.9) and (5.10) are the usual flow constraints that make the solution feasible. An illustration of the connectivity constraints is given in Figure 5.1.

5.2.2 Flow constraints

One of the challenges in the MILP formulation of the islanding problem is the formulation of flow constraints. Interconnecting lines do not carry flow and all other lines are subject to the DC power flow equations. In order to form sustaining islands, the flow on the lines is also required to respect the corresponding line capacities. These requirements all considered in the following constraints:

$$|f_{ij}| \leq (1 - |\sigma_i - \sigma_j|)c_{ij} \qquad \forall i, j = 1, \ldots, N \tag{5.11}$$

$$|b_{ij}(\delta_i - \delta_j) - f_{ij}| \leq a_{ij}|\sigma_i - \sigma_j| \cdot 2\pi \max_{i \in V} b_i \qquad \forall i, j = 1, \ldots, N \tag{5.12}$$

$$|\delta_{gen(g)}| \leq (1 - \xi_{gen(g)}) \cdot 2\pi \qquad \forall g = 1, \ldots, n_{gens}. \tag{5.13}$$

Recall that the DC power flow model implies that line (i, j) experiences a power flow

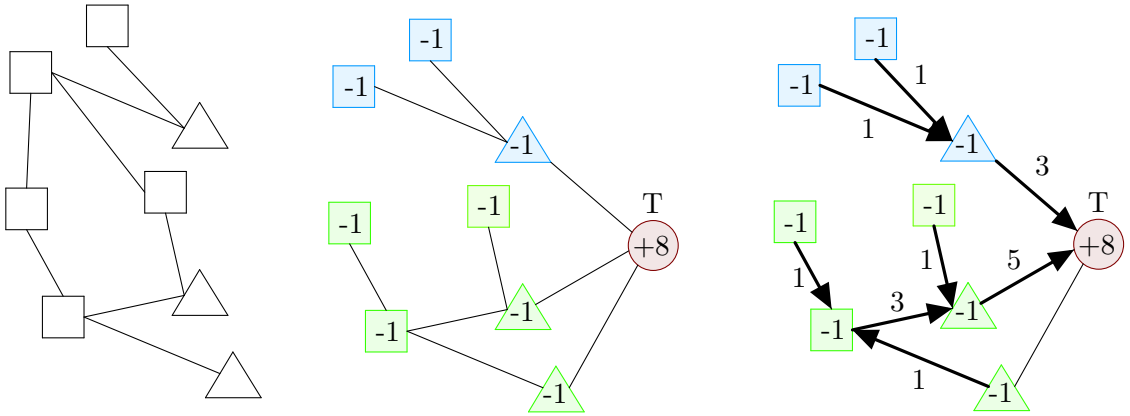

(a) Island scheme I

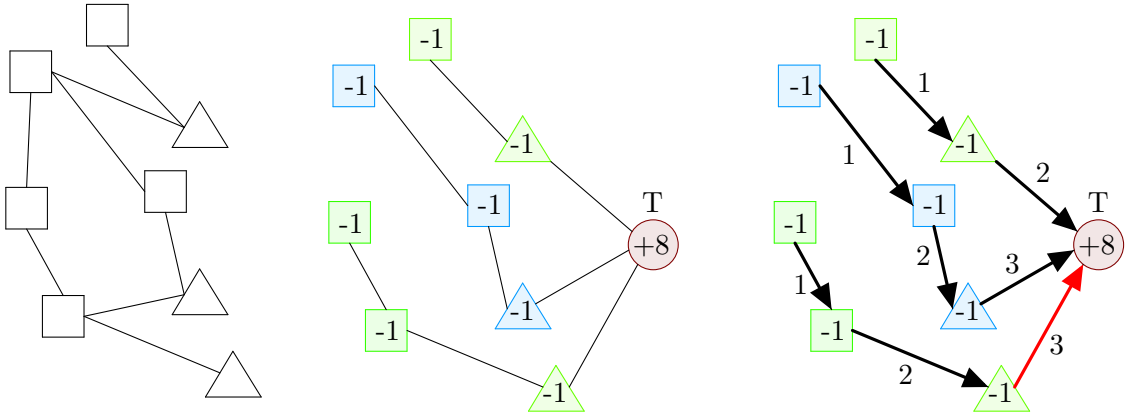

(b) Island scheme II

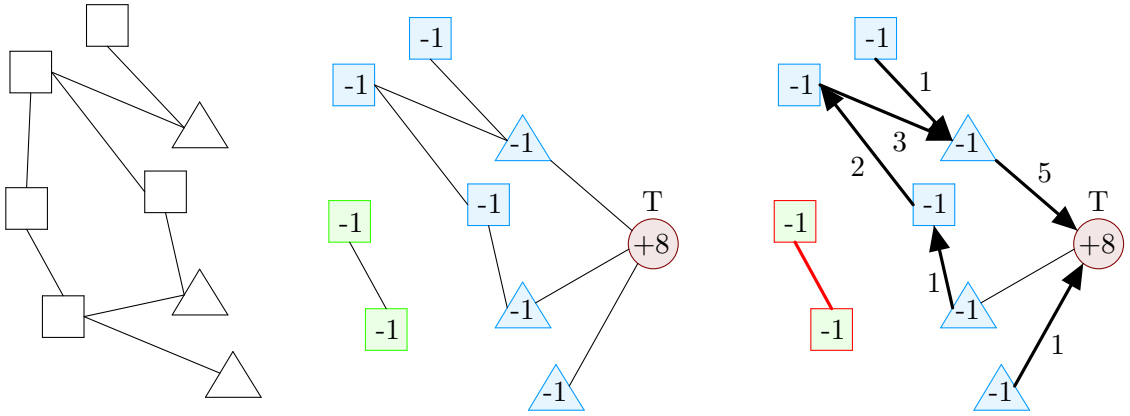

(c) Island scheme III

Figure 5.1: Visualization of connectivity constraints. Generators are illustrated by triangles and the imaginary flow z_{ij} by arrows. The arrows have been directed to correspond with positive flow and should not be confused with the undirected nature of the graph. Islanding scheme I shows that connected components with at least one generator can transport flow from all nodes to the generator and then to the supersink T. When the components are not connected, as illustrated in Islanding scheme II, it is not possible to use only two links adjacent to T. That is, constraint (5.8) can not be satisfied. Island scheme III shows that components without a generator are not able to transport flow to T, so the flow balance constraints (5.5) and (5.6) can not be satisfied.

of $b_{ij}(\delta_i - \delta_j)$ where b_{ij} is the electrical susceptance of the line (imaginary part of the admittance Y, see Section 4.2) and δ_i and δ_j are the voltage angles at the ends of the line. The term $b_{ij}(\delta_i - \delta_j)$ thus corresponds to the power flow on a line (i, j).

We want the line flow f_{ij} to equal zero for interconnecting lines and to equal $b_{ij}(\delta_i - \delta_j)$ for the lines in the island or its complement. First assume that $\sigma_i = \sigma_j$. Then line (i, j) is in the island or its complement, and $|\sigma_i - \sigma_j| = 0$. From (5.12) it follows that $f_{ij} = b_{ij}(\delta_i - \delta_j)$ and (5.11) makes sure that the capacity of the line is respected; $|f_{ij}| \leq c_{ij}$. Now assume that $\sigma_i \neq \sigma_j$, so line (i, j) is interconnecting. Constraint (5.11) then reduces to $f_{ij} = 0$ and (5.12) is respected since $2\pi \max_{i \in V} b_i$ is an upper bound for $|b_{ij}(\delta_i - \delta_j)|$. Finally, lines that do not exist have $b_{ij} = c_{ij} = 0$ and zero flow will be assigned by (5.11) without restricting δ_i and δ_j in (5.12). The constraints above will thus assign flow – subject to the DC power flow equation – to a line if and only if the line exists and is not interconnecting.

Constraint (5.13) forces precisely one generator in each island to have voltage angle zero (the generators assigned by the connectivity constraints). Since only the relative values of the voltage angles are relevant, fixing one of them does not change the practical solution space whereas it does remove an infinite number of equivalent solutions. In other words, this constraint does not imply a new physical condition on the problem, but it makes the computation easier. The constant 2π is an upper bound on the δ_i and should not alter the solution space.

Given the power flows, it is possible to compute the power d_i at each node and make them subject to the following constraints:

$$d_j = \sum_{i=1}^{N} f_{ij} \qquad \forall i = 1, \ldots, N \tag{5.14}$$

$$d_{gen(g)} \leq 0 \qquad \forall g = 1, \ldots, n_{gens} \tag{5.15}$$

$$d_{gen(g)} \geq 1.05 \cdot power_{gen(g)} \qquad \forall g = 1, \ldots, n_{gens} \tag{5.16}$$

$$d_{load(l)} \leq power_{load(l)} \qquad \forall l = 1, \ldots, n_{loads} \tag{5.17}$$

$$d_{load(l)} \geq (1 - \sigma_{load(l)}) \cdot \alpha \cdot power_{load(l)} \qquad \forall l = 1, \ldots, n_{loads}. \tag{5.18}$$

Constraints (5.15) and (5.16) require the power at all generators to be negative, meaning that they have a supply, and bounded by 105% of the initial generation. That is, generators are assumed to able to deliver an additional 5% power output after islanding to make the system stable. The margin of 5% has been adopted from [63]. Load nodes can not receive more energy than they require (5.17), and their lower bound is given by (5.18). This lower bound equals zero (complete load shed) for nodes in the island, and a fraction α of the initial node load for nodes in the complement.

5.2.3 Cost constraints

Recall the cost function (5.1). For the cost function we need a distinction between the load shed in the island and the load shed in the complement, as the latter has to be penalized harder than the former. For this reason we need constraints that assign $p^{s=2}_{load(l)} = 0$ if $load(l)$ is in the island and $power_{load(l)} - d_{load(l)}$ otherwise, and vice versa for $p^{s=1}_{load(l)}$.

Consider the following constraints:

$$p^{s=2}_{load(l)} \geq (1 - \sigma_{load(l)}) \cdot power_{load(l)} - d_{load(l)} \qquad \forall l = 1, \ldots, n_{load} \tag{5.19}$$

$$p^{s=1}_{load(l)} \geq \sigma_{load(l)} \cdot power_{load(l)} - d_{load(l)} \qquad \forall l = 1, \ldots, n_{load} \tag{5.20}$$

$$p^{s}_{load(l)} \geq 0 \qquad \forall l = 1, \ldots, n_{load}, s = 1, 2. \tag{5.21}$$

The combination of (5.19) and (5.21) assigns every $p^{s=2}_{load(l)}$ a minimum value of zero for all island nodes and the amount of load shed for all nodes in the complement. Inequalities (5.20) and (5.21) do the opposite for $p^{s=1}_{load(l)}$. Since the cost function of the MILP is to minimize the positive sum of all $p^{s}_{load(l)}$, a minimum value of every individual $p^{s}_{load(l)}$ will be forced by the algorithm. We may conclude that every $p^{s}_{load(l)}$ is assigned precisely the value that has been described in the preceding paragraph. By setting $C = 0$ in the cost function and removing all $p^{s=1}_{load(l)}$ constraints, the load shed within the islands is not accounted for at all.

5.2.4 Absolute value transformations

One may have noted that there are absolute values in constraints (5.4), (5.13), (5.11) and (5.12). Absolute values, however, are no linear functions. Fortunately, there is a elegant way to work around these problems that will be described in the following paragraphs.

Consider the following relations:

$$|X| \leq M \Leftrightarrow X \leq M \text{ and } -X \leq M \tag{5.22}$$

$$X \leq |\sigma_i - \sigma_j| \Leftrightarrow X \leq \sigma_i + \sigma_j \text{ and } X \leq 2 - \sigma_i - \sigma_j \tag{5.23}$$

$$X \leq (1 - |\sigma_i - \sigma_j|) \Leftrightarrow X \leq \sigma_i + (1 - \sigma_j) \text{ and } X \leq (1 - \sigma_i) + \sigma_j. \tag{5.24}$$

The first relation is used very often. It follows directly from the definition of the absolute value $|X|$, which equals X for $X \geq 0$ and $-X$ for $X < 0$. That is, $|X| = \max\{-X, X\}$. If both $-X$ and X are bounded by M, then $|X|$ is bounded by M too.

The second and third relations are less obvious but can easily be checked with a logical table. Recall that $|\sigma_i - \sigma_j|$ should indicate whether nodes i and j are in different components,and that $1 - |\sigma_i - \sigma_j|$ should indicate whether the nodes are both in the island or both in the complement. Verification of (5.23) and (5.24) is done in Tables 5.1 and 5.2, respectively. The relations are correct because the AND-columns (corresponding to the right-hand expressions) are identical to the last columns (corresponding to the left-hand expressions).

σ_i	σ_j	$\sigma_i + \sigma_j$	$2 - \sigma_i - \sigma_j$	AND	Indicator different component, $\lvert\sigma_i - \sigma_j\rvert$
0	0	0	2	0	0
0	1	1	1	1	1
1	0	1	1	1	1
1	1	2	0	0	0

Table 5.1: Verification of (5.23). Column AND states the logical value of the right-hand expression of (5.23). This is equal to the multiplication of the third and forth column entries. The last column is the indicator of σ_i and σ_j being in a different component, or rather the left-hand expression of (5.23).

σ_i	σ_j	$\sigma_i + (1 - \sigma_j)$	$(1 - \sigma_i) + \sigma_j$	AND	Indicator same component, $1 - \lvert\sigma_i - \sigma_j\rvert$
0	0	1	1	1	1
0	1	0	2	0	0
1	0	2	0	0	0
1	1	1	1	1	1

Table 5.2: Verification of (5.24). Same concept as in Table 5.1, yet now the last column is the indicator of σ_i and σ_j being in the same component.

5.2.5 Additional remark

Recently, a similar MILP formulation has been presented by Trodden et al. [78]. Although there are striking similarities, the author wants to emphasize that these are purely coincidental and that he was unfamiliar with the article by Trodden et al. until after completion of this chapter. The formulation presented in this chapter is completely based on the article by Pahwa et al. [63], the author's visit to Kansas (Appendix D) and the author's own work and insight. This being said, it should be mentioned that Trodden et al. [78] performed extensive simulations with real data. Their results include an evaluation of optimization speed versus performance, accuracy of the MILP islands when compared to AC power flow solutions and response of machine rotor angles to islanding. Readers who are interested in more research on MILP formulations for islanding are recommended to read Trodden et al. [78].

Constants		
a_{ij}	binary	Indicator matrix for lines in the undirected network. Equals one if line (i, j) exists and zero else.
b_{ij}	real	Electrical susceptance of line (i, j), equals zero if line does not exist.
c_{ij}	real	Capacity of line (i, j), equals zero if line does not exist.
$power_i$	real	Initial power generation (negative) in or load (positive) of node i.
$power_{ij}$	real	Initial power flow (directed) over line (i, j).
Decision variables		
σ_i	binary	Indicator for all nodes. Equals one if node is in the island and zero if in its complement.
$\xi_{gen(g)}$	binary	Indicator for all generators. Equals one if there is non-zero flow to supersink T and zero else. Needed for connectivity constraints.
z_{ij}	real	Imaginary flow on line (i, j) for connectivity constraints.
$z_{gen(g),T}$, $z_{T,gen(g)}$	real	Imaginary flow on lines between generators and supersink T for connectivity constraints.
δ_i	real	Voltage angles of nodes.
f_{ij}	real	Power flow (directed) on line (i, j) after islanding.
d_i	real	Power in node i after islanding. Negative for generators, positive for loads.
$p^{s=1}_{load(l)}$	real	Load shed at node $load(l)$ if the node is in the island, and zero if it is in the complement.
$p^{s=2}_{load(l)}$	real	Load shed at node $load(l)$ if the node is in the complement, and zero if it is in the island.

Table 5.3: Overview constants and decision variables MILP formulation.

5.3 Theoretical impact of islanding

To get a first impression of the impact of islanding, the MILP problem has been solved for the IEEE 118 bus network[16]. First, the optimization problem has been solved without constraint (5.2) to calibrate the model. Flow values from this solution were used to fix $power_i$ and $power_{ij}$ for all $i = 1, \ldots, N$. Secondly, the MILP problem has been solved with all constraints. This yielded the following solution:

- Nodes 1 to 14 and node 117 are all in the island, all other nodes are in the complement. Forming islands requires disconnecting only four links: (8,30), (12,16), (13,15) and (14,15). This is visualized in Figure 5.2.
- Slightly more than 10% (183 MW) of the total system load is contained in the island. Almost 90% (1611 MW) of the total system load is in the 'protected' component.

[16] Computation only took a few seconds. However, solving the MILP formulation for the large UCTE network repeatedly terminated with out-of-memory warnings. For this reason no results on islanding for the UCTE network are presented in this thesis.

- The amount of load shed in the island equals 2.7 MW. This is 1.5% of the total load of the corresponding nodes before islanding.
- No load was shed in the complement.
- The total flow shift equals 148.6 MW. This is 2.3% of the combined flows before islanding.

These results look very promising. For simplicity assume that the system serves 10 million consumers. The above results imply that islanding separates 1 million consumers from the other 9 million so that those 9 million are protected against eventual problems. If no problems occur, the 1 million consumers only receive enough power for 985,000 consumers. However, if problems are likely then this is a fair price to pay in order to save 9 million others. The flow shift of 2.3% could induce stability problems and should therefore be examined carefully. However, the relatively small change in flows does not seem threatening at first sight.

It should be noted that the island is designed for a network that operates under optimal conditions. All links are in service and the island that has been formed does not isolate an actual failure. Section 6.3 evaluates the effect of islanding in more severe circumstances so that the actual consequences can be analyzed. In particular, we study the effect of islanding when one line has tripped and an island is designed to isolate this failure[17].

[17] A line $l = (i, j)$ can be forced in the island by adding the constraints $\sigma_i = 1$ and $\sigma_j = 1$.

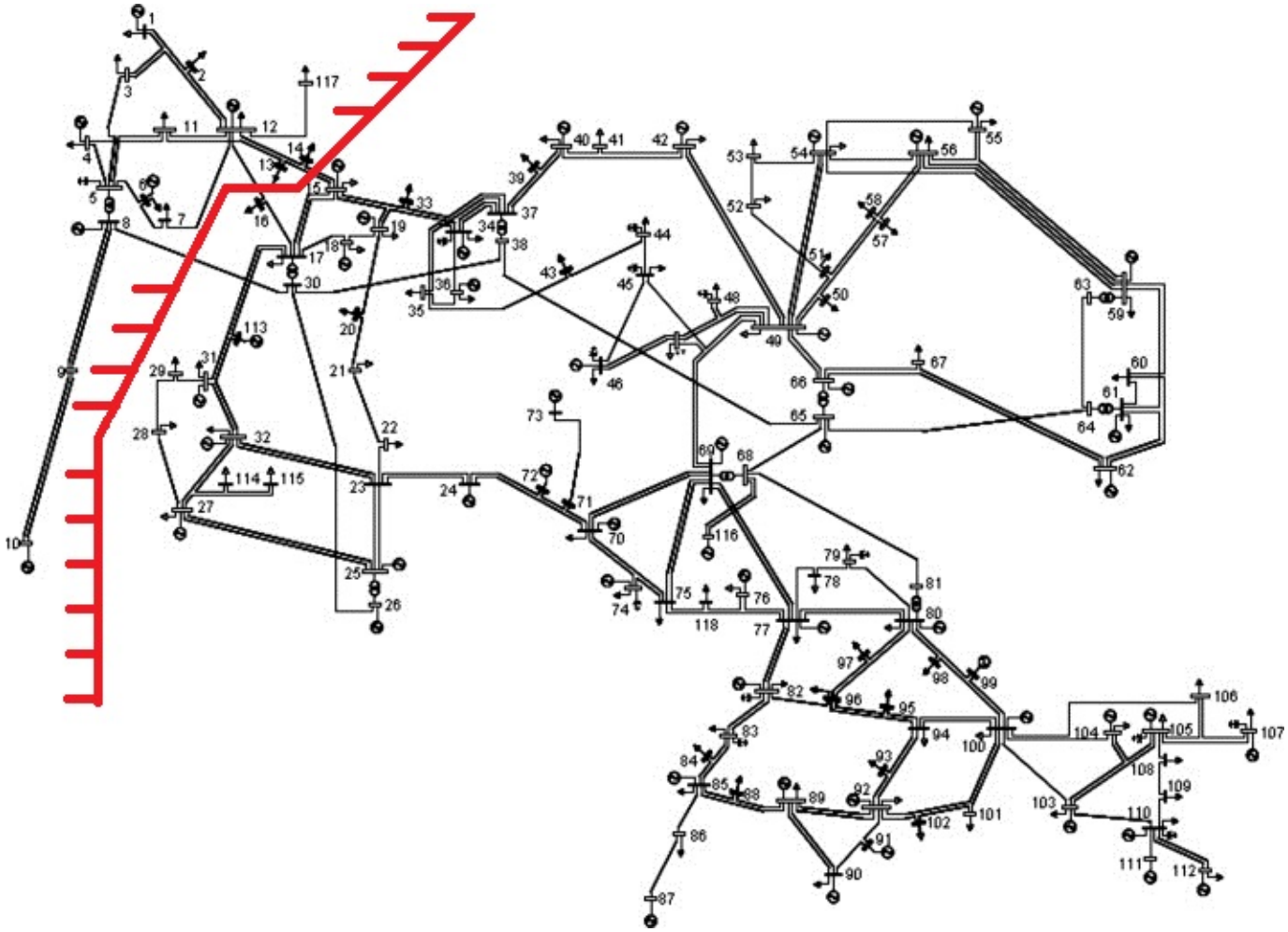

Figure 5.2: Optimal island for the IEEE 118 bus network. The left part of the network is isolated by disconnecting only four transmission lines. The big component (complement) is now protected to insecure system states in the small component (island). Original single line diagram from [47]

Chapter 6

Experiments and results

Chapters 4 and 5 introduced the reader to a mathematical model for simulating the high voltage power grid and a MILP formulation to design optimal islands. This chapter presents the results and analyzes of the various simulations that have been done. In particular, Section 6.1 introduces the reader to the simulation algorithm that is used and explains how the output of simulations can be interpreted. Next, Section 6.2 evaluates the various importance measures from Chapter 4 to find the most important links. Section 6.3 shows the results of cascading failure simulations for three different islanding schemes and discusses the impact of islanding. Finally, a brief sensitivity analysis is done in Section 6.4.

Many simulations have been performed during the research to the extent of obtaining reliable results. Therefore, in order to reduce computing time required, not all simulations have been performed on the UCTE network with 1254 nodes. In particular, the simulations for Figures 6.4 and 6.5 have been performed on the IEEE 118 bus network. All simulations have been performed in Matlab 2012b and IBM ILOG CPLEX Optimization Studio 12.5 on a Windows 7 machine with a Intel i7 processor and 6 GB memory.

6.1 First simulations

This section will introduce the reader to the algorithm used. Furthermore, the output of the algorithm is explained so that the results in the next sections can be interpreted correctly.

The algorithm (see below) is based on an eventlist; a list that keeps track of all events to come. This includes all failures and repair events that have been discussed in Chapter 4. Entries in the eventlist specify the time of the event, the component that is involved and the actual event. In every iteration, the first event in the list is evaluated. That is, lines and generators can fail or they can be repaired. After the event, flows are redistributed and new events are added to the eventlist. This process is repeated until the simulation time exceeds the maximum simulation time. A warmup period of 100 days is included to bring the network in a realistic (non-perfect) condition.

- Input: network in Matpower format, maximum simulation time, mean failure time, importance measure.
- Initialize: $t = 0$, warmup = 100 days, eventlist is empty, compute line capacities.
- Initialize: determine first failure time and corresponding failure (link and generator) and add to eventlist. Sort eventlist to ascending failure times.

- While $t <$(maximum simulation time + warmup) repeat the following steps.

  Step 1. Progress time t to first event in eventlist.

  Step 2. Start event.
  - For a repair event, put the component back into service.
  - For a line (generator) failure event, put component out-of-service and add repair event to eventlist. For a line failure event, check for hidden failures and put those lines out-of-order. Add new line (generator) failure to eventlist. Also add repair events for hidden failures.

  Step 3. Shed load if necessary, then redistribute flow according to DC power flow equations.

  Step 4. Check for generator stability failures. If generators fail, put them out-of-order, add repair events to the eventlist and return to Step 3.

  Step 5. Compute line overload times and add to eventlist. Remove previously computed overload times.

  Step 6. Sort eventlist to ascending time.

- Remove data for all events with $t <$warmup.
- Plot results.

The remainder of this section will explain and discuss these plots. There are two different plots after each run of the algorithm: the main plot and the interdanger time distribution plot.

- Main plot – Number of active lines versus simulation time and fraction of unserved energy versus simulation time. Furthermore, markers in the plot indicate the type of event that happened.
- Interdanger time distribution plot – Distribution plot of time between subsequent system states with two or more tripped lines, as well as an exponential distribution fit.

The plots will be now be explained in more detail. Examples can be found in Figures 6.1 and 6.2. The first figure shows the main plot for a 30 day simulation of the IEEE 118 bus network, the second figure shows both the main plot and the interdanger time distribution plot for a 50-year simulation of the UCTE network.

The main plots display the most relevant data. It is a compact overview of the most important aspects of the model. The blue stairs function displays the number of lines that is available. This number is almost directly related to the system state of the power grid operator (see Appendix B). In particular, a system state where two or more lines are out-of-order is considered to be critical as it can easily jeopardize the safety of the entire network. We will refer to such states as *danger states*. In the main plot it is easy to see when such danger states occur. Times between two danger states are referred to as *interdanger times*.

By looking at the markers in the plot, it is also easy to see how the system got into a certain (danger) state. Many times this will be either the random failure of two lines or the

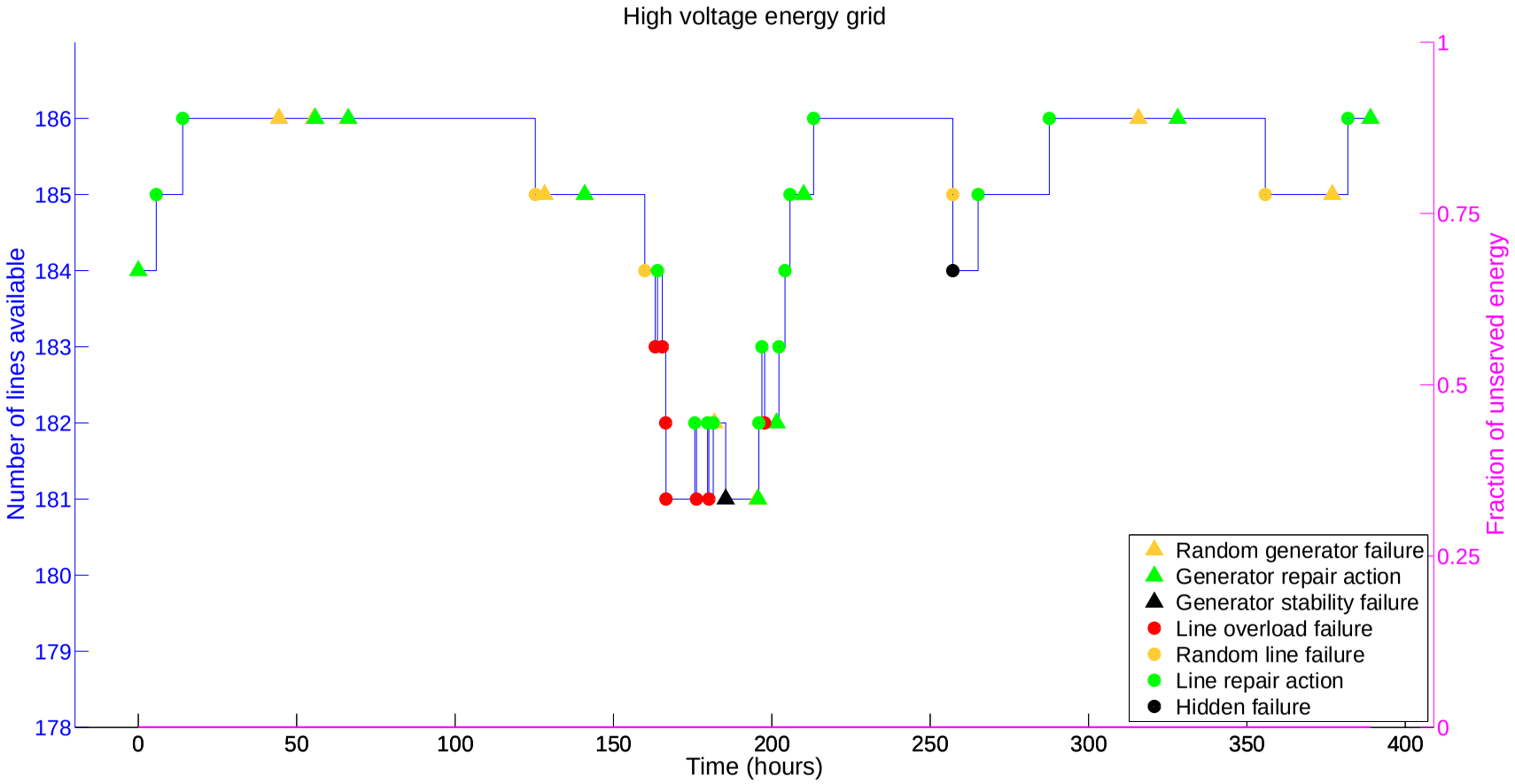

Figure 6.1: Illustration of main plot as outputs of the model. Based on a 30 day simulation of the IEEE 118 bus network. Since all demand is met in this simulation, the fraction of unmet energy equals zero and coincides with the time-axis.

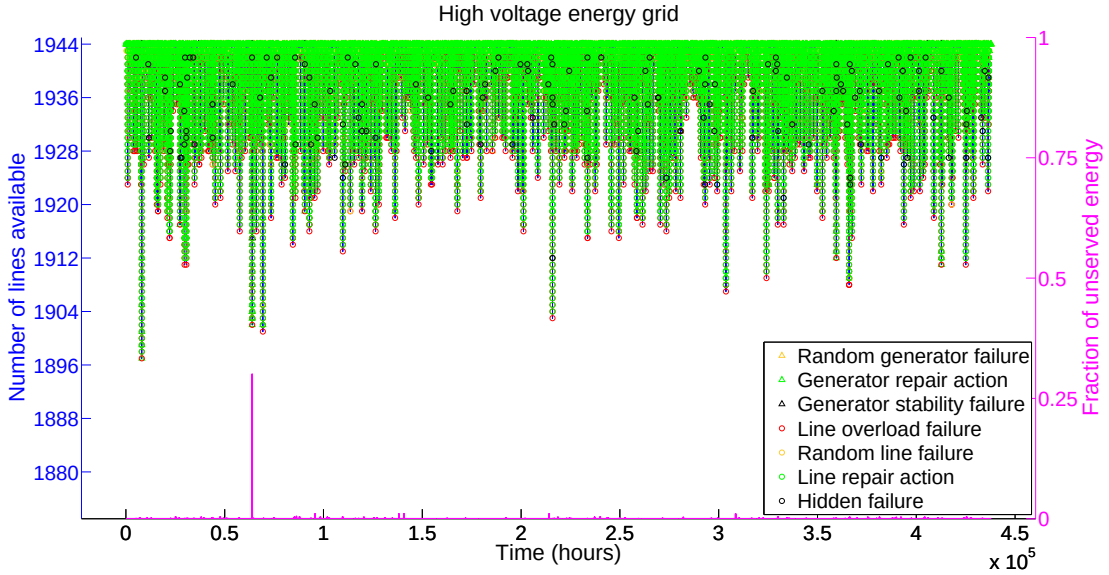

(a) Main plot

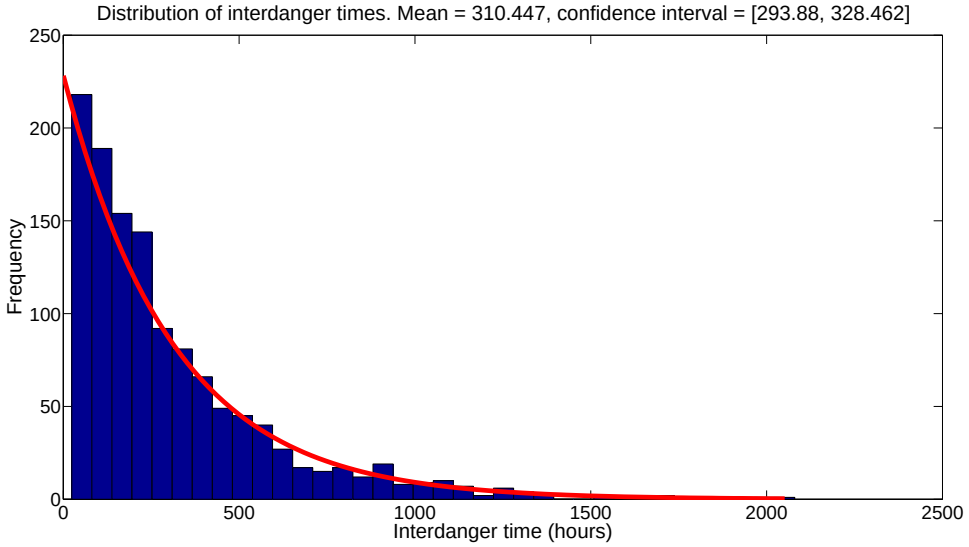

(b) Interdanger time distribution plot

Figure 6.2: Illustration of main plot as outputs of the model. Based on a 50 year simulation of the UCTE network. Artificial increase of failures was forced by initial flow bias on random failures to ensure load shed for illustrative purposes.

failure of a generator and a line, causing overload on other lines due to the redistribution of flow. For example, the first danger state in Figure 6.1 is caused by two random line failures (orange circles). These two failures caused other lines to overload (red circles) so that eventually five lines were out-of-service. During the repairs that followed (green circles), one of the generators tripped for stability reasons (black triangle). At $t = 230$ hours, all lines and generators were back to service again. The next random failure exposed a hidden failure in a relay, which tripped an additional line (black circle). This is the second danger state for the given simulation. During these danger states, no load was shed (that is, no customers experienced a blackout) and the operators would've been lucky. The simulation results in Figure 6.2(a) do show load shed; the magenta lines at the bottom of the plot indicate load shed was necessary in order to keep the network secure. Load shed is displayed as the fraction of total demand, so a real world load shed of 0.3 over 500 million consumers (UCTE network) implies that roughly 150 million people experience a blackout. Fortunately, real world networks perform better than the network in Figure 6.2 (e.g. better generator allocation and corrective actions in case of failures).

Roughly stating that the first danger state in Figure 6.1 was restored at 210 hours and the second danger state started at 260 hours, it follows that the interdanger time equals 50 hours. If more simulation data were available, it would be possible to accurately estimate the mean interdanger time. Figure 6.2(a) provides this simulation data for the UCTE network. Individual interdanger times can be extracted from this data (analogously to the short example), visualized with a frequency plot and fitted to a similar distribution. This is shown in the mean interdanger time plot in Figure 6.2(b). One can see that the distribution of mean interdanger times is well approximated by the exponential fit[18]. This is a direct consequence of the assumption that interfailure times are exponentially distributed[19]. Deviation from the exponential distribution will be discussed in the next section.

The frequency of danger situations is a good measure for system reliability, since it reflects how often the system is in danger rather than for how long. Operators would have more trouble with two danger situations than with one danger situation that is twice as long (especially because this would imply that they have more time to take actions). The frequency of danger states therefore seems representative to measure the robustness of the network. In particular, the distribution of interdanger times can be used to compare different simulations. A long interdanger time will indicate that the system is more robust than a system with a short mean interdanger time. Also, these plots will prove to provide more insight in the factors that lead to danger states.

6.2 Evaluation of importance measures

In this section, different importance measures will be compared to each other. As argued in the previous section, the mean interdanger time will be used to compare the different importance measures. First, we compare the results of random sampling and biased random sampling with edge betweenness. Interdanger distribution plots for both line failure approaches after 500 year simulations on the UCTE network can be found in Figure 6.3.

[18] The exponential distribution fits are made by the Matlab function `expfit` from the Statistics Toolbox.

[19] Interdanger times of less than 24 hours have been removed from the data. It is assumed that the corresponding dangerous states belong to the same event.

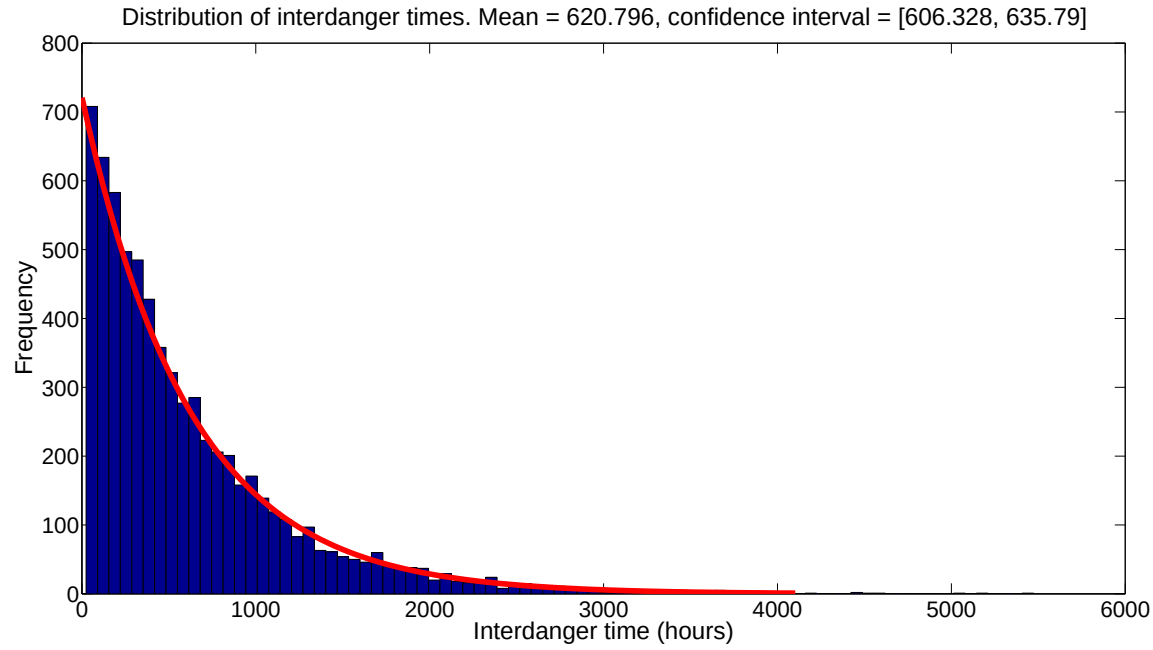

(a)

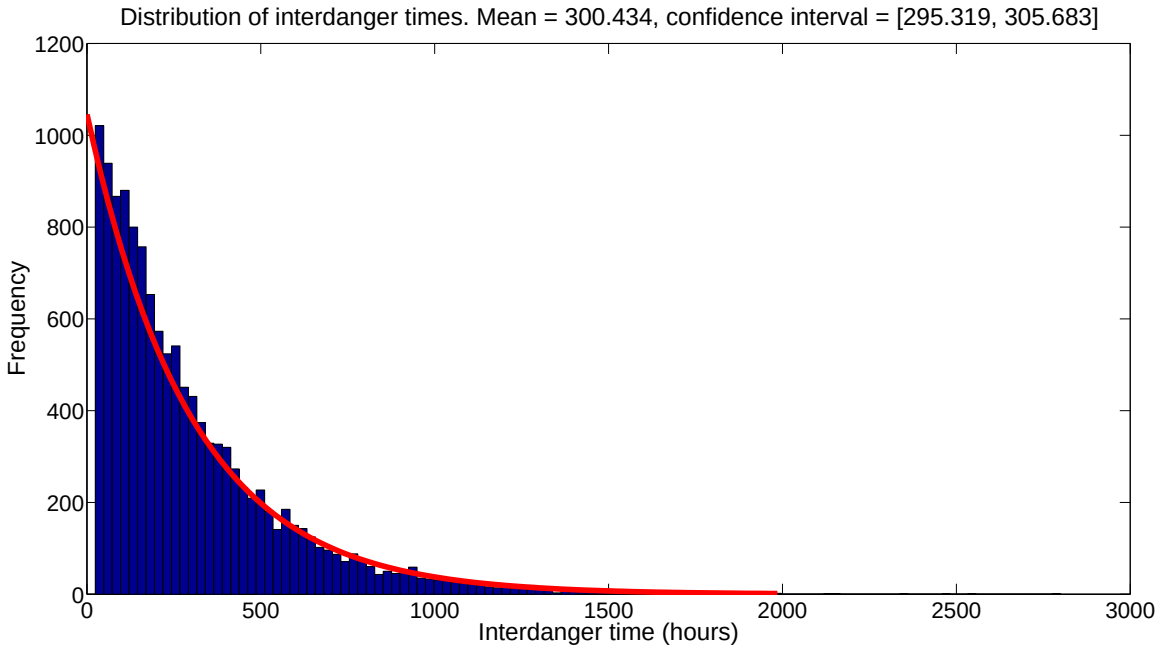

(b)

Figure 6.3: Interdanger distribution plot for random failures (a) and biased random failures w.r.t. edge betweenness (b) for 500 year simulations on the UCTE network.

An important piece of information can be found in the titles of the respective figures, which state that the random failure approach had a mean interdanger time of 621 hours versus 300 hours for edge betweenness bias. From these numbers it can be concluded that the edge betweenness measure is significantly better in revealing important links than the random method. This can be explained intuitively. The shortest path between two nodes is likely to also be the path with least resistance. Therefore, the links with high edge betweenness are likely to transfer a lot of flow. Tripping of these lines will cause a relatively big shift in power flows, which may cause overloads on other lines as well as disturbances in voltage and frequency.

We will now take a moment to consider the exponential fit. As noted before, the exponential fit is a direct consequence of the exponential distribution of interfailure times. However, it is interesting to see that the head of the experimental distribution is heavier than that of the exponential fit. This implies that there are relatively many short interdanger times, which would not occur when the physical aspects (overload, hidden failures, stability failures) were left out. Also, physical aspects play a smaller role for random failures and indeed the *heavy body* of the distribution[20] is not observed in Figure 6.3(a). This is another indication that the heavy body is caused by physical aspects. We will postpone the rest of this discussion to Section 7.1.

In Figure 6.3, we assumed biased probability on failures with respect to an importance measure. It is also possible to work the other way around. Instead of having a measure and simulating failures with respect to this measure, one may gather failure data and simulate failures with respect to this empirical data. That is, we simulate a given failure method for a long time. In every dangerous situation, the failed links are determined and they are stored. After the simulation, a list with all links is sorted in descending order of the number of occurrences in the aforementioned count. This is the empirical importance of every link with respect to the original measure. A new simulation is now started with the empirical importance. One would expect that the most important links have failed most often in the first simulation, meaning that their empirical importance is high. The empirical simulation is thus expected to have a lower mean interfailure time.

Table 6.1 shows the mean interdanger times for random failures and biased random failures with respect to edge degree, node significance, edge betweenness and initial flow, along with empirical simulations based on the data of the corresponding method. From this table, one can see that lines with high initial flow are in general more important for the network stability than other lines. Also, lines with a larger edge betweenness are slightly more important than general lines yet less important than the initial flow lines. This is in agreement with the analysis of Figure 6.3(b).

Unfortunately, Table 6.1 also shows that the empirical bias fails to identify more vulnerable lines. One explanation for this result is that the empirical data only looks for individual lines that are involved in a dangerous situation, rather than combinations of links. It is possible that some links are not very important on their own, but very important after another contingency. If the empirical method would consider combinations of links and failures would be modeled dependent, then a more structural analysis could be performed. For instance, the failures could be made dependent (e.g. failure of line 1 increases failure probability of line 2) to simulate worst-case scenarios. This could de-

[20] With the body of a distribution we refer to the part of the distribution that contains most of the mass (highest density), as opposed to the tail of a distribution.

	Random line failure method				
	Random	Edge degree	Node significance	Edge betweenness	Initial flow
Importance measure	621	599	428	300	213
Empirical data	965	942	687	870	1067

Table 6.1: Mean interdanger times for different failure methods. Interdanger times have been based on 500 year simulations on the UCTE network except for initial flow. Initial flow has been based on 50 year simulations since 500 year simulations always ended in complete blackouts. Empirical importance lists have been extracted from the simulation data of the initial simulations, whose results are in the top row.

crease the mean interfailure time of empirical simulations. However, researching how the importance of one line depends on failures of other lines is beyond the scope of this thesis.

All simulations so far used the biased random method with parameter $\beta = 0.8$ to allow some randomness in the simulations. The remainder of this section will show the impact of β and discuss the importances measures to a greater extent. Concretely, we analyze the change in mean interfailure times when the bias parameter β is varied from .01 to 1. Recall that $\beta = 1$ is equivalent to uniform random sampling (regardless of the importance measure chosen) and $\beta \downarrow 0$ limits to deterministic selection. Plots of mean interfailure time verses β are presented in Figure 6.4. This figure shows the mean interdanger times for hundred simulations with bias to all importance measures, where the parameter β is gradually increased from 0.01 to 1. The shaded regions indicate a 95% confidence interval for the mean interdanger times. The confidence interval is smoothed by taking the 7-points moving average[21]. As mentioned in Section 4, the biased probabilities range from uniform random ($\beta = 1$) to deterministic ($\beta \downarrow 0$). Indeed, all figures show similar results for $\beta = 1$. Figure 6.4 reveals interesting insights, which will be discussed figure-by-figure.

(a) More bias with respect to edge degree actually makes the system more robust than uniform random failures. When only links with high edge degree are removed, less danger states are experienced. This implies that the links with high edge degree are in general not more important than other lines. We may conclude that edge degree is a bad importance measure in our model.

(b) Opposed to edge degree, node significance performs better when β is decreased. Apparently, links with high node significance are often involved in danger states and possibly cascading failures. High values for the parameter β significantly increase the probability that lower entries in the list $\bar{E}$ are selected for removal. For $\beta \geq .9$ one may observe that node significance bias is comparable to uniform random failures. It thus follows that only the links with highest node significance are actually important, and that links with moderate node significance (not on top of $\bar{E}$) are not necessarily important.

(c) The most fascinating figure. Edge betweenness shows the same behaviour as edge

[21] 7-Points moving average: Every data point is corrected to the mean of itself, the three preceding data points and the three following data points. This smoothens the original confidence intervals to damp the variability caused by relatively short simulation times.

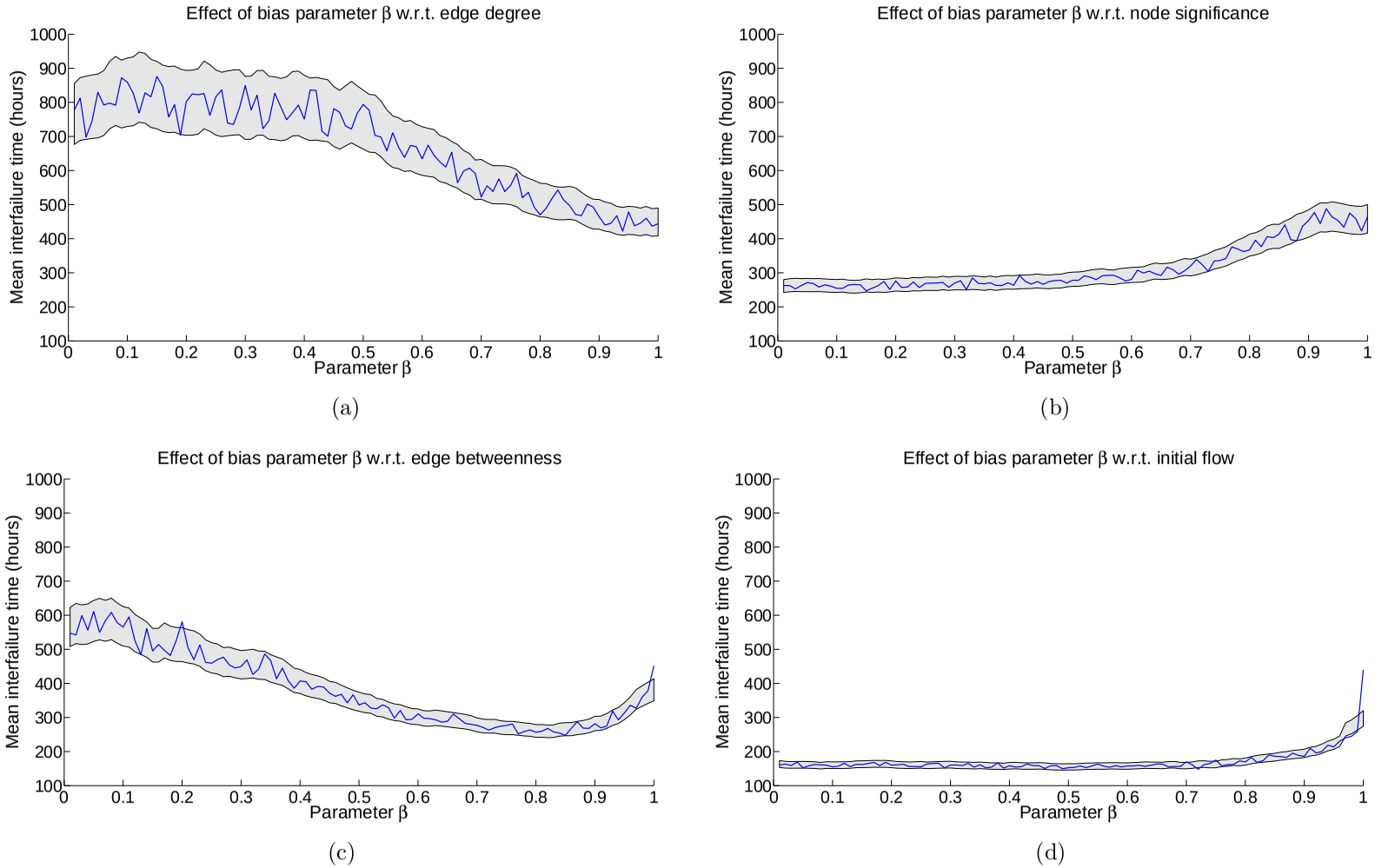

Figure 6.4: Effect of parameter β for biased probabilities on mean interdanger times. Results from 25 year simulations on the IEEE 118 bus network with bias for (a) edge degree, (b) node significance, (c) edge betweenness and (d) initial flow. The blue line is the mean of the exponential fit. The shaded regions indicate the 7-points moving average of the corresponding 95% confidence interval.

degree for lower values of β. However, as β goes from .5 to 1 the mean interdanger times actually drop below the uniform random performance at $\beta = 1$. One possible explanation for this behaviour is that links with high edge betweenness are not the most important links, but their failure is essential in triggering a cascade. Only when high edge betweenness links *and* more random lines are selected to trip, the mean interdanger time obtains its minimum value. In any case, this plot shows that there is a connection between edge betweenness bias and mean interdanger times that was not revealed in our earlier analysis.

(d) Clearly, initial flow performs best in indicating important lines for every value of the bias parameter β. However, recall that in this model line capacity is related to initial flow. Hence, care should be taken when generalizing these results.

Concluding, we have seen that node significance and initial flow are both good indicators of links that are often involved in danger states. Also, links with high edge betweenness are important in worsening the system state after an initial failure. They are less likely to initiating a danger state. Finally, edge degree is a bad measure for indicating important links. It would be interesting to do the same analysis for biased failures of generators and the combination of both. However, this is beyond the scope of this thesis.

6.3 Evaluation of islanding

In the previous section we found that initial flow is the best importance measure to indicate important links in our model. When these links are given a higher probability to fail the simulations show more consecutive failures than for simulations with bias to other importance measures. This observation is the motivation for our heuristic island design. The island design is heuristic as it does not compute the optimal island for every link but rather chooses the best island from a predefined set of islands. In order to save both computing time for island design and reaction time in case islanding is requested, we constructed a set of islands using the procedure below. This resulted in 11 islands for the IEEE 118 bus network. Every island has been designed as to isolate the most important line that was not yet in an other island. Hence, optimal islands are constructed for the most likely cascade triggers. Concretely, we constructed islands by the following steps:

Step 1. Start an empty island set.

Step 2. Pick the most important link $l = (i, j)$ with respect to initial flow that is not yet in an island.

Step 3. Solve the MILP formulation as described in Chapter 5 where the endpoints of l are forced in an island, e.g., $\sigma_i = 1$ and $\sigma_j = 1$. All other nodes are free, regardless of previous MILP solutions.

Step 4. Add this island and its solution value to the island set.

Step 5. If there are links that have not been assigned to at least one island, return to Step 2.

For any given single line failure, it is now possible to isolate the failure in an island. In particular, when the link is part of multiple islands one can implement the island with the lowest solution value. Recall that the solution value corresponds to a shift in flow (stability) and load shed, and that a lower solution value indicates a better island in the sense that has been described in Chapter 5. This heuristic approach is suboptimal in most cases, yet we hope that the focus on important lines makes the heuristic reasonably accurate. Comparison with actual computation of all islands (one for every initial failure) is outside the scope of this thesis.

It is hard to create a simulation that initiates islanding for several reasons. First, the model needs a way to determine the right moment to initiate islanding. Initiating islanding when this is not needed may yield undesired results both directly (load shed) and indirectly (synchronisation afterwards). Not initiating islanding when this would be helpful may result in a cascade throughout the entire network. Secondly, it is challenging to model the restoration process afterwards. When should this process be started? How much time is needed to synchronize the islands and what other complications may occur? Solving these issues is beyond the scope of this thesis and we thus chose for a different approach.

Consider the following three simulations:

- No islanding – Normal simulation without islanding.
- Timely islanding – If the first simulation experiences a cascading failure leading to a complete blackout, run the same simulation (same random seed). This time islanding is initiated right after the trigger event of the normal simulation.
- Initial islanding – The last simulation initiates islanding immediately at time $t = 0$. If the second simulation has been performed, the same islands are formed.

After the islanding set procedure has finished, the above three simulations are performed sequentially (simulation set). If more runs are requested, a new simulation set is performed using the same islanding set as before. Note that the islanding procedure is deterministic and as such will always yield the same results for a given importance measure. In all cases, generator output is assigned using (4.3), which implies that no care is taken for the generator limit (5.16) and generator outputs as proposed by the MILP solution. This is done to ensure compatibility with the non-islanding simulations.

Average results over 25 runs of the above simulation set with random line failures biased to any importance measure can be found in Figure 6.5. Comparing these results reveals information on the effect of islanding. First, Figure 6.5(a) shows the mean interfailure times. One can see that initial islanding will decrease system robustness in almost all cases. Thus, a big network is in general less vulnerable than several small islands. Of course, this is the very reason that the power grid has become the extensive network that it is today. Initial islanding only performs better when the most important lines fail often. Timely islanding outperforms the other islanding schemes in all but one case. For this exceptional case, no islanding sometimes resulted in a complete blackout (Figure 6.5(c)) where timely islanding was able to sustain. However, after timely islanding was performed the interdanger times reduced and consequently reduced the overall mean interdanger time. This observation also illustrates that the mean interdanger time plot can give a distorted view of actual performance and should be considered along with the other plots.

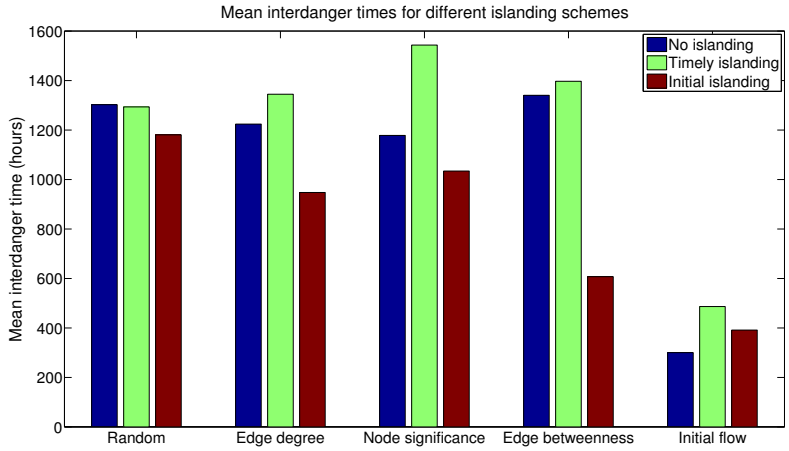

(a)

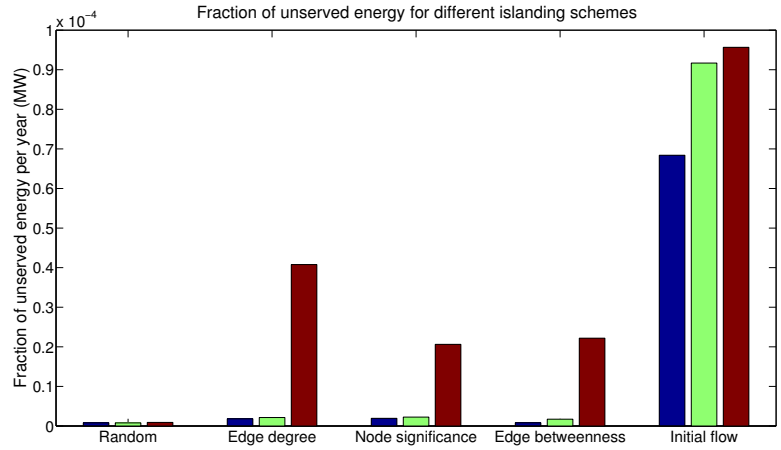

(b)

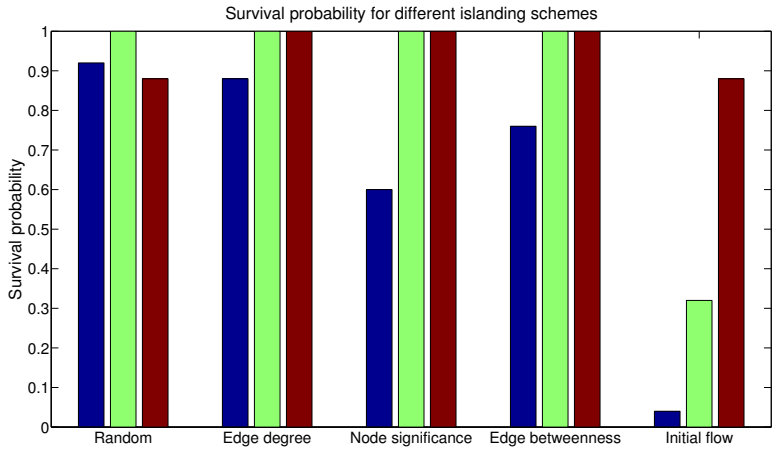

(c)

Figure 6.5: Effect of islanding on the IEEE 118 bus network. Results for 25 runs for every islanding scheme and every importance measure. Mean interdanger times are shown in (a), yearly fraction of unserved energy in (b) and survival probability in (c). Simulation time: 50 years for initial flow and 500 years for all others. 500 year simulation of initial flow shows the same results, but survival probability for non-initial islanding equals zero.

Figure 6.5(b) shows that initial islanding causes more load shed. This a direct consequence of the high frequency of danger states displayed in Figure 6.5(a) and again this is supported by the size of the real-life networks. Timely islanding shows the same qualitative behaviour for the more extreme line failure approaches, although the fraction of unserved energy is less than that of initial islanding. Both islanding methods perform worse than the simulations without islanding.

So far, initial islanding performs poorly and timely islanding shows little benefits. However, mean interdanger times and load shed are only monitored until a blackout. In particular, load shed during a blackout is not shown in Figure 6.5(b). Therefore the analysis should also consider Figure 6.5(c), which shows the fraction of times that a simulation terminated with a blackout. Here it is shown that initial islanding drastically increases the survival (non-blackout) probability for simulations with failure bias to important lines. Timely islanding also increases the survival probabilities, although it should be kept in mind that this is inevitable by the construction of timely islanding.

The analysis so far is based on the islands that were obtained by the islanding procedure described at the beginning of this section. Every island is forced to contain a certain link, namely the most important link that is not yet in an other island. Thus, the set of islands that is acquired in this manner clearly depends on the relative importance of links and hence the importance measure that is used. Therefore, we will briefly discuss the results of islanding simulations when islands are designed with respect to edge degree, node significance or edge betweenness. The analysis is based on figures similar to Figure 6.5.

Qualitatively, all results are very much like the initial flow case. The mean interdanger time of timely islanding is often better than that of no islanding and, apart from the initial flow biased random failures simulations, both perform better than initial islanding. Also, the amount of unserved energy is low in the no islanding and timely islanding schemes, whereas initial islanding shows relatively high amounts. All simulations with initial flow biased random failures show considerably more load shed than other biased and unbiased random failures regardless of the islanding scheme. Finally, the survival probabilities for both timely and initial islanding schemes are significantly higher than those of the no islanding scheme.

Considering the different aspects shown in Figure 6.5 and the remark on islanding with respect to other importance measures, we conclude the following: A large network is more robust than two (or more) smaller networks. Less danger states are observed and less load is shed. However, increased failure of important lines makes the network vulnerable to blackouts. Our results show that islanding can greatly reduce this effect when initiated just before a cascade propagates, that is, timely islanding.

6.4 Sensitivity analysis

The model presented in Chapter 4 relies on a lot of input variables. Many of these variables could be extracted from data, if appropriate data sets were available. However, by lack of these sets one can not be sure that the values that have been used for the input variables are correct. Moreover, the use of incorrect variables may result in inaccurate output of the model. This section will shortly discuss the sensitivity of the model to changes in

the input variables. Concretely, the effect of mean interfailure time (Λ_{FD}^{-1}), repair time, hidden failure probability and load shed will be analyzed. The fraction of unserved energy is discussed only if a clear trend is visible, since the precise values are fluctuating between computations.

Recall that the time between two consecutive random failures equals Λ_{FD}^{-1}, where Λ_{FD} is the failure density parameter used in the exponential distribution. In our model we have assumed that $\Lambda_{FD}^{-1} = 24 \cdot 7$ hours for both line failures and generator failures. Thus, on average one could expect a single line failure and a single generator failure in every week. For the sensitivity analysis, we decreased or increased Λ_{FD}^{-1} by 10 or 20% before running a 500 year simulation on the UCTE network with unbiased random line failures. Increasing Λ_{FD}^{-1} means that the mean interfailure time has increased and thus one would expect less dangerous situations. On the other hand, decreasing Λ_{FD}^{-1} effectively decreases the average time between consecutive failures and one may expect that the system is less robust. Our results indeed show that a change in Λ_{FD}^{-1} of $X\%$ causes a change of $1.5X\%$ in the mean interfailure time. Also, increasing Λ_{FD}^{-1} decreases the fraction of unserved energy and visa versa.

The same sensitivity analysis has been performed on the repair times. Repair times were decreased or increased by 10 or 20% before running simulations on the UCTE network. Opposed to change in mean interfailure times, one would now expect that a decrease of repair times has a positive effect on the mean interdanger time. An increase of repair times would keep the network insecure for a longer time and thus decrease the mean interdanger time. However, our results show that the repair time has a negligible effect on the mean interdanger time. This indicates that the repair time is too long to suppress follow-up failures and that small changes in the repair time can not overcome this problem. On the other hand, the fraction of unserved energy shows a decreasing trend for shorter repair times and an increasing trend for longer repair times. As discussed before, the values corresponding to unserved energy are fluctuating a lot and therefore only the qualitative behaviour is discussed.

Hidden failures in our model are induced by the tripping of a link. All links that share a node with the tripping link are subject to a hidden failure with probability 0.001. Instead, the hidden failure probability was increased to analyze the effect of hidden failures. Increasing the hidden failure probability to 0.005 and 0.01 decreased the mean interdanger time by 7 and 14% respectively. Decreasing the hidden failure probability to 0.0005 and 0.0001 increased the mean interdanger time by 1 and 3% respectively. This shows that hidden failures play a significant role in power grids when the hidden failure probability is increasing. Aging of equipment and reduction of maintenance budget may increase the hidden failure probability and therefore reduce the network reliability. The fraction of unserved energy showed no clear trends when the hidden failure probability was changed.

Finally, the effect of load shed schemes was analyzed. The presented model assumes three load shedding steps of 15, 15 and 20% respectively, as indicated by TenneT (Appendix B). Alternatively, smaller or bigger steps can be modeled to evaluate the effect of load shed schemes. A maximum load shed of 50% was achieved in uniform steps of 5, 10 or 25% at a time. That is, the 5% scheme would take at most 10 steps to shed maximum load whereas the 25% scheme would shed maximum load in at most two steps. Simulations with these changes showed that the mean interdanger times hardly changed and no clear trends in the fraction of unserved energy were observed.

The sensitivity analysis shows that the presented model is robust to variations in the input variables. Variations in the input variables result in expected behaviour of the output variables and the change in output variables is proportional to the change in input variables. We may therefore conclude that the output provides a solid basis for analysis on the model, as has been performed in this chapter.

Chapter 7

Conclusions and future research

7.1 Conclusions

The aim of this thesis was to understand the power grid and reduce the damage done by cascading failures. More precisely, we wanted to answer the primary research question:

> *How can the damage caused by cascading failures in a power grid be reduced by means of intentional islanding?*

Since this question could not be answered without further research, the following secondary research questions were answered first:

- *What is the power grid and how does it work?*
- *What kind of power grid models have been studied in literature?*
- *Can we propose a power grid model that is reasonably accurate and yet fast enough to run many simulations?*
- *How can we determine topological islands for a certain power grid that are optimal in some sense?*
- *Which transmission lines are most important to the power grid's robustness?*

Every chapter has been assigned to one of these questions and every question has been carefully examined. This section summarizes the considerations and concluding remarks for every question.

As seen in Chapter 2, the power grid is a complex network designed for transporting electrical energy from generators to consumers. Many physical aspects make this service non-trivial to say the least. Non-linear AC power flow dynamics, voltage angles between generators, active and reactive power and continuous shifts in demand and supply are just a handful of obstacles in power grid operation and management. This is even more difficult when components of the network fail due to any of the various possible causes. Although power grid operators try to respect the $N-1$ criterion in all cases, sometimes the grid can no longer do what it should. Protection mechanisms like relays have been installed to keep the power grid from damaging itself, cutting of power for many consumers in worst case. This motivates the scientific community to devote their research to power grids in order to understand and enhance its behaviour.

Many models for power grid and cascading failure simulation have been proposed in the literature. Ranging from purely topological, stochastic models to complex real-time physical models, there is a wide variety in physical accuracy and computational requirements. Models may simulate the overall dynamics to understand how the cascade propagates, or they may zoom into a specific component to understand how this component may contribute to a more reliable power grid. Analysing literature has provided a clear overview of the different modeling possibilities and their individual benefits and limitations.

Based on the literature review in Chapter 3, we proposed a model that includes many physical aspects in a very simplistic manner. The simplicity of the model allows relatively fast computation of the many different simulations that have been performed in this thesis. Including physical aspects made the model more realistic and – equally important – aimed to illustrate the complex nature of power grids. Running (physically) accurate simulations with all aspects that have been included in this model would require 1) more complex programming 2) stronger computational software and 3) better computer hardware than those used for this thesis. We believe that a good trade-off between performance and computational cost was achieved in the presented model of Chapter 4.

The presented model made use of a linear approximation of flow dynamics; the DC power flow equations. The linearity of these equations is exploited in the islanding problem that was faced. In Chapter 5 of this thesis a mixed integer linear programming (MILP) formulation is proposed to find 'optimal' islands. Optimal between quotation marks, since there are lots of issues for islanding and the 'optimal' island is a trade-off between these issues. The proposed MILP formulation allowed flexibility for the user to give priority to stability (expensive flow shift) or demand satisfaction (expensive load shed). Solutions of the MILP formulation show optimal islanding with a flow shift of 2.3% of total flow, a 1.5% load shed in the island and no load shed in the complement.

Surely, power grid operators aim to make the grid as reliable as possible to prevent cascades from happening. Essential information in this process is the relative importance of transmission lines; both for new investments as for cascade simulation. From the various importance measures that have been tested, we may conclude that purely topological measures do not cover the importance of a link.

Physical aspects are essential in valuing transmission lines. Although the results suggest that initial flow is the best tested importance measure, one should be careful when stating conclusions on this. We are well aware of the fact that in our model, initial flow is directly related to capacity and indirectly related to generator locations and generator output via DC power flow equations. That is, topological aspects have implicitly affected initial load and therefore capacity. Concluding that topological aspects are not relevant is therefore not justified, and some of the suggestions in the next section aim to reduce this bias. Also, initial flow is something unrealistic for real power networks. Power flows adapt continuously as demand changes over time (hourly, daily, summer/winter) and initial flow has no meaning. Alternatively one could suggest that transmission lines with high *average* flow are important lines.

Another indication that physical and topological properties are both important is the second placed importance measure: node significance. Node significance performed surprisingly well, taking into account that the original node significance was not designed as an importance measure. Especially the effect of the bias parameter β demonstrated

that node significance is comparable to initial flow. Finally, edge betweenness showed very interesting results. It made clear that the links with high edge betweenness do not necessarily initiate cascades, but that they are important in the follow-up failures. This is a strong indicator that high edge betweenness links play a major role in neutralizing disturbances.

Using both the MILP formulation for islanding and simulating severe grid conditions with the biased random failures, we were able to analyze the effects of islanding. Specifically, we compared the situations without islanding, with timely islanding[22] and with islanding from the start. This crude comparison gave intuitive results on islanding:

- Under normal (non-severe) conditions, the big network always outperforms islanded networks. Sharing generation facilities that are interconnected via a network of transmission lines minimizes load shed throughout the year, and less dangerous situations are encountered.
- Under severe conditions, islanding (both timely and initially) outperforms non-islanding. The islands are more robust, as their individual problems are not spread over the network. Less dangerous situations are experienced and load shed is reduced.
- Restricting islanding to times where there is a high probability of a cascading failure is a desirable alternative. It combines the benefits of a large interconnected network and the robustness of smaller islands.

However, deciding whether islanding is needed and if so, determining the optimal timing are complex problems on their own. This remark and more thoughts on future research will be discussed in the next section.

7.2 Future research

Getting into power grid literature, talking to professionals in the field and working on a new model has provided a lot of insight. This section will summarize some of these insights so that the reader may get a better idea of challenges in power grid modeling and possibly see interesting directions for his or her own research. Insights have been listed in three categories: Accurate modeling, Flexible protection mechanisms, and Other.

Accurate modeling:

- Data availability – As has been mentioned in Chapter 4, power grid modeling in general faces a shortage of relevant data. Availability of this data would make models more accurate and results could be verified. Also, this would encourage closer cooperation between researchers and industry experts.
- AC power flows – Modeling with AC power flows has two major benefits over DC power flows. First, the power flows are far more accurate. Second, voltage and

[22] Here, timely islanding refers to islanding that is initiated at a trigger event that is known to cause a cascade a priori. For a more detailed explanation, see Section 6.3.

frequency profile and reactive power flows are considered as well. This additional information can be used for realistic relay and generator protection device modeling. Approximations of the AC power flows (e.g. the ones proposed in [21] and [66]) that consider the same aspects as the real AC power flows can also be used to save computational costs.

- Fluctuating demand – Demand is continuously changing. Modeling this behaviour makes the model more realistic, although this may not be particular useful for the current research question. The model in this thesis is testing the grid under severe circumstances to analyze the benefits of islanding in general. It shows *what islanding can do in worst-case scenarios*. Fluctuating demand is more realistic but it also makes that islanding may be less beneficent. For example, demand is low in the middle of the night. This makes cascading failures less probable and there is less need for islanding. This raises a new question, namely *whether to initiate islanding at a given moment*. Fluctuating demand is useful in researching this question rather than our own research question. Timing of islanding is discussed by [1]. The article by Aponte and Nelson [3] does similar research on time optimal load shedding after islanding.

- Shifting generation – Instead of assuming that all generators give equal weighted output, it is more realistic to allow deviations from this output as done by Anghel et al. [2] and Carreras et al. [17]. This is a better simulation of the market/auction process in power generation. Furthermore, the changing flows are more representative of the conditions that transmission lines are subject to. Incorporating this with AC power flows is challenging, since the shift in generation has to be modeled carefully to keep the system stable. Of course, shifting generation is also coupled to varying demand.

Flexible protection mechanisms:

- Operator interaction – Instead of performing load shed when this is inevitable, operators may decide to shed load earlier to prevent possible worse outcomes. Also, overloaded lines could intentionally be taken out-of-service when this is preferred and islanding could be initiated manually. Implementing operator interaction in a stochastic manner (as done in Anghel et al. [2]) makes the model more realistic and also provides new model aspects to research.

- Islanding with AC power flows – Our MILP formulation made use of DC power flow equations to predict the post-islanding power flows. The same is done by Trodden et al. [78], who compared the predicted power flows for the islands with their actual AC power flow solutions. Their results indicated a limited ability of the DC-based MILP formulation to predict the AC islanding solutions. Therefore, it would be interesting to formulate a MILP that incorporates a linear approximation of the AC power flows (e.g. the approximation byCoffrin and Van Hentenryck [21]). Alternatively a completely different non-linear optimization problem could be formulated. For example, [1] and [83] use AC power flow properties in their island design through slow coherency theory.

- Combine islands in the restoration process – Islanding may follow from a cascading failure or it may be initiated intentionally to protect the power grid. In both cases, individual islands have been formed and generators in different islands are probably

out of synchronism. The generators have to be synchronized again in order to combine the various islands and restore the power grid. Also, other restoration problems may be at hand. Incorporating island synchronization in the model requires more literature research, and modeling with AC power flows. The author is not familiar with these kind of papers.

Other:

- Biased random generator failures – All non-stability failures for generators were uniformly random and no attention was paid to the important generators. It may be interesting to perform an importance analysis – similar to the analysis on links in this thesis – to determine generator importances. After this it would also be possible to perform a combined link/generator importance analysis to discover the interaction between the two.
- Random failures with memory – In our model, all importance measures were evaluated once at the start of a simulation. However, as the network topology changes it may be valuable to update the link importances accordingly. One could even introduce importance measures with memory or measures that depend on the current network state. For example, some measure could assign a higher probability to trip link i in system state A than in system state B.
- Empirical importance – The results of the simulations with empirical bias were disappointing. Its performance can probably be enhanced, e.g. by allowing the memory aspect described above.
- Relation flow shift versus stability issues – More research on stability issues and flow shift can be used to improve the MILP cost function. Possibly another cost function is more representative for stability issues, or maybe a good indication of the costs A and B in the MILP can be found.

This extensive chapter on future research shows that there are many, many things to do. The proposed model is relatively simple, yet it already shows some of the complexity of power grid modeling. Even though this thesis is completed the work is not finished. We hope that the presented work gives the reader a better idea about the power grid and that it may serve as motivation to continue research on this subject.

Appendix A

PTDF update method

A.1 Notation

Before introducing the PTDF matrix and LODF vector, we list a few notations that will be used throughout this appendix. Readers who are familiar to the Matlab software should have no problems with the notations.

First, a logical vector can be used as index for a vector or matrix. Let A be an arbitrary $m \times n$ matrix and I_1, I_2 be logical vectors (entries 0 and 1) of lengths m and n, respectively. We define $A(I_1, I_2)$ as the submatrix of A whose entries are given by the intersection of rows indicated by I_1 and columns indicated by I_2. For example, let

$$A = \begin{bmatrix} 1 & 2 \\ 3 & 4 \\ 5 & 6 \end{bmatrix}, I_1 = \begin{bmatrix} 1 \\ 0 \\ 1 \end{bmatrix} \text{ and } I_2 = \begin{bmatrix} 1 \\ 1 \end{bmatrix}.$$

Then $A(I_1, I_2)$ denotes the submatrix of A that is the intersection of rows 1 and 3 and columns 1 and 2, e.g.

$$A(I_1, I_2) = \begin{bmatrix} 1 & 2 \\ 5 & 6 \end{bmatrix}.$$

Instead of using a vector of ones of appropriate length we will use a colon (:) to imply that all rows or columns are requested, e.g., $A(I_1, :) = A(I_1, I_2)$. The $\neg$ symbol is used as the logical operator 'not', e.g., $\neg I_1 = \neg[1, 0, 1] = [0, 1, 0]$. Thus,

$$A(\neg I_1, :) = A(\neg I_1, I_2) = \begin{bmatrix} 3 & 4 \end{bmatrix}.$$

When a logical vector is used to state the size of a matrix, we refer to the number of ones in the vector. For instance, a matrix of size $(I_1 \times I_2)$ is a matrix with $\mathbf{1} \cdot I_1 = 1 + 0 + 1 = 2$ rows and $\mathbf{1} \cdot I_2 = 1 + 1 = 2$ columns. This is in agreement with the size of $A(I_1, I_2)$.

There are two reasons to use this notation. First, this notation provides an easy way to keep overview of the various matrix-matrix multiplications that will be encountered in this appendix. Many of those multiplications remove some rows or columns from another matrix. When some of these matrix-matrix multiplications are written down, it is easy to forget the essence of the manipulation. By writing the outcome in the Matlab notation, it is easier to see and understand what has been done. Second, the Matlab notation is also used in the actual programming. Instead of programming several matrix-matrix multiplications, one can just remove some rows or columns from the original matrix. This latter method is computationally cheaper than the former method. Similarly, it is (in general) cheaper to find the inverse of a small matrix rather than the inverse of a large

matrix. It is important to understand these statements, because the benefits of the update method that will be presented relies on this kind of argumentation.

A.2 Introduction

Power Transfer Distribution Factors (PTDFs) are a useful tool in sensibility analysis of power systems. They are derived from the DC power flow equations and are stored in the PTDF matrix H. The PTDF matrix is dependent on the so-called slack node, which can be any node in the network. Entry h_{li} of the PTDF matrix is interpreted as follows: when one unit of energy is injected in node i and rejected at the slack node, the change in link l is h_{li}. This implies that the change in link l for an injection of a units in node i and a rejection in node j is given by $a \cdot (h_{li} - h_{lj})$. An example is given in Figure A.1. Given the PTDF matrix for a slack node s, it is possible to convert this matrix to the PTDF matrix for another slack node s_{new} by subtracting the PTDF column corresponding to s_{new} from all columns of the PTDF matrix.

Another tool that has been mentioned in Section 4.2 are Line Outage Distribution Factors (LODFs). The LODF vector corresponding to link $l = (i, j)$ shows the change in all links when link l is removed. Note that l is directed, but that negative flow f_l is possible. This corresponds to positive flow from j to i. For such a link l, the LODF vector can be computed directly from the PTDF matrix:

$$LODF_{l=(i,j)} = \frac{f_l}{1 - (h_{li} - h_{lj})}(H(:, i) - H(:, j)). \tag{A.1}$$

This can be interpreted as follows. Before removing link l, there is a flow of $f_{other} + f_l$ from node i to j, where f_{other} represents the total flow from non-l links from i to j. We basically want to find an injection (rejection) a for node i (j) such that the flow f_l is carried by other links in the network, i.e. $f^{new}_{other} = f_{other} + f_l$. Link l can then be removed, resulting in the same amount of flow from i to j as before the injection and removal. By definition of the PTDF matrix, an injection of one unit of flow in i and an equal rejection at j results in an transportation shift of $h_{li} - h_{lj}$ units of flow over l. Thus, $1 - (h_{li} - h_{lj})$ units of flow are transported over all other links. It follows that an injection (rejection) or $a = f_l/(1 - (h_{li} - h_{lj}))$ units at i (j) results in a shift of f_l over all non-l links, explaining the factor in (A.1). The vector $H(:, i) - H(:, j)$ translates this factor to the individual links, according to their PTDF values for transport from i to j. For a given initial flow F, the flow F_{new} after removal of link l equals $F_{new} = F + LODF_{l=(i,j)}$, where the rows corresponding to link l have been removed.

The model that has been described in this thesis is not the first model that the author worked on. An earlier model was studied to some extent before we decided to create a new model. The algorithm corresponding to this first model computed the PTDF matrix of the given network for hundreds or thousands of iterations. Calculating the PTDF matrix over and over again caused a major problem in the computation speed. However, every iteration altered the network only slightly and we were able to update the PTDF matrix every iteration instead of computing it from scratch. In particular, every iteration removed one node k and all links adjacent to k. The outline of the algorithm that updates the PTDF matrix for this change is given below:

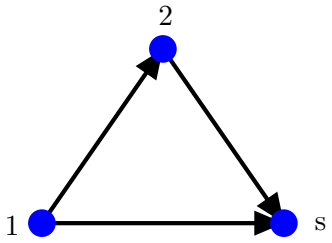

(a) Network

	node 1	node 2	node s
link $(1, s)$	$2/3$	$1/3$	0
link $(1, 2)$	$1/3$	$-1/3$	0
link $(2, s)$	$1/3$	$2/3$	0

(b) PTDF matrix

Figure A.1: Example of PTDF matrix. The rows correspond to links in the network, the columns to the nodes. In this example, all link susceptances (related to resistance) are assumed identical. From the PTDF matrix it can be seen that an injection of one unit of flow in node 1 and an equal rejection at the slack node s is transported directly for $2/3$ and the remaining $1/3$ via node 2. This makes sense, because links $(1, 2)$ and $(2, s)$ have a combined susceptance that is twice the susceptance of link $(1, s)$. Also, transporting 5 additional units of flow from node 2 (injection) to 1 (rejection) changes the flow in link $(1, 2)$ by $5 \cdot (-1/3 - 1/3) = -10/3$, the flow in link $(2, s)$ by $5 \cdot (2/3 - 1/3) = 5/3$ and the flow in link $(1, s)$ by $5 \cdot (1/3 - 2/3) = -5/3$. Thus, most energy is send directly from node 2 to node 1 and some energy is sent via node s.

- Determine islands that will be formed by removing k. With islands we refer to connected components of maximal size, i.e., no other node from the network can be added such that the component is still connected.
- Update PTDF by removing as many links adjacent to k as possible without disconnecting the network. This computation is difficult.
- Special update of PTDF for removing the other links. Islands will be formed in this step. This computation is easy.
- Extract PTDF sub-matrices for islands formed. Those matrices are correct PTDF matrices for the new islands and every island has a known slack node.

This process is illustrated in Figures A.2-A.4. Recall that the graph is originally undirected and that arbitrary link directions are assigned to indicate the direction of flow. Negative flow is also possible, indicating flow in the reverse direction. In the remainder of this chapter we assume – without loss of generality – that all links are directed to the slack node when this makes sense (links adjacent to k in Figures A.2-A.4). Directions of all other links are not important. This assumption ensures that all PTDF entries corresponding to links adjacent to k have non-negative values; reversing their orientation will also change the sign.

The main theorem and a detailed theoretical construction of the update are described in Section A.3. Section A.4 shows that the update only (and always) works by removing the links in two steps as described above. Experimental comparison with direct PTDF computations are presented in Section A.5.

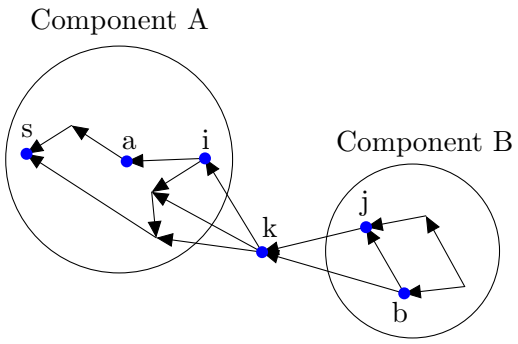

(a) Network before removal of links

Component	A			k	B	
	s		i	k	j	
$A \to A$	0	XXX	X	X	X	XXX
	0	XXX	X	X	X	XXX
	0	XXX	X	X	X	XXX
$k \to i$	0	XXX	X	X	X	XXX
$k \to A/\{i\}$	0	XXX	X	X	X	XXX
$j \to k$	0	0 0 0	0	0	X	XXX
$B/\{j\} \to k$	0	0 0 0	0	0	X	XXX
$B \to B$	0	0 0 0	0	0	X	XXX
	0	0 0 0	0	0	X	XXX
	0	0 0 0	0	0	X	XXX

(b) PTDF matrix

Figure A.2: Initial network topology. Many connections to node k, which will be removed later. Links $A \to B$ refer to all links from nodes in A to nodes in B, e.g., $i \to a \in A \to A$ and $b \to k \in B/\{j\} \to k$. $X \in [-1, 1]$ values in the PTDF matrix correspond to flows whose exact values are not relevant. This PTDF matrix shows that flow from nodes in B to s is possible along multiple paths and no line is essential, e.g., no single line is on every path. This follows from the fact that there are no 1-valued entries h_{ij} in the PTDF matrix, which would indicate that link i is on every path from node j to slack node s.

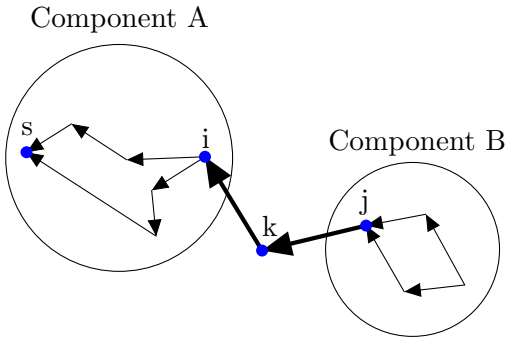

(a) Network after first removal of links

Component	A			k	B	
	s		i	k	j	
$A \to A$	0	XXX	X	X	X	XXX
	0	XXX	X	X	X	XXX
	0	XXX	X	X	X	XXX
$k \to i$	0	0 0 0	0	1	1	1 1 1
$j \to k$	0	0 0 0	0	0	1	1 1 1
$B \to B$	0	0 0 0	0	0	0	XXX
	0	0 0 0	0	0	0	XXX
	0	0 0 0	0	0	0	XXX

(b) PTDF matrix

Figure A.3: The maximum number of links has been removed such that network is still connected and PTDF matrix is updated. This update requires most of the work. Only one connection from each component to node k is still in the network. The PTDF matrix shows that flow from B to s is only possible via (j, k) and (k, i), since those entries equal one. Note that column j has only zeros in rows $B \to B$ because power in j can only reach s via links that are not in $B \to B$.

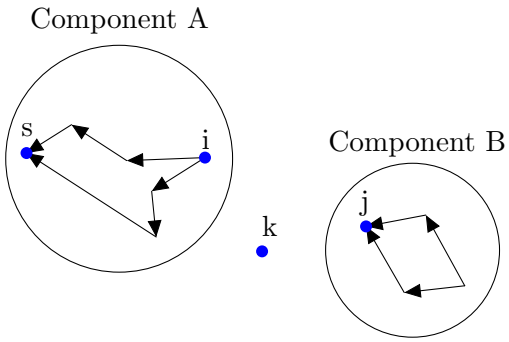

(a) Network after second removal of links

Component	A				k	B			
	s			i	k	j			
$A \to A$	0	X	X	X	0	0	0	0	0
	0	X	X	X	0	0	0	0	0
	0	X	X	X	0	0	0	0	0
$k \to i$	0	0	0	0	0	0	0	0	0
$j \to k$	0	0	0	0	0	0	0	0	0
$B \to B$	0	0	0	0	0	0	X	X	X
	0	0	0	0	0	0	X	X	X
	0	0	0	0	0	0	X	X	X

(b) PTDF matrix

Figure A.4: All links adjacent to k have been removed and the PTDF matrix is updated. This simple update replaces the upper-right blocks by the zero-filled matrix. The PTDF matrix shows some different components, all of which have a slack node. In particular, the last node that was connected to k from component B, node j, is now the slack node of component B. Node s is still the slack node of component A and node k is the slack node of the single-node component k.

A.3 Basic approach

The PTDF matrix H is computed in a few steps. These steps have been described by Zimmerman et al. [86] and are directly taken from the algorithms in their Matlab package Matpower. Also, the matrix names used in this appendix have been adopted from the algorithms. We will go through these steps and, given the node and lines that are to be removed from the network, present a method that updates the PTDF matrix. An overview of symbols in this appendix is given in Table A.1.

Ultimately, we want to solve

$$H(:, noslack) = Bf(:, noref) \cdot Bbus(noslack, noref)^{-1}.$$

as cheap as possible. Here, *noslack* (*noref*) is the logical vector where the slack node (reference node) entry equals zero and all other entries equal one. Recall that the slack node is the node where power is rejected. The reference node is more technical of nature; it is the node where the voltage angle equals zero. Both the slack node and the reference node are not special nodes in the network; the reason that they are included in the calculations is to ensure non-singularity of the matrix *Bbus*. This non-singularity will be proven in Section A.4. The slack node and reference node can be chosen arbitrarily. In particular, one may initialize them as the same node.

Theorem 1. *Let the previous PTDF matrix H_{old}, the slack vector noslack, the reference vector $noref$ and the indicator of removed links rl be given for a power system. Let Cft_{old} be the link-node incidence matrix of the power system topology before removal of the links rl. If the removal of links rl does not disconnect the network, then the new PTDF matrix H_{new} is given by*

$$\begin{aligned} H_{new}(:, noslack) = H_{old}(\neg rl, noslack) \cdot \\ \left\{ I_{noslack} + Cft_{old}(rl, noslack)^T \cdot \right. \\ \left[I_{rl} - H_{old}(rl, noslack) \cdot Cft_{old}(rl, noslack)^T \right]^{-1} \\ \left. \cdot H_{old}(rl, noslack) \right\}, \end{aligned} \quad \text{(A.2)}$$

and the inverse of the term between square brackets exists.

Proof. The proof is given in the remainder of Section A.3 (construction) and Section A.4 (invertibility) and uses Theorem 2, which is part of the latter section. □

Theorem 2. *Let A be an irreducible, diagonally dominant[23] $n \times n$ matrix. Let B_{ij} denote the $(n-1) \times (n-1)$ submatrix that is obtained from A by deleting the i-th row and j-th column. Then for any $i \in \{1, \ldots, n\}$ the submatrix B_{ii} is invertible. Moreover, if A is symmetric and has a strictly positive diagonal, then for any two row indices $i, j \in \{1, \ldots, n\}$ that correspond to rows with non-positive off-diagonal elements the submatrix B_{ij} is invertible.*

Proof. The proof is given in Subsection A.4.1 for the matrix *Bbus* which satisfies all properties that are listed in the theorem. It actually satisfies stronger properties (listed in the remark below), but the proof in Subsection A.4.1 does not rely on those properties. □

[23] See Definition 1 on page 77.

nb	Number of nodes. (scalar)
nl	Number of links. In the update method, nl is the number of links in the previous (old) iteration. (scalar)
rl	Indicator of links that were removed in the previous iteration. Entry equals one if the corresponding link is removed and zero else. ($nl \times 1$ logical vector)
$D_{\neg rl}$	Indicator matrix of non-removed links. Diagonal matrix with $\neg rl$ as its diagonal. Equals $T_{\neg rl}^T \cdot T_{\neg rl}$. ($nl \times nl$ matrix)
$T_{\neg rl}$	Transformation matrix for non-removed links. If I_{nl} is the $nl \times nl$ identity matrix, then $T_{\neg rl} = I_{nb}(\neg rl, :)$. ($(nl - rl) \times nl$ matrix)
$noslack$	Indicator of nodes that are not the slack node. ($(nb - 1) \times 1$ logical vector)
$T_{noslack}$	Transformation matrix for non-slack nodes. If I_{nb} is the $nb \times nb$ identity matrix, then $T_{noslack} = I_{nb}(:, noslack)$. ($nb \times (nb - 1)$ matrix)
$noref$	Indicator of nodes that are not the reference node. ($(nb - 1) \times 1$ logical vector)
T_{noref}	Transformation matrix for non-reference nodes. If I_{nb} is the $nb \times nb$ identity matrix, then $T_{noref} = I_{nb}(:, noref)$. ($nb \times (nb - 1)$ matrix)
I_{rl}	Let k be the number of removed links. Then $k = \mathbf{1} \cdot rl$ and I_{rl} is the $k \times k$ identity matrix.

Table A.1: List of symbols. Basically, if some matrix A is multiplied by $D_{...}$ then all entries in A that belonged to 'wrong' nodes or links are set to zero, e.g., $A \cdot D_{\neg rb}$ replaces the columns of A that correspond to removed nodes by zero-filled columns. $T_{...}$ does not replace rows/columns but rather removes them from A, e.g., $T_{\neg rb} \cdot A$ removes the columns of A that correspond to removed nodes.

Remark: The following statement follows directly from Theorem 2, but is slightly weaker. Let A be an irreducible, symmetric $n \times n$ matrix. If additionally (1) all diagonal elements are strictly positive, (2) all off-diagonal elements are non-positive and (3) all rows have a zero sum, then any $(n - 1) \times (n - 1)$ submatrix of A is invertible.

The formulation of Theorem 1 doesn't look very attractive. However, note that the terms with rl are computationally very easy since they remove a lot of rows. Also, the matrix Cft_{old} has only two non-zeros in every row. Nevertheless, the most important feature is the inverse matrix computation. A direct calculation of the PTDF matrix requires inverting a $nb \times nb$ matrix – i.e. 1254×1254 for the UCTE network – which takes a lot of time. In our update, we only invert a $rl \times rl$ matrix – generally not larger than 10×10 – which is quickly done. It is this feature that reduces computing time significantly.

We will now go through the proof of Theorem 1 in steps parallel to the Matpower algorithm. First, the vector b and incidence matrix Cft are introduced. Both are needed in the construction of Bf and $Bbus$, which is the second step. Thirdly, the construction of H is presented. Variables with the subscript old and new will always refer to the corresponding variables in the previous and current iteration, respectively. Always keep

in mind that the goal is to minimize the computational cost, which can be achieved by inverting only small matrices.

A.3.1 Preparations

1. The first step is the computation of the tap ratio vector b ($nl \times 1$ vector). The exact definition of the vector is not relevant here; it suffices to know that b accounts for the link susceptances of the active links. Link susceptances are are also found the DC power flow equations as explained in Section 4.2.

   As the link susceptances are constant, the values in b for each link do not change during or between iterations. However, all links that were removed in the last iteration will not appear in the new b. It follows that

   $$b_{new} = T_{\neg rl} \cdot b_{old},$$

   which can be presented in Matlab notation as

   $$b_{new} = b_{old}(\neg rl). \tag{A.3}$$

2. In the second step of the algorithm, the incidence matrix Cft ($nl \times nb$ matrix) of the network is determined. For each row i there are exactly two non-zero entries that correspond to link i. If u and v are respectively the tail and head of link i, then $Cft(i,u) = 1$, $Cft(i,v) = -1$ and $Cft(i,w) = 0$ for all $w \neq u, v$. Alternatively one could say that for every column v, corresponding to node v, all incoming and outgoing links are indicated with -1 and +1 respectively[24].

   The incidence matrix update Cft_{new} can now be constructed from Cft_{old} by removing all lines indicated by rl:

   $$Cft_{new} = T_{\neg rl} \cdot Cft_{old},$$

   or

   $$Cft_{new} = Cft_{old}(\neg rl, :). \tag{A.4}$$

3. In this step, the algorithm constructs the matrix Bf ($nl \times nb$ matrix) that is related to branch power injections. It is almost the same as Cft, but instead of indicating links Bf indicates the b-value corresponding to the links. If u and v are respectively the tail and head of link i, then $Bf(i,u) = b(i)$, $Bf(i,v) = -b(i)$ and $Bf(i,w) = 0$ for all $w \neq u, v$. It can be seen that row i of Bf equals row i of Cft times $b(i)$, i.e. $Bf(i,:) = b(i) \cdot Cft(i,:)$.

   The update for Bf requires the same correction as Cft:

   $$Bf_{new} = T_{\neg rl} Bf_{old}.$$

   or

   $$Bf_{new} = Bf_{old}(\neg rl, :). \tag{A.5}$$

   Note that the aforementioned relation $Bf_{new}(i,:) = b_{new}(i) \cdot Cft_{new}(i,:)$ still holds after the update.

[24] Recall that the network is undirected of nature and that a direction is only needed to correctly indicate flows.

4. We will now consider the last matrix that is computed in the algorithm before the PTDF matrix. The update for the matrix $Bbus = Cft^T \cdot Bf$ ($nb \times nb$ matrix) can be determined directly from the previous updates:

$$\begin{aligned} Bbus_{new} &= Cft_{new}^T \cdot Bf_{new} \\ &= Cft_{old}^T \cdot T_{\neg rl}^T \cdot T_{\neg rl} \cdot Bf_{old}. \end{aligned} \tag{A.6}$$

   One may check that $T_{\neg rl}^T \cdot T_{\neg rl}$ equals the $nl \times nl$ diagonal matrix with diagonal $\neg rl$; $D_{\neg rl}$. Substituting this into the equality above yields

$$\begin{aligned} Bbus_{new} &= Cft_{old}^T \cdot D_{\neg rl} \cdot Bf_{old} \\ &= Cft_{old}^T \cdot [I_{nl} - D_{rl}] \cdot Bf_{old} \\ &= Cft_{old}^T \cdot Bf_{old} - Cft_{old}^T \cdot D_{rl} \cdot Bf_{old} \\ &= Bbus_{old} - Cft_{old}^T \cdot D_{rl} \cdot Bf_{old}. \end{aligned}$$

   Using the relation $D_{rl} = T_{rl}^T \cdot T_{rl}$ gives

$$Bbus_{new} = Bbus_{old} - \left(T_{rl} \cdot Cft_{old}\right)^T \cdot \left(T_{rl} \cdot Bf_{old}\right), \tag{A.7}$$

   which can be written as

$$Bbus_{new} = Bbus_{old} - Cft_{old}(rl,:)^T \cdot Bf_{old}(rl,:) \tag{A.8}$$

   in the Matlab representation. This is a good point to take a moment and reconsider the Matlab notation. Equation (A.7) is long and not easy to read. It involves three matrix-matrix multiplications and on first sight it is more troublesome than the starting equation (A.6). However, equation (A.8) shows that two of the multiplications are actually a removal of rows. This offers two insights. First, (A.8) shows that $Bbus_{new}$ equals $Bbus_{old}$ with a correction that depends exclusively on the removed links. Second, it shows that not three matrix-matrix multiplications have to be computed but rather one matrix-matrix multiplication of two relatively small matrices. Computationally, this may be far more efficient than direct computation of (A.6).

5. The PTDF matrix H ($nl \times nb$ matrix) can now be found by solving

$$H_{new} \cdot T_{noslack} = Bf_{new} \cdot T_{noref} \cdot \left(T_{noslack}^T \cdot Bbus_{new} \cdot T_{noref}\right)^{-1}, \tag{A.9}$$

   or in alternative notation,

$$H_{new}(:, noslack) = Bf_{new}(:, noref) \cdot Bbus_{new}(noslack, noref)^{-1}. \tag{A.10}$$

   The slack and reference buses have been explained at the beginning of the chapter. For this update method it is required that the slack node (reference node) in both the previous and current iteration is the same. Also, it is important that the slack and reference node have not been removed in the previous iteration. Invertibility of $Bbus$ is discussed in Section A.4. Finally note that (A.9) is also correct for H_{old}, i.e. when all subscripts *new* are replaced by *old*.

   Instead of analyzing H directly in a chaos of matrix manipulations and substitutions, we will perform a number of manipulations on beforehand and put them together in the end. First, we are interested in the inverse of $T_{noslack}^T \cdot Bbus_{new} \cdot T_{noref}$. Existence of this inverse is proven in Section A.4. The inverse can be found using the following theorem:

Theorem 3. ***(Woodbury Matrix Identity)***
Let A be an invertible $n \times n$ matrix and let U, C, V be $n \times k, k \times k$ and $k \times n$ matrices, respectively. The inverse of $A + UCV$ exists if C and $C^{-1} + VA^{-1}U$ are invertible, and it is given by

$$(A + UCV)^{-1} = A^{-1} - A^{-1}U\left[C^{-1} + VA^{-1}U\right]^{-1} VA^{-1}$$

Proof. The theorem will be proven by direct substitution.

$$\begin{aligned}
&(A + UCV)\left(A^{-1} - A^{-1}U\left[C^{-1} + VA^{-1}U\right]^{-1} VA^{-1}\right) \\
&\qquad = I + UCVA^{-1} - (A + UCV)A^{-1}U\left[C^{-1} + VA^{-1}U\right]^{-1} VA^{-1} \\
&\qquad = I + UCVA^{-1} - \left(U + UCVA^{-1}U\right)\left[C^{-1} + VA^{-1}U\right]^{-1} VA^{-1} \\
&\qquad = I + UCVA^{-1} - UC\left(C^{-1} + VA^{-1}U\right)\left[C^{-1} + VA^{-1}U\right]^{-1} VA^{-1} \\
&\qquad = I + UCVA^{-1} - UCVA^{-1} = I,
\end{aligned}$$

and

$$\begin{aligned}
&\left(A^{-1} - A^{-1}U\ \left[C^{-1} + VA^{-1}U\right]^{-1} VA^{-1}\right)(A + UCV) \\
&\qquad = I + A^{-1}UCV - A^{-1}U\left[C^{-1} + VA^{-1}U\right]^{-1} VA^{-1}(A + UCV) \\
&\qquad = I + A^{-1}UCV - A^{-1}U\left[C^{-1} + VA^{-1}U\right]^{-1}\left(V + VA^{-1}UCV\right) \\
&\qquad = I + A^{-1}UCV - A^{-1}U\left[C^{-1} + VA^{-1}U\right]^{-1}\left(C^{-1} + VA^{-1}U\right)CV \\
&\qquad = I + A^{-1}UCV - A^{-1}UCV = I.
\end{aligned}$$

This completes the proof. □

The Woodbury Matrix Identity is very useful in matrix update methods like the one that is presented here. For notational convenience, define

$$T_s^T := T_{noslack}^T, B_o := Bbus_{old} \text{ and } T_r := T_{noref}. \tag{A.11}$$

Rewriting (A.8) with this identity and the above theorem yields

$$\begin{aligned}
&\left(T_{noslack}^T \cdot Bbus_{new} \cdot T_{noref}\right)^{-1} \\
&\qquad = \left\{T_s^T B_o T_r - T_s^T \cdot Cft_{old}(rl,:)^T \cdot Bf_{old}(rl,:) \cdot T_r\right\}^{-1} \\
&\qquad = \left(T_s^T B_o T_r\right)^{-1} + \left(T_s^T B_o T_r\right)^{-1} \cdot T_s^T \cdot Cft_{old}(rl,:)^T \cdot \\
&\qquad\qquad \left[I_{rl} - Bf_{old}(rl,:) \cdot T_r \cdot \left(T_s^T B_o T_r\right)^{-1} \cdot T_s^T \cdot Cft_{old}(rl,:)^T\right]^{-1} \\
&\qquad\qquad\qquad \cdot Bf_{old}(rl,:) \cdot T_r \cdot \left(T_s^T B_o T_r\right)^{-1},
\end{aligned} \tag{A.12}$$

provided that $T_s^T B_o T_r$ and the term between square brackets are invertible. This will be proven in the next section, for now assume that they are. Substituting this expression and (A.5) into (A.9) gives

$$\begin{aligned}
H_{new} \cdot T_{noslack} = T_{\neg rl} \cdot Bf_{old} \cdot T_r \cdot &\left(T_s^T B_o T_r\right)^{-1} \\
&\left\{I_{noslack} + T_s^T \cdot Cft_{old}(rl,:)^T \cdot \right. \\
&\left[I_{rl} - Bf_{old}(rl,:) \cdot T_r \cdot \left(T_s^T B_o T_r\right)^{-1} \cdot T_s^T \cdot Cft_{old}(rl,:)^T\right]^{-1} \\
&\left. \cdot Bf_{old}(rl,:) \cdot T_r \cdot \left(T_s^T B_o T_r\right)^{-1}\right\},
\end{aligned}$$

where $I_{noslack}$ is the (number of nodes)×(number of nodes) identity matrix. The above equation is rewritten as

$$H_{new} \cdot T_{noslack} = A \cdot (I_{noslack} + B), \tag{A.13}$$

where

$$A = T_{\neg rl} \cdot Bf_{old} \cdot T_{noref} \cdot \left(T_s^T B_o T_r\right)^{-1} \tag{A.14}$$

and

$$B = T_s^T \cdot Cft_{old}(rl,:)^T \cdot \left[I_{rl} - Bf_{old}(rl,:) \cdot T_r \cdot \left(T_s^T B_o T_r\right)^{-1} \cdot T_s^T \cdot Cft_{old}(rl,:)^T\right]^{-1} \cdot Bf_{old}(rl,:) \cdot T_r \cdot \left(T_s^T B_o T_r\right)^{-1} \tag{A.15}$$

We will show that the computation of both A and B can be greatly reduced with the information from the previous iteration.

A.3.2 Construction of A

Substitution of (A.11) into (A.14) yields

$$A = T_{\neg rl} \cdot Bf_{old} \cdot T_{noref} \cdot \left(T_{noslack}^T \cdot Bbus_{old} \cdot T_{noref}\right)^{-1}. \tag{A.16}$$

Recall that H_{old} satisfies

$$H_{old} \cdot T_{noslack} = Bf_{old} \cdot T_{noref} \cdot \left(T_{noslack}^T \cdot Bbus_{old} \cdot T_{noref}\right)^{-1}, \tag{A.17}$$

where we make use of the fact that both the slack node and the reference node are the same as in the previous iteration. Comparing (A.16) and (A.17) gives the following relation between A and H_{old}:

$$A = T_{\neg rl} \cdot H_{old} \cdot T_{noslack}, \tag{A.18}$$

which is the same as

$$A = H_{old}(\neg rl, noslack).$$

A.3.3 Construction of B

It is now time to analyze B. The matrix B is given by

$$B = T_s^T \cdot Cft_{old}(rl,:)^T \cdot Z^{-1} \cdot Y \tag{A.19}$$

where Z and Y are the second and third line of the right-hand side of (A.15), respectively. In particular, substitution of (A.11) gives

$$Y = T_{rl} \cdot Bf_{old} \cdot T_{noref} \cdot \left(T_{noslack}^T \cdot Bbus_{old} \cdot T_{noref}\right)^{-1}$$

which can be compared to (A.17) along the same lines as before in the construction of A to find

$$Y = T_{rl} \cdot H_{old} \cdot T_{noslack},$$

or

$$Y = H_{old}(rl, noslack).$$

Finally, Z can be simplified to

$$\begin{aligned} Z &= I_{rl} - Bf_{old}(rl,:) \cdot T_{noref} \cdot \left(T_s^T B_o T_r\right)^{-1} \cdot T_{noslack}^T \cdot Cft_{old}(rl,:)^T \\ &= I_{rl} - Y \cdot T_{noslack}^T \cdot Cft_{old}(rl,:)^T \\ &= I_{rl} - H_{old}(rl,:) \cdot T_{noslack} \cdot T_{noslack}^T \cdot Cft_{old}(rl,:)^T \end{aligned}$$

A.3.4 Merging the pieces

From all the manipulations and insights so far, it is possible to rewrite (A.13) in terms of old iteration matrices:

$$\begin{aligned} H_{new} \cdot T_{noslack} &= A \cdot (I_{noslack} + B) \\ &= A \cdot (I_{noslack} + T_{noslack}^T \cdot Cft_{old}(rl,:)^T \cdot Z^{-1} \cdot Y) \\ &= T_{\neg rl} \cdot H_{old} \cdot T_{noslack} \cdot \\ &\quad \left\{ I_{noslack} + T_{noslack}^T \cdot Cft_{old}^T \cdot T_{rl}^T \cdot \right. \\ &\quad\quad \left[I_{rl} - T_{rl} \cdot H_{old} \cdot T_{noslack} \cdot T_{noslack}^T \cdot Cft_{old}^T \cdot T_{rl}^T \right]^{-1} \\ &\quad\quad\quad \left. \cdot T_{rl} \cdot H_{old} \cdot T_{noslack} \right\}. \end{aligned}$$

Or in alternative notation:

$$\begin{aligned} H_{new}(:, noslack) = H_{old}(\neg rl, noslack) \cdot & \\ \left\{ I_{noslack} + Cft_{old}(rl, noslack)^T \cdot \right. & \\ \left[I_{rl} - H_{old}(rl, noslack) \cdot Cft_{old}(rl, noslack)^T \right]^{-1} & \\ \left. \cdot H_{old}(rl, noslack) \right\}. & \quad \text{(A.2 revisited)} \end{aligned}$$

This formulation doesn't look very attractive. However, note that the matrix multiplications that include $T_{...}$ are computationally very easy since they only remove rows or add empty rows. Also, the matrix Cft_{old} has only two non-zeros in every row. Nevertheless, the most important feature is the inverse matrix computation. A direct calculation of the PTDF matrix requires inverting a $nb \times nb$ matrix – i.e. 1254×1254 for the UCTE network – which takes a lot of time. In our update, we only to invert a $rl \times rl$ matrix – generally not larger than 10×10 – which is quickly done. It is this feature that reduces computing time significantly.

Applying the Woodbury Matrix Identity to the part of (A.2) between curly brackets, it follows that

$$\begin{aligned} H_{new}(:, noslack) = H_{old}(\neg rl, noslack) \cdot & \\ \left[I_{noslack} - Cft_{old}(rl, noslack)^T \cdot H_{old}(rl, noslack) \right]^{-1}. & \quad \text{(A.20)} \end{aligned}$$

This gives a nice representation of (A.2) which will be used in Subsection A.4.2. Unfortunately, this representation also requires inverting a large matrix.

After the removal of the first set of links, the removal of the second set of links (hereby disconnecting the network) is easily done. As shown in Figure A.4, all entries h_{li} that correspond to a link l that does not have both ends in the component with i, can be replaced by zero. After that, submatrices that correspond to a component can be extracted from the PTDF matrix. Note that the update for the second set of links is implicitly done by extracting submatrices, but it is good to see how everything works out.

A.4 Tie up loose ends

During the derivation of (A.2), two important assumptions has been made without verification so far. Inverses of $Bbus_{old}$ and $Bbus_{new}$ do not need to exist, and the inverse of Z in (A.19) does not need to exist. Note that Z is the same as the term between square brackets in (A.12). We will discuss these problems and show how that all matrices are non-singular when the underlying network is connected. By construction of the update method, this implies that (A.2) is well-defined.

A.4.1 Invertibility of $Bbus$

Invertibility of $Bbus_{old}(noslack, noref)$ and $Bbus_{new}(noslack, noref)$ is proven in the same way. The only requirement is that the underlying network is connected, which is true for both matrices. For this reason we prove invertibility of $Bbus(noslack, noref)$, without specifying the previous or current iteration. Before the proof is stated, some definitions are introduced.

Definition 1. *A matrix A is called **diagonally dominant** if*

$$|a_{ii}| \geq \sum_{j \neq i} |a_{ij}| \tag{A.21}$$

*holds for all rows i. If A.21 holds with strict inequality for all i, A is called **strictly diagonally dominant**.*

Definition 2. *A matrix A is called **irreducibly diagonally dominant** if all of the following properties hold.*

1. *A is irreducible.*
2. *A is diagonally dominant.*
3. *At least one row of A satisfies* (A.21) *with strict inequality.*

We will now introduce some results on the singularity of matrices. The presented theorems are used to prove invertibility of $Bbus$ and are stated without proof.

Theorem 4. *An adjacency matrix A of the undirected graph G is irreducible if and only if G is connected.*

Theorem 5. ***(Gershgorin's Circle Theorem)*** *Any eigenvalue λ of a matrix A is located in one of the closed discs of the complex plane centered at a_{ii} and having radius $\rho_i = \sum_{j \neq i} |a_{ij}|$. In other words, $\forall \lambda \in \delta, \exists\, i : |\lambda - a_{ii}| \leq \rho_i$. Here, $\delta(A)$ is the set of eigenvalues of A [33].*

Theorem 6. ***(Gershgorin's Theorem 2)*** *Let A be an irreducible $n \times n$ matrix and assume that an eigenvalue λ of A lies on the boundary of the union of the n Gershgorin discs. Then λ lies on the boundary of all Gershgorin discs [81].*

Corollary 1. *If a matrix A is strictly diagonally dominant or irreducibly diagonally dominant, then it is non-singular [81].*

One may check from the previous section that the matrix $Bbus$ equals

$$Bbus = Cft^T \cdot D_b \cdot Cft,$$

where D_b is the diagonal matrix with the entries of b as its diagonal. Recall that the vector b has strictly positive entries. It follows that

$$Bbus_{ii} = \sum_{\text{link } l \text{ is adjacent to } i} b_l$$
$$Bbus_{ij} = - \sum_{\text{link } l \text{ is has endpoints } i \text{ and } j} b_l,$$

where the direction of a link is not relevant. Assuming that $b = \mathbf{1}$, it can be seen that the diagonal entries $Bbus_{ii}$ equal the degree of node i and the off-diagonal entries $Bbus_{ij}$ equal the number of links between i and j with a minus sign. Intuitively, the matrix $Bbus$ can thus be considered as a weighted, undirected adjacency matrix.

Some properties of the matrix $Bbus$ are stated before the proof:

(1) The matrix $Bbus$ is irreducible since the underlying graph is connected.

(2) The matrix $Bbus$ is symmetric.

(3) All row sums of $Bbus$ equal zero.

(4) The diagonal elements of $Bbus$ are strictly positive. This follows from the fact that every node has at least one adjacent link and b is strictly positive. For the same reason, all off-diagonal elements are non-positive (there may be no link between i and j so that $Bbus_{ij} = 0$).

(5) Let j be an arbitrary node. From definition of the $Bbus$, it follows that $Bbus_{ij}$ is non-positive for every $i \neq j$. Thus, removing the column that corresponds to j makes the sum of row i ($i \neq r$) non-negative. In particular, every node i that shares a link with j satisfies $Bbus_{ij} < 0$ and removal of column j will make the sum of row i strictly positive.

It follows from (3) and (4) that $Bbus$ is diagonally dominant. We will now show that the matrix $Bbus(noslack, noref)$ is invertible.

Case I: slack node equals reference node

This is the easier case since invertibility immediately follows from the above theorems and the following observations. Without loss of generality we assume that the slack and reference node is the last node. Removing the last row and column of $Bbus$ results in $Bbus(noslack, noref)$. Its underlying graph G' equals that of $Bbus$ with the exception that the last node has been removed. Hence, the new graph G' may consist out of several components or it is still connected (one component).

Let k be the number of maximum size components in G'. Without loss of generality we may now assume that $Bbus(noslack, noref)$ is a block diagonal matrix with k irreducible submatrices on its diagonal[25]. Note that property (4) still holds. Since every component was connected to the slack node, it follows from (5) that every submatrix has at least one row with a strictly positive sum and no row has a negative sum. Therefore, every submatrix is irreducibly diagonally dominant and hence invertible by Corollary 1. This implies that the inverse of $Bbus(noslack, noref)$ also exists and it is given by the block diagonal matrix with the k inverse submatrices on its diagonal.

Case II: slack node is not equal to reference node

The matrix $Bbus$ can be represented in the following way:

$$Bbus = \begin{bmatrix} \alpha_0 & \alpha_1 & \dots & \alpha_{n-2} & \gamma \\ \alpha_1 & & & & \beta_1 \\ \vdots & & B & & \vdots \\ \alpha_{n-2} & & & & \beta_{n-2} \\ \gamma & \beta_1 & \dots & \beta_{n-2} & \beta_{n-1} \end{bmatrix}. \tag{A.22}$$

Here we make use of the fact that $Bbus$ is symmetric. The submatrix B is symmetric, diagonally dominant and invertible, where the latter property can be proven by applying the proof of Case I to the last node and then to the first node. Since B is diagonally dominant and invertible it also follows that its eigenvalues are strictly positive. We will use the given representation of $Bbus$ and the properties of B in the proof of Case II.

Without loss of generality we assume that the slack node is the first node and the reference node is the last node. Like before, this can be achieved by renumbering the nodes. It follows from (A.22) that $Bbus(noslack, noref)$ is given by

$$Bbus(noslack, noref) = \begin{bmatrix} \alpha_1 & & \\ \vdots & B & \\ \alpha_{n-2} & & \\ \gamma & \beta_1 \ \dots \ \beta_{n-2} & \end{bmatrix}. \tag{A.23}$$

[25] One way to see this is that the nodes can be renumbered component-wise. That is, the n_1 nodes in the first component have numbers 1 to n_1, the n_2 nodes in the second component have numbers $n_1 + 1$ to $n_1 + n_2$, etc. This will lead to k blocks in $Bbus(noslack, noref)$. Since every component is connected, the corresponding submatrices are irreducible. This construction does not change the properties of $Bbus(noslack, noref)$, but it makes the discussion easier.

For sake of a contradiction, assume that $Bbus(noslack, noref)$ is not invertible. Then there exists a nonzero vector $\mathbf{x} = (x_1, \ldots, x_{n-1})^T = (x_1, \bar{\mathbf{x}})^T$ such that

$$Bbus(noslack, noref) \cdot \mathbf{x} = \mathbf{0}. \tag{A.24}$$

Let $\bar{\alpha} = (a_1, \ldots, a_{n-2})^T$ and $\bar{\beta} = (b_1, \ldots, b_{n-2})^T$. Using representation (A.23), equation (A.24) is equivalent to

$$\bar{\alpha} \cdot x_1 + B \cdot \bar{\mathbf{x}} = \mathbf{0} \tag{A.25}$$

and

$$\gamma \cdot x_1 + \bar{\beta}^T \cdot \bar{\mathbf{x}} = 0. \tag{A.26}$$

Since B is invertible, equation (A.25) implies

$$\bar{\mathbf{x}} = -B^{-1} \cdot \bar{\alpha} \cdot x_1. \tag{A.27}$$

For $x_1 = 0$ it follows that $\mathbf{x} = \mathbf{0}$, which is a contradiction. We may thus assume $x_1 = 1$ so that the righthand side of (A.27) becomes independent of $\mathbf{x}$;

$$\bar{\mathbf{x}} = -B^{-1} \cdot \bar{\alpha}. \tag{A.28}$$

Substituting (A.28) into (A.26) and using $x_1 = 1$ yields

$$\bar{\beta}^T \cdot B^{-1} \cdot \bar{\alpha} = \gamma. \tag{A.29}$$

or

$$\left(\bar{\beta}, B^{-1}\bar{\alpha}\right) = \gamma. \tag{A.30}$$

From our assumption that $Bbus(noslack, noref) = T_{noslack}^T \cdot Bbus \cdot T_{noref}$ is not invertible, it follows that its transpose $T_{noref}^T \cdot Bbus^T \cdot T_{noslack}$ is also not invertible. Using the fact that $Bbus$ is symmetric, it follows that the transpose of $Bbus(noslack, noref)$ equals $Bbus(noref, noslack)$ which can be represented as

$$Bbus = \left[\begin{array}{ccc|c} \alpha_1 & \ldots & \alpha_{n-2} & \gamma \\ \hline & & & \beta_1 \\ & B & & \vdots \\ & & & \beta_{n-2} \end{array}\right]., \tag{A.31}$$

since B is symmetric. As the matrix $Bbus(noref, noslack)$ is not invertible, there exists a nonzero vector $\mathbf{y} = (\bar{\mathbf{y}}, y_{n-1})^T$ such that

$$Bbus(noref, noslack) \cdot \mathbf{y} = \mathbf{0}, \tag{A.32}$$

or equivalently

$$\bar{\beta} \cdot y_{n-1} + B \cdot \bar{\mathbf{y}} = \mathbf{0} \tag{A.33}$$

and

$$\gamma \cdot y_{n-1} + \bar{\alpha}^T \cdot \bar{\mathbf{y}} = 0. \tag{A.34}$$

Analogously to the matrix $Bbus(noslack, noref)$, the above equations lead to the condition

$$\left(\bar{\alpha}, B^{-1}\bar{\beta}\right) = \gamma. \tag{A.35}$$

Summing (A.30) and (A.35) yields

$$\left(\bar{\alpha} + \bar{\beta}, B^{-1}(\bar{\alpha} + \bar{\beta})\right) = 2\gamma. \tag{A.36}$$

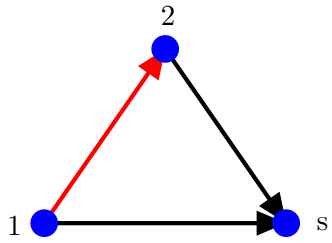

(a) Network

	node 1	node 2
node 1	1/3	−1/3
node 2	−1/3	1/3

(b) Matrix $Cft(rl, noslack)^T \cdot H(rl, noslack)$

Figure A.5: Example of $CH = Cft(rl, noslack)^T \cdot H(rl, noslack)$ matrix, assuming that link $(1, 2)$ will be removed ($= rl$ links). In Figure A.1 it was shown that an injection of one unit flow in node 1 results in a 1/3 unit flow to node 2. This is also the net flow leaving node 1 though adjacent rl links, and so entry (1,1) equals 1/3. Also, for the given injection, node two receives a net flow of 1/3 through adjacent rl links and thus entry (1,2) equals -1/3. The same reasoning can be applied for an injection in node 2. Note that the rejection is still in the slack node for both cases.

Recall that the matrix B has strictly positive eigenvalues. This implies that the eigenvalues of B^{-1} are also strictly positive and thus the matrix B^{-1} is positive definite. The lefthand side of (A.36) is therefore non-negative. Furthermore, γ is an off-diagonal element of $Bbus$ and thus $\gamma \leq 0$. It follows that (A.36) can be satisfied if and only if $\bar{\alpha} + \bar{\beta} = 0$ and $\gamma = 0$. All elements in $\bar{\alpha}$ and $\bar{\beta}$ are off-diagonal elements of $Bbus$ and hence $\bar{\alpha} = \bar{\beta} = \mathbf{0}$. This implies that α_0 is the only element in the first row and in the first column of $Bbus$. However, this means that $Bbus$ is reducible which is a contradiction to property (1). We may thus conclude that $Bbus(noslack, noref)$ is invertible for any slack node and reference node.

A.4.2 Invertibility of Z

Using the Woodbury Matrix Identity on (A.2) yielded (A.20). Thus, showing that the inverse in (A.2) exists is equivalent to showing that the inverse in (A.20) exists. We will prove the latter statement since this is more intuitive and hereby also prove that (A.2) is well-defined.

Define $CH = Cft_{old}(rl, noslack)^T \cdot H_{old}(rl, noslack)$ and assume that only one link is removed. The matrix $I_{noslack} - CH$ is invertible if the spectral radius of CH, $\rho(CH)$, is smaller than one, e.g. $\rho(CH) = \max_i(|\lambda_i|) < 1$ where λ_i are the eigenvalues of CH. We thus need to show that the eigenvalues of CH are strictly less than one.

It can be verified that CH_{ij} equals the net change of energy in node i due to flows over removed links adjacent to i when one unit of flow is injected at j and rejected at the slack node. This is illustrated in Figure A.5. Since only two nodes are adjacent to the one link that is removed, it follows that there are only two non-zero rows in CH. All flow leaving node i via link (i, j) enters j, and thus $CH_{i,x} = -CH_{j,x}$ for all x. The characteristic

polynomial $p_{CH}(\lambda)$ is given by

$$\begin{aligned} p_{CH}(\lambda) &= \lambda^{n-3}\left[(\lambda - CH_{ii})(\lambda - CH_{jj}) - CH_{ij}CH_{ji}\right] \\ &= \lambda^{n-3}\left[\lambda^2 - \lambda(CH_{ii} + CH_{jj}) + CH_{ii}CH_{jj} - CH_{ij}CH_{ji}\right] \\ &= \lambda^{n-3}\left[\lambda^2 - \lambda(CH_{ii} + CH_{jj}) + CH_{ii}CH_{jj} - CH_{jj}CH_{ii}\right] \\ &= \lambda^{n-2}(\lambda - (CH_{ii} + CH_{jj})) \end{aligned}$$

The eigenvalues of CH are the roots of $p_{CH}(\lambda)$, which equal 0 (with multiplicity $n-2$) and $CH_{ii} + CH_{jj}$. It follows that $\rho(CH) = |CH_{ii} + CH_{jj}|$ and CH is invertible if $CH_{ii} + CH_{jj} < 1$. Note that CH_{xx} is always non-negative. By definition of CH, this implies that

$$\begin{aligned} Cft_{old}(rl,i)^T \cdot H_{old}(rl,i) + Cft_{old}(rl,j)^T \cdot H_{old}(rl,j) < 1 \\ Cft_{old}((i,j),i)^T \cdot H_{old}((i,j),i) + Cft_{old}((i,j),j)^T \cdot H_{old}((i,j),j) < 1 \\ H_{old}((i,j),i) - H_{old}((i,j),j) < 1. \end{aligned}$$

The last equation can be recognized as the change in link (i,j) when one unit of flow is injected in i and removed in j. Clearly, this is smaller than one if and only if (i,j) is not the only path from (i,j) so that other paths carry part of the flow too. If (i,j) is the only path, then all flow must go though this link and the change $H_{old}((i,j),i) - H_{old}((i,j),j)$ equals 1. We may conclude that the inverse in (A.20) is defined when only one link is removed, and this link does not disconnect the network. This also holds for the special case where i (j) is the slack node and the corresponding CH_{ii} (CH_{jj}) equals zero.

The fact that multiple links can be removed in one iteration follows from an induction argument. We have just seen that the inverse of $I_{noslack} - CH$ exists if one link is removed. Assume that the inverse exists after removal of $k < K$ links, and that link K can be removed without disconnecting the network. Let $H_{old}, H_{new}, H_{new,K}$ and $Cft_{old}, Cft_{new}, Cft_{new,K}$ denote the matrices H and Cft for respectively the initial situation, the situation after removal of the first $K-1$ links, and the situation after removal of all K links. Also, let T_x be the transformation matrix that removes the rows indicated by x as defined before in Table A.1. The indicators x are rl_K, rl_{K-1} and rl_k, removing all K links, the first $K-1$ links or only the K-th link k, respectively. The transformation matrix $\widetilde{T}_x$ is corrected for the removal of the first $K-1$ links, e.g. $\widetilde{T}_{\neg rl_k} \cdot T_{\neg rl_{K-1}}$ removes links $K-1$ first and then link k and thus this product equals $T_{\neg rl_K}$, the removal of all K links at once.

The update method states that H_{new} satisfies

$$\begin{aligned} H_{new}(:, noslack) = T_{\neg rl_{K-1}} \cdot H_{old}(:, noslack) \cdot \\ \left[I_{noslack} - \left(T_{rl_{K-1}} \cdot Cft_{old}(:, noslack)\right)^T \cdot T_{rl_{K-1}} \cdot H_{old}(:, noslack)\right]^{-1}. \end{aligned} \quad \text{(A.37)}$$

and $H_{new,K}$ is found by updating H_{new},

$$\begin{aligned} H_{new,K}(:, noslack) = \widetilde{T}_{\neg rl_k} \cdot H_{new}(:, noslack) \cdot \\ \left[I_{noslack} - \left(\widetilde{T}_{rl_k} \cdot Cft_{new}(:, noslack)\right)^T \cdot \widetilde{T}_{rl_k} \cdot H_{new}(:, noslack)\right]^{-1}. \end{aligned} \quad \text{(A.38)}$$

Substituting (A.37) into (A.38) yields

$$H_{new,K}(:,noslack) = \widetilde{T}_{\neg rl_k} \cdot T_{\neg rl_{K-1}} \cdot H_{old}(:,noslack) \cdot \Big[I_{noslack} - \big(T_{rl_{K-1}} \cdot Cft_{old}(:,noslack)\big)^T \cdot T_{rl_{K-1}} \cdot H_{old}(:,noslack)\Big]^{-1} \cdot \Big[I_{noslack} - \Big(\widetilde{T}_{rl_k} \cdot Cft_{new}(:,noslack)\Big)^T \cdot \widetilde{T}_{rl_k} \cdot T_{\neg rl_{K-1}} \cdot H_{old}(:,noslack) \cdot \Big[I_{noslack} - \big(T_{rl_{K-1}} \cdot Cft_{old}(:,noslack)\big)^T \cdot T_{rl_{K-1}} \cdot H_{old}(:,noslack)\Big]^{-1}\Big]^{-1}. \quad (A.39)$$

Using $X^{-1} \cdot Y^{-1} = (YX)^{-1}$, the following equation can be derived from (A.39):

$$H_{new,K}(:,noslack) = \widetilde{T}_{\neg rl_k} \cdot T_{\neg rl_{K-1}} \cdot H_{old}(:,noslack) \cdot \Big[I_{noslack} - \big(T_{rl_{K-1}} \cdot Cft_{old}(:,noslack)\big)^T \cdot T_{rl_{K-1}} \cdot H_{old}(:,noslack) - \Big(\widetilde{T}_{rl_k} \cdot Cft_{new}(:,noslack)\Big)^T \cdot \widetilde{T}_{rl_k} \cdot T_{\neg rl_{K-1}} \cdot H_{old}(:,noslack)\Big]^{-1}. \quad (A.40)$$

Since $Cft_{new} = T_{\neg rl_{K-1}} \cdot Cft_{old}$ and $\widetilde{T}_{\neg rl_k} \cdot T_{\neg rl_{K-1}} = T_{\neg rl_K}$ and $\widetilde{T}_{rl_k} \cdot T_{\neg rl_{K-1}} = T_{rl_k}$ one finds

$$H_{new,K}(:,noslack) = T_{rl_K} \cdot H_{old}(:,noslack) \cdot \Big[I_{noslack} - \big(T_{rl_{K-1}} \cdot Cft_{old}(:,noslack)\big)^T \cdot T_{rl_{K-1}} \cdot H_{old}(:,noslack) - \big(T_{rl_k} \cdot Cft_{old}(:,noslack)\big)^T \cdot T_{rl_k} \cdot H_{old}(:,noslack)\Big]^{-1}. \quad (A.41)$$

or

$$H_{new,K}(:,noslack) = H_{old}(rl_K,noslack) \cdot \big[I_{noslack} - Cft_{old}(rl_{K-1},noslack)^T H_{old}(rl_{K-1},noslack) - Cft_{old}(rl_k,noslack)^T \cdot H_{old}(rl_k,noslack)\big]^{-1}. \quad (A.42)$$

Finally, this can be simplified to

$$H_{new,K}(:,noslack) = H_{old}(rl_K,noslack) \cdot \big[I_{noslack} - Cft_{old}(rl_K,noslack)^T H_{old}(rl_K,noslack)\big]^{-1}, \quad (A.43)$$

which is identical to the update method for removing all K links at once. We may thus conclude that (A.20) is valid for the removal of any set of links that do not disconnect the network. Since (A.2) is equivalent to (A.20), update equation (A.2) is valid under the same condition. This condition is always satisfied by construction of the update algorithm and we conclude that the update method is correct.

A.5 Results

The PTDF update method has been compared to the direct computation on the IEEE 14, 30, 57 and 118 bus networks, as well as on the 1254 bus UCTE network. Comparing the methods has been done in the following way:

1. Compute initial PTDF matrix.
2. For every island I with at least two nodes, choose one node at random and execute steps 3. to 6.
3. Determine sub-islands S that will be formed by removing this node (common computation time).
4. Compute PTDF matrices with the update method (update-C = update time - common time). If the slack node of the old PTDF matrix is the node to be removed, determine a new slack node and transform the PTDF matrix by subtracting the new slack column from all columns. This operation transforms the PTDF matrix corresponding to the old slack node to the PTDF matrix that corresponds to the new slack node.
5. Compute PTDF matrices with the direct method (direct-C = direct time - common time).
6. Sum entry-wise absolute differences for all matrices of both methods (deviation).
7. If there are sub-islands S with at least two nodes left, define those as new islands I and return to 2.

Thus, every comparison removes nodes until the resulting network has been disconnected. Big networks will need a lot of iterations before the comparison algorithm terminates. This implies that the original PTDF matrix will be updated many times. A large deviation at termination of the comparison algorithm would show that the numerical implementation of the update method is unstable. Fortunately, Table A.2 shows that the deviations are very small compared to the network size and thus the method is very accurate.

Table A.3 shows that the computation time of the update method is approximately 30 to 45% faster than the direct method, depending on the network size. Variation in the computation time difference is caused by both the common and the characteristic computing part. A relatively large common computing time will push the factor update/direct (both terms including the common time) to one, indicating that the total computing time is comparable but concealing the enhanced performance in the characteristic part.

Column 5 in the table shows that characteristic part of the update method is 58 to 60% faster than the characteristic part of the direct method for the smaller networks. The 1254 bus UCTE network shows an improvement of 43%. This are good improvements, but it should be noted that our construction plays a big part. We only remove one node at a time, thereby limiting the number of links that is removed. Recall that the update method has to invert a (number of removed links)×(number of removed links) matrix opposed to the (number of remaining links)×(number of remaining links) matrix in the direct method. This implies that the update method works best for removing a small fraction of links at a time. Removing a lot of links at a time is a big change in the network topology and will cause longer computation time to update the PTDF matrix. In such cases, direct computation is probably faster. A more thorough analysis on this has not been performed, but it is expected that the update method performs worse than the direct method when removing, say, 30% of the network.

	mean deviation	max deviation
IEEE 14	$2.6324 \cdot 10^{-14}$	$9.1544 \cdot 10^{-14}$
IEEE 30	$2.1769 \cdot 10^{-13}$	$9.9879 \cdot 10^{-13}$
IEEE 57	$1.1995 \cdot 10^{-12}$	$8.6490 \cdot 10^{-12}$
IEEE 118	$2.1284 \cdot 10^{-11}$	$1.1920 \cdot 10^{-10}$
UCTE	$5.4931 \cdot 10^{-8}$	$4.8657 \cdot 10^{-7}$

Table A.2: Experimental comparison of direct PTDF and PTDF update methods for the same 1000 runs as in Table A.3. Deviations have been calculated as the total sum of entry-wise absolute differences between PTDF matrices of both methods for the same run. Thus, networks with more nodes and links are expected to show larger deviations.

	mean common	mean update-C	mean direct-C	mean update/direct	mean update-C/direct-C
IEEE 14	0.0054	0.0066	0.0165	0.5517	0.4051
IEEE 30	0.0146	0.0142	0.0341	0.5914	0.4174
IEEE 57	0.0413	0.0307	0.0726	0.6324	0.4234
IEEE 118	0.1401	0.0708	0.1732	0.6725	0.4089
UCTE	18.9295	20.5763	36.1574	0.7171	0.5689

Table A.3: Experimental comparison of direct PTDF and PTDF update methods for 1000 runs. Both methods consist of a common part (finding islands) and a characteristic part (computing the PTDF matrix). The characteristic part is denoted by update-C and direct-C. The ratio update/direct corresponds to the averaged fraction of the total computing times $\frac{update}{direct}$ and the ratio update-C/direct-C corresponds to the averaged fraction of the characteristic computing time $\frac{update-C}{direct-C}$ of every run. This value is in general not equal to the fraction of the second and third values.

Appendix B

Visit TenneT, Arnhem (NL)

B.1 Introduction

Most people will agree that theory and reality are often two separate worlds. This has been identified as a key issue in many real-world problems and in the evaluation of research results. It is in everybody's best interest to bridge this gap so that research can contribute to the problems that are faced. Much can be gained by simply bringing the two sides together and having a conversation. We decided to contact TenneT, the electricity transmission operator in the Netherlands and member of ENTSO-E, the European Network of Transmission System Operators for Electricity. One of TenneT's missions is to protect the electricity supply and restore it when necessary. TenneT explained about their daily operations and the more extreme situations in which the system is vulnerable or subject to blackouts. Their cooperation has provided new insights and is greatly valued for the writing of this thesis.

The website of TenneT [76] provides a compact description of the organization's objectives:

> "TenneT is the electricity transmission operator in the Netherlands and a large part of Germany. We monitor the balance between the supply of and demand for electricity – 24 hours a day and 7 days a week. We are the linking pin between electricity producers and consumers, ensuring a reliable and uninterrupted supply of electricity to our 36 million end-users. TenneT is responsible for the continuity of the electricity supply. In addition, we aim to develop an integrated European energy market. TenneT has an international focus, working with government authorities, non-governmental organisations, trading partners and private investors all over the world. TenneT is working hard, both on land and at sea, to ensure that vital infrastructure is developed, realised and efficiently managed, now and in the future."

Evidently, this is the industry equivalent of our research. The professionals at TenneT have vast knowledge about and experience with operating the power grid. Their input has been very helpful in increasing the author's sense of reality in power grid modeling and therefore in evaluating the variety of different models. The remainder of this appendix is a summary of the meeting on April 16$^{\text{th}}$, 2013.

B.2 Meeting

TenneT distinguishes between two aspects of operating the transmission of electricity: system services and transport services. System services include balancing the network, controlling import and export to other countries and maintaining the programme responsibility system. Transport services include controlling the flow, compensation for grid losses and maintaining voltage with reactive power supplies. The two services are now described in more detail.

B.2.1 System services

Balancing the network is one of the priorities for an electricity transmission operator. Supply and demand are ever changing and it is essential for a transmission network that the difference is minimal. For example, under-supply causes under-frequency in the network, jeopardizing the safety of the network. Operators are given additional authorizations based on the Grid and Systemcode when the safety of the network is threatened so that they can secure the network. This is considered in more detail in Subsection B.2.3.

Import and export to other countries are closely related to balancing the network. Under normal operation conditions, import and export have been forecast and communicated with other countries' operators. However, when power production is unexpectedly cut down due to some cause, power is involuntary drawn from other countries' networks. This may in turn endanger their network balance. It is important for both countries to communicate and solve these issues as soon as possible (see ENTSO-E policies [30]).

Any party that is connected to the network in the Netherlands bears programme responsibility for those connections (Programme Responsibility System). Every such party is required to draw up daily programmes that include the expected supply and demand for every connection. System conditions are forecast according to these programmes. Differences between expected and actual generation and demand are measured and reported to TenneT. Differences are penalized as they threaten system security.

B.2.2 Transport services

Transport services make transport of energy possible. TenneT is responsible for 20,000 km of transmission lines that are subject to various weather conditions, copper theft and other external events. Usually, some transmission lines are out-of-service every day for maintenance. All of these maintenance activities state a so-called give-back period on beforehand. If the line is required to be put back into service, this give-back period is the estimated amount of time that is needed to do so. The give-back periods normally range from hours to days. These periods are important in scheduling maintenance activities so that unforeseen difficulties in the network can be taken care of within a couple of hours.

Increasing market transactions force more transport over the network. TenneT is expected to build new transmission lines and substations to ensure safety in the network. Slower expansion of the network can cause higher loads on transmission lines. To prevent N-1 violations, congestion management is needed in some cases. Decisions on maintenance

and new equipment – and equally important the location of this equipment – are becoming more challenging and allow for interesting research (see also Appendix C for research challenges in power systems).

B.2.3 Abnormal system conditions

Transmission lines and generators are both subject to unforeseen tripping[26] and may disturb the system balance. TenneT has defined a set of states to indicate the condition of the system. Each state implies additional authorizations to restore grid security and the system balance.

- **Normal.** When the system conditions are normal, the $N-1$ criterion is respected and no single contingency can instantly bring the system out of its operational limits.
- **Alert.** The first abnormal system state. The $N-1$ criterion is violated and TenneT is required to protect the system. They are authorized to claim production from all generators (both real and reactive power) to get the system back to normal. For instance, a geographical shift in generation may reduce the load on threatened transmission lines. Temporarily transformer overload is possible, allowing operators to respond.
- **Emergency.** Frequency, voltage or load levels have exceeded normal operating security limits. Automatic load shedding is performed in three steps (shedding respectively 15%, 15% and 20% of load) when the frequency drops below 49 Hz. Manual load shedding at substations is authorized to get back to the Alert state as soon as possible.
- **Blackout.** In this state the grid is disturbed. The restoration process will be started.

Operators may decide to restore out-of-service transmission lines. This choice is based on time of the day (short-term demand forecast), severity of the disturbance and give-back periods.

During Emergency, actions often need to be taken within seconds. Automatic load shedding systems operate within this time frame and are essential to relieve the system. Operators require several minutes to analyze the situation and take corrective actions such as manual load shedding.

The blackout state, possibly during a cascading failure, is a worst-case situation. Literature describes a wide variety on 1) intentional islanding schemes to stop cascading and 2) islanding schemes to restore unintentional islands after cascading. These latter islanding schemes are also defined at TenneT. Pre-engineered (black-start[27]) islands have been designed to facilitate restoration of the network. Islands are chosen for reasons of frequency and voltage stability, and (black-start) generation facilities available.

[26] Most terminology, e.g. *tripping* and $N-1$ *criterion*, is introduced in Chapter 2.
[27] Black-start islands contain equipment that can be activated without energy supply from the grid.

The restoration procedure starts by restoring the pre-engineered islands. When all islands have been formed and are working properly, they are connected two at a time at synchronization locations. Those locations contain physical equipment needed to synchronize the generators in both islands. In contrast to some papers on intentional islanding, TenneT aims to form as least islands as possible. Synchronization of islands is time-consuming and should be limited especially in case the grid can be energized from the surrounding ENTSO-E system.

Appendix C

Visit Energy Systems Week 2013, Cambridge (GB)

The energy industry provides a vast amount of unanswered questions and motivates many years of research in many different research directions. In order to identify some of the problems that are faced today and problems that will be faced tomorrow, the Isaac Newton Institute in Cambridge (UK) organized and hosted the Energy Systems Week 2013. Most participants were mathematicians from universities and professionals from the energy industry. Other participants included some economists and government officials. To enhance understanding and cooperation between different fields, non-mathematically schooled participants are encouraged to visit future sessions. A more elaborated overview of the week is given below (cited from the website of the Isaac Newton Institute [44]).

> This meeting is a one-week research and scoping workshop to discuss applications of mathematics to the management of complex energy systems. It will be held at the Isaac Newton Institute in Cambridge from 22 to 26 April this year. It is intended as a follow-up to the Spring 2010 Programme in Stochastic Processes in Communication Sciences, and the one-week Energy Systems workshop which formed part of that programme, and subsequent one-day events on the theme of mathematics in the management of energy (Energy Systems Day and Maths Underpinning Energy Workshop). The aims of the meeting are:
>
> 1. To address and make progress with some of the difficult problems now arising in large electrical energy networks (e.g. that supplying Great Britain) and concerned with the management of variability and uncertainty in these systems. These problems are primarily:
>   a. the characterisation and prediction of complex patterns of variability in both supply and demand, notably those in supply arising from an increased reliance on renewable sources of energy such as wind and solar power;
>   b. the management of the system in response to uncertainty, via scheduling, the use of storage, and time-shifting of demand;
>   c. the design of market mechanisms so as to ensure economically efficient operation of the overall system, particularly in the balancing of supply and demand.
>
>   The solution of these problems requires the expert application of systems mathematics, i.e. probability and stochastic modelling, statistics and optimization, together with strong computational expertise in these areas.
> 2. To set up sustainable and lasting industrial-academic partnerships in

> these areas, and also to obtain a greater mutual understanding between industry and academia of how they may better combine their respective approaches to work for the common good.
>
> It is intended that the meeting should focus on identifying where and how mathematics can contribute to the pressing system management problems now facing the energy industry. To that end there will be a relatively small number of talks, which are by invitation, together with substantial time for brainstorming and discussion.

The workshop has provided good insight in problems for power grid management. All presentations have been recorded and can be found at `http://www.newton.ac.uk/programmes/SCS/scsw09p.html`. A summary of problems discussed has been formed and discussed on Friday, as well as proposals of the skills and/or educations needed in order to solve the problems. Unfortunately, this summary is only available as a recording of the discussion and not in document format.

Appendix D

Visit Kansas State University, Manhattan, Kansas (US)

This Appendix is a document that has been written during the author's visit to Kansas. It was intended for discussion with Pahwa et al. on their work [63] and can not be considered as a stand-alone. Section D.1 has been referred to in the thesis and is comprehensible without additional literature. All further sections assume that the reader is familiar with the work of Pahwa et al. [63] – in particular their Appendix A – and has the paper available for reference.

Optimal Intentional Islanding to Enhance the Robustness of Power Grid Networks – Further Research

This document will summarize some relevant issues from the May, 20th meeting with dr. C. M. Scoglio, dr. S. Starrett, dr. M. Youssef, S. Pahwa and N. Kamphorst. Next, we will propose some alternative constraints for the MILP model in [63]. Some of the alternative constraints are consistent with the model in the paper, some are additional constraints based on the meeting.

D.1 Meeting

This section does is not intended to cover the entire meeting but rather to enumerate discussion points for the model and actions to be undertaken before the next meeting on May, 23rd.

- Optimal islanding is an interesting topic of research. Next to topologically based research, there is also is also stability based research on islanding. Topological based papers tend to optimize islanding in the sense that load shedding is kept to a minimum. Stability based research is based on slow coherency of generators; generators that contribute to the same eigenvalue contribute to a stable system and disconnecting them makes the system more vulnerable. Unfortunately, computational costs of stability-related equations are high and a model that integrates both perspectives is not achievable in the current time frame.

- The current model allows disconnecting heavily loaded lines to form islands. It can be assumed that disconnecting heavily loaded lines induces more stability issues than the disconnecting of lightly loaded lines. For this reason it is proposed that a new cost function will also take this into account.

- The current model forces the complete network to be split up in a user-defined number of non-overlapping islands. The purpose of islanding is that any failure in the grid will be located in an island and this island can be disconnected from the complement of the island (the rest of the network). Thus, the other islands are not important for this failure. Since the constraint of non-overlapping islands is likely to reduce the quality of the individual islands, it is suggested that islands may overlap one other. So long as all nodes and links are in at least one island, it is still possible to isolate the cascade in one island whereas load shedding is reduced further.

- Good results have been obtained with the MILP formulation for both the IEEE 14 and 30 bus networks. However, the algorithm did not converge for larger systems. For this reason, there are two aspects to look into:

  - The constraints of the MILP. Maybe some of them can be removed or altered in order to reduce the computing times.

  - Load shedding constraints. At this moment, the load shed per node is limited to at most $(1 - \alpha)$ of initial load, where α is user-defined. It is noted that people in real life are not wanting to suffer a blackout for faults that happened hundreds of miles away. For this reason it may be interesting to allow complete load shed in the island that is suffering the problem and give priority to minimum load shed in the complement.

- Finally, the heuristics in [63] are not able to correct decisions made in order to achieve better results. Methods that allow correction of earlier decisions may lead to better solutions, so it is interesting to look into this.

D.2 Topological line constraints

This section will propose changes to the work of Pahwa et al. [63] from Kansas. It is assumed that the reader is familiar with their work – in particular Appendix A – and has the paper available for comparison.

Some of the constraints in Appendix A of the original paper [63] can be altered to allow removal of other constraints. All constraints from the original paper will be labelled with $P.x$, where x is the label of the corresponding constraint. Alternative constraints are labelled with $M.xb$ where x is the corresponding constraint from the original paper that is replaced. New constraints will be labelled with $N.y$.

The constraints that we consider are the following:

$$\sum_{k=1}^{n_{isl}} \mu_{ij}^{k,1} \leq a_{i,j} \qquad \forall i,j = 1,\ldots,N \tag{P.1}$$

$$\mu_{ij}^{k,1} + \mu_{ij}^{k,2} \leq 1 \qquad \forall i,j = 1,\ldots,N, k = 1,\ldots,n_{isl} \tag{P.2}$$

$$\sum_{k=1}^{n_{isl}} (\mu_{ij}^{k,1} + \mu_{ij}^{k,2}) \leq a_{ij} n_{isl} \qquad \forall i,j = 1,\ldots,N \tag{P.5}$$

$$\left(\sum_{j=1}^{N} \mu_{ij}^{k,1} \geq 1\right) \Rightarrow \left(\sum_{j=1}^{N} \sum_{k'=1,k'\neq k}^{n_{isl}} \mu_{ij}^{k',1} = 0\right) \qquad \forall i = 1,\ldots,N, k = 1,\ldots,n_{isl}. \tag{P.9}$$

We propose the following constraint to replace (P.1), (P.2) and (P.5):

$$\mu_{ij}^{k,1} + \mu_{ij}^{k,2} \leq a_{ij} \qquad \forall i,j = 1\ldots N, k = 1\ldots n_{isl}. \tag{M.2b}$$

This constraint sets all $\mu_{ij}^{k,s}$ to equal zero when link (i,j) does not exist, and else that the link can not be in an island and its complement both. We will show that constraints (M.2b) and (P.9) imply the same solution space as the constraints P above.

We will show that (M.2b) and (P.9) imply all constraints P. Assume that these two constraints are satisfied.

- If $a_{ij} = 0$, then (P.1) is satisfied by (M.2b). Now let (i,j) be fixed and assume $a_{ij} = 1$. Then (M.2b) allows $\mu_{ij}^{k,1} \in \{0,1\}$ for all k. If $\mu_{ij}^{k,1} = 0$ for all k, (P.1) is respected. Assume $\mu_{ij}^{K,1} = 1$ for some K. Then by (P.9), $\mu_{ij}^{k,1} = 0$ for all $k \neq K$ and thus $\sum_{k=1}^{n_{isl}} \mu_{ij}^{k,1} = 1 = a_{i,j}$.
- Since $a_{ij} \in \{0,1\}$, (M.2b) implies (P.2).
- Assume (M.2b) is met for all k. Summing over all k yields (P.5).

So indeed, (M.2b) and (P.9) imply all constraints P. Now assume that (P.1), (P.2), (P.5) and (P.9) are satisfied. We only need to show that (M.2b) is also satisfied.

- If $a_{ij} = 1$ then (P.2) equals (M.2b) and we are done.
- Instead assume $a_{ij} = 0$. From (P.5) it follows that $\mu_{ij}^{k,1} + \mu_{ij}^{k,2} = 0$ for all $k = 1,\ldots,n_{isl}$, thus implying (M.2b).

This completes the proof. Equations (P.1), (P.2), (P.5) can thus be replaced by constraint (M.2b). Note that the second part of the proof did not need (P.1). This is due to the fact that (P.5) and (P.9) imply (P.1).

D.3 Topological logical constraints

Consider the following constraints:

$$\left(\sum_{j=1}^{N}(\mu_{ij}^{k,1}+\mu_{ji}^{k,1})\geq 1\right)\Rightarrow\left(\sum_{j=1}^{N}(\mu_{ij}^{k,2}+\mu_{ji}^{k,2})=0\right)\qquad\forall i=1,\ldots,N,k=1,\ldots,n_{isl} \tag{P.7}$$

$$\left(\sum_{j=1}^{N}(\mu_{ij}^{k,2}+\mu_{ji}^{k,2})\geq 1\right)\Rightarrow\left(\sum_{j=1}^{N}(\mu_{ij}^{k,1}+\mu_{ji}^{k,1})=0\right)\qquad\forall i=1,\ldots,N,k=1,\ldots,n_{isl} \tag{P.8}$$

$$\mu_{ij}^{k,s}=\mu_{ji}^{k,s}\qquad\forall i,j=1,\ldots,N,k=1,\ldots,n_{isl},s=1,2. \tag{P.10}$$

Basically, (P.7) forces that any link to a node i that has at least one link in the island, can not be part of the complement. Constraint (P.8) does the same thing for nodes that have at least one link in the complement. These constraint make sure that all nodes belong to either an island or its complement, but not both. Also note that links are counted in both directions. By (P.10), this is not necessary and all $\mu_{ji}^{k,1}$ and $\mu_{ji}^{k,2}$ can be removed from (P.8) and (P.9) without changing the solution space.

At this moment, the constraints check all links connected to the node to find out where the node is assigned to. Instead, we propose binary decision variables σ_i^k for every node i and island k that indicate whether the node is in the island ($\sigma_i^k=1$) or the complement ($\sigma_i^k=0$). Let $deg(i)$ be the degree of node i. Then the inequalities

$$\sum_{j=1}^{N}\mu_{ij}^{k,2}\leq(1-\sigma_i^k)\cdot deg(i)\qquad\forall i=1,\ldots,N,k=1,\ldots,n_{isl} \tag{M.7b}$$

$$\sum_{j=1}^{N}\mu_{ij}^{k,1}\leq\sigma_i^k\cdot deg(i)\qquad\forall i=1,\ldots,N,k=1,\ldots,n_{isl} \tag{M.8b}$$

are equivalent to (P.7) and (P.8). To see this, assume that $\sum_{j=1}^{N}\mu_{ij}^{k,1}\geq 1$ for some node i and island k. This implies that node i is part of the island and so we expect σ_i^k to equal one. From our assumption and (M.8b) it indeed follows that $\sigma_i^k=1$. However, this implies that the righthand side of (M.7b) equals zero and no link adjacent to node i can be part of the complement. This is equivalent to (P.7). In the same way it can be shown that $\sigma_i^k=0$ if a link adjacent to node i is in the complement, and that (P.8) is satisfied. The righthand side limits $deg(i)$ are tight upper bounds for the number of links adjacent to node i and thus impose no additional constraints.

The new formulation also allows to replace both (P.6),

$$\sum_{j=1}^{N}\sum_{k=1}^{n_{isl}}\mu_{ij}^{k,1}\geq 1\qquad\forall i=1,\ldots,N, \tag{P.6}$$

and (P.9) by

$$\sum_{k=1}^{n_{isl}} \sigma_i^k = 1 \qquad \forall i = 1, \ldots, N, \tag{M.6b}$$

which assigns every node to precisely one island. This constraint can be relaxed so that nodes are in *at least* one island. Also, the new formulation can be used to force at least one generator in every island by the new constraint

$$\sum_{g=1}^{n_{gen}} \sigma_{gen(g)}^k \geq 1 \qquad \forall k = 1, \ldots, n_{isl}, \tag{N.1}$$

where *gen* is the subset of nodes that correspond to generators.

D.4 Cost function and power flow constraints

One of the interesting observations during the meeting was that consumers in the island have a lower priority than consumers in the complement. This can be captured in two ways:

- Alter the minimum amount of load served to consumers in the island.
- Alter the cost function to prioritize consumers in the complement. The cost function can also take the power of the interconnecting lines into account (another point in Chapter 1).

The first way can be implemented easily now that we know which consumers are in the island: $\sigma_i^k = 1$. We will allow the algorithm to shed all load of customers in the island and a minimum load of $\alpha \cdot power_i$ for all non-island nodes i with initial load of $power_i$. This requires only a slight change in (P.17) to

$$d_{load(l)}^k \geq (1 - \sigma_{load(l)}^k) \cdot \alpha \cdot power_{load(l)} \qquad \forall i = 1, \ldots, n_{loads}, k = 1, \ldots, n_{isl}, \tag{M.17b}$$

where the only change from (P.17) is the factor $(1 - \sigma_{load(l)}^k)$.

The second way can also be implemented changing the cost function to

$$\text{Minimize } \frac{A}{2} \sum_{k=1}^{n_{isl}} \sum_{i=1}^{N} \sum_{j=1}^{N} |power_{ij} - f_{ij}^k| + B \sum_{k=1}^{n_{isl}} \sum_{l=1}^{n_{load}} p_{load(l)}^{k,2} + C \sum_{k=1}^{n_{isl}} \sum_{l=1}^{n_{load}} p_{load(l)}^{k,1}, \tag{N.2}$$

where $p_{load(l)}^{k,2} = 0$ if $load(l)$ is in the island and $power_{load(l)} - d_{load(l)}^k$ otherwise, and visa versa for $p_{load(l)}^{k,1}$. That is, the change in power flow is accounted for with factor A (note that all links are counted twice), the load shed in the complement is accounted for with factor B and the load shed in the island is accounted for with factor C. Also, load shed and load shift was penalized equally in the original cost function.

For example, a load shed of 10 MW was equally bad as a generator shift of 10 MW. The new cost function takes account for load shift in the first part, but the main cost for load shedding is in the second part. Adjusting A, B and C will set the priority between these situations (with $B > C$ so that non-island nodes have priority over island nodes).

The real variable $p^{k,s}_{load(l)}$ just has to satisfy two constraints:

$$p^{k,2}_{load(l)} \geq (1 - \sigma^k_i) \cdot power_{load(l)} - d^k_{load(l)} \qquad l = 1, \ldots, n_{load}, k = 1, \ldots, n_{isl}, \quad \text{(N.3)}$$

$$p^{k,1}_{load(l)} \geq \sigma^k_i \cdot power_{load(l)} - d^k_{load(l)} \qquad l = 1, \ldots, n_{load}, k = 1, \ldots, n_{isl} \quad \text{(N.4)}$$

and

$$p^{k,s}_{load(l)} \geq 0 \qquad l = 1, \ldots, n_{load}, k = 1, \ldots, n_{isl}, s = 1, 2. \quad \text{(N.5)}$$

The combination of (N.3) and (N.5) assigns every $p^{k,2}_{load(l)}$ a minimum value of zero for all island nodes and the amount of load shed for all others. Inequalities (N.4) and (N.5) do the opposite to $p^{k,1}_{load(l)}$. Since the cost function of the minimization problem involves the sum of all $p^{k,s}_{load(l)}$, a minimum value of every individual $p^{k,s}_{load(l)}$ will be forced by the algorithm. We may conclude that every $p^{k,s}_{load(l)}$ gets precisely the value that has been described in the preceding paragraph. By setting $C = 0$ and removing all $p^{k,1}_{load(l)}$ constraints, the load shed within the islands is not accounted for at all.

D.5 Conclusion

After analysing the paper of [63] and a fruitful discussion, some variations to the original model have been proposed. These variations include combining several constraints to one constraint and changing a subset of logical constraints to linear constraints at the cost of additional binary constraints. These binary constraints have proved helpful in allowing additional assumptions for the model. Also, a new cost function has been proposed. This cost function takes into account the total amount of flow rerouted and the amount for load shed in non-island nodes.

Bibliography

[1] Ahmed, S., Sarker, N., Khairuddin, A., Ghani, M., and Ahmad, H. (2003). A scheme for controlled islanding to prevent subsequent blackout. *Power Systems, IEEE Transactions on*, 18(1):136–143. [14, 15, 62]

[2] Anghel, M., Werley, K. A., and Motter, A. E. (2007). Stochastic model for power grid dynamics. In *System Sciences, 2007. HICSS 2007. 40th Annual Hawaii International Conference on*, page 113. [14, 16, 17, 19, 21, 22, 23, 25, 26, 27, 28, 62]

[3] Aponte, E. and Nelson, J. (2006). Time optimal load shedding for distributed power systems. *Power Systems, IEEE Transactions on*, 21(1):269–277. [14, 15, 62]

[4] Arianos, S., Bompard, E., Carbone, A., and Xue, F. (2009). Power grid vulnerability: A complex network approach. *Chaos*, 19(1):013119. [17]

[5] Bae, K. and Thorp, J. S. (1999). A stochastic study of hidden failures in power system protection. *Decision Support Systems*, 24(3-4):259–268. [11]

[6] Baldick, R., Chowdhury, B., Dobson, I., Dong, Z., Gou, B., Hawkins, D., Huang, H., Joung, M., Kirschen, D., Li, F., Li, J., Li, Z., Liu, C.-C., Mili, L., Miller, S., Podmore, R., Schneider, K., Sun, K., Wang, D., Wu, Z., Zhang, P., Zhang, W., and Zhang, X. (2008). Initial review of methods for cascading failure analysis in electric power transmission systems IEEE PES CAMS task force on understanding, prediction, mitigation and restoration of cascading failures. In *Power and Energy Society General Meeting - Conversion and Delivery of Electrical Energy in the 21st Century, 2008 IEEE*, pages 1–8. [17]

[7] Baldick, R., Chowdhury, B., Dobson, I., Dong, Z., Gou, B., Hawkins, D., Huang, Z., Joung, M., Kim, J., Kirschen, D., Lee, S., Li, F., Li, J., Li, Z., Liu, C.-C., Luo, X., Mili, L., Miller, S., Nakayama, M., Papic, M., Podmore, R., Rossmaier, J., Schneider, K., Sun, H., Sun, K., Wang, D., Wu, Z., Yao, L., Zhang, P., Zhang, W., and Zhang, X. (2009). Vulnerability assessment for cascading failures in electric power systems. In *Power Systems Conference and Exposition, 2009. PSCE '09. IEEE/PES*, pages 1–9. [17]

[8] Bao, Z., Cao, Y., Wang, G., and Ding, L. (2009). Analysis of cascading failure in electric grid based on power flow entropy. *Physics Letters A*, 373(34):3032 – 3040. [16]

[9] Barabási, A.-L. and Albert, R. (1999). Emergence of scaling in random networks. *Science*, 286(5439):509–512. [20]

[10] Bhavaraju, P., Nour, N., Institute, E. P. R., Electric, P. S., and Company, G. (1992). *TRELSS: A Computer Program for Transmission Reliability Evaluation of Large-scale Systems : Final Report*. EPRI TR. The Institute. [16]

[11] Bienstock, D. (2011). Optimal control of cascading power grid failures. In *Decision and Control and European Control Conference (CDC-ECC), 2011 50th IEEE Conference on*, pages 2166–2173. [14, 15, 16]

[12] Boccaletti, S., Latora, V., Moreno, Y., Chavez, M., and Hwang, D.-U. (2006). Complex networks: Structure and dynamics. *Physics Reports*, 424(4-5):175–308. [17]

[13] Bompard, E., Gao, C., Masera, M., Napoli, R., Russo, A., Stefanini, A., and Xue, F. (2007). Approaches to the security analysis of power systems: defence strategies against malicious threats. Technical report, Joint Research Centre, Institute of the Protection and Security of the Citizen (IPSC). [13]

[14] Bompard, E., Napoli, R., and Xue, F. (2009). Analysis of structural vulnerabilities in power transmission grids. *International Journal of Critical Infrastructure Protection*, 2(12):5–12. [17]

[15] Carreras, B., Newman, D., Dobson, I., and Poole, A. (2000). Initial evidence for self-organized criticality in electric power system blackouts. In *Proceedings of the 33rd Annual Hawaii International Conference on System Sciences*. [13]

[16] Carreras, B., Newman, D., Dobson, I., and Poole, A. (2004). Evidence for self-organized criticality in a time series of electric power system blackouts. *Circuits and Systems I: Regular Papers, IEEE Transactions on*, 51(9):1733–1740. [13]

[17] Carreras, B. A., Lynch, V. E., Dobson, I., and Newman, D. E. (2002). Critical points and transitions in an electric power transmission model for cascading failure blackouts. *Chaos: An Interdisciplinary Journal of Nonlinear Science*, 12(4):985–994. [15, 16, 22, 62]

[18] Chen, G., Dong, Z. Y., Hill, D. J., Zhang, G. H., and Hua, K. Q. (2010). Attack structural vulnerability of power grids: A hybrid approach based on complex networks. *Physica A: Statistical Mechanics and its Applications*, 389(3):595–603. [11, 14, 16, 17, 26]

[19] Chen, J., Thorp, J. S., and Dobson, I. (2005). Cascading dynamics and mitigation assessment in power system disturbances via a hidden failure model. *International Journal of Electrical Power & Energy Systems*, 27(4):318–326. [11, 15, 16, 17]

[20] Chen, J., Thorp, J. S., and Parashar, M. (2001). Analysis of electric power system disturbance data. In *HICSS'01*. [13]

[21] Coffrin, C. and Van Hentenryck, P. (2012). A linear-programming approximation of AC power flows. *ArXiv e-prints*. [16, 62]

[22] Crucitti, P., Latora, V., and Marchiori, M. (2004). A model for cascading failures in complex networks. *Phys. Rev. E*, 69:045104. [15, 16, 17]

[23] Diao, R., Vittal, V., Sun, K., Kolluri, S., Mandal, S., and Galvan, F. (2009). Decision tree assisted controlled islanding for preventing cascading events. In *Power Systems Conference and Exposition, 2009. PSCE '09. IEEE/PES*, pages 1–8. [14, 15]

[24] Dimitrovski, A. and Tomsovic, K. (2005). Slack bus treatment in load flow solutions with uncertain nodal powers. *International Journal of Electrical Power & Energy Systems*, 27(9):614–619. [20]

[25] Dobson, I., Carreras, B., Lynch, V., and Newman, D. (2001). An initial model for complex dynamics in electric power system blackouts. In *Proceedings of the 34th Annual Hawaii International Conference on System Sciences (HICSS-34)*, volume 2 of *HICSS '01*, pages 2017–, Washington, DC, USA. IEEE Computer Society. [13, 16]

[26] Dobson, I., Carreras, B. A., Lynch, V. E., and Newman, D. E. (2007). Complex systems analysis of series of blackouts: Cascading failure, critical points, and self-organization. *Chaos: An Interdisciplinary Journal of Nonlinear Science*, 17(2):026103. [13]

[27] Dobson, I., McCalley, J., and Liu, C.-C. (2010). Fast simulation, monitoring and mitigation of cascading failure. Technical report, Power Systems Engineering Research Center. [15]

[28] Dola, H. and Chowdhury, B. (2006). Intentional islanding and adaptive load shedding to avoid cascading outages. In *Power Engineering Society General Meeting, 2006. IEEE*. [14, 15]

[29] Elizondo, D. and De La Ree, J. (2004). Analysis of hidden failures of protection schemes in large interconnected power systems. In *Power Engineering Society General Meeting, 2004. IEEE*, volume 1, pages 107–114. [11]

[30] ENTSO-E policies (2013). `https://www.entsoe.eu/publications/system-operations-reports/operation-handbook/`. [88]

[31] Erdös, P. and Rényi, A. (1960). On the evolution of random graphs. In *Publication of the Mathematical Institute of the Hungarian Academy of Sciences*, pages 17–61. [20]

[32] FERC/NERC staff (2012). Arizona-southern california outages on september 8, 2011: Causes and recommendations. Federal Energy Regulatory Commission and North American Electric Reliability Corporation. [5, 11, 15, 16]

[33] Gershgorin, S. A. (1931). Uber die abgrenzung der eigenwerte einer matrix. . , (6):749–754. [78]

[34] Girvan, M. and Newman, M. E. J. (2002). Community structure in social and biological networks. *Proceedings of the National Academy of Sciences*, 99(12):7821–7826. [24]

[35] Great Britain Security and Quality of Supply Standard (2004). `http://www.nationalgrid.com/NR/rdonlyres/FBB211AF-D4AA-45D0-9224-7BB87DE366C1/15460/GB_SQSS_V1.pdf`. Paragraph 5.1. [10]

[36] Güler, T., Gross, G., and Liu, M. (2007). Generalized line outage distribution factors. *Power Systems, IEEE Transactions on*, 22(2):879–881. [30]

[37] Hayashi, Y. and Miyazaki, T. (2005). Emergent rewirings for cascades on correlated networks. Technical Report cond-mat/0503615, Japan Advanced Institute of Science and Technology. [15, 16]

[38] Hines, P., Balasubramaniam, K., and Sanchez, E. (2009). Cascading failures in power grids. *Potentials, IEEE*, 28(5):24–30. [13, 17, 22]

[39] Hines, P., Liao, H., Jia, D., and Talukdar, S. (2005). Autonomous agents and cooperation for the control of cascading failures in electric grids. In *Networking, Sensing and Control, 2005. Proceedings. 2005 IEEE*, pages 273–278. [15]

[40] Holme, P. (2002). Edge overload breakdown in evolving networks. *Phys. Rev. E*, 66:036119. [16, 17]

[41] Holme, P. and Kim, B. J. (2002). Vertex overload breakdown in evolving networks. *Phys. Rev. E*, 65:066109. [16]

[42] Holme, P., Kim, B. J., Yoon, C. N., and Han, S. K. (2002). Attack vulnerability of complex networks. *Phys. Rev. E*, 65:056109. [16, 17]

[43] Hopkinson, K., Wang, X., Giovanini, R., Thorp, J., Birman, K., and Coury, D. (2006). Epochs: a platform for agent-based electric power and communication simulation built from commercial off-the-shelf components. *Power Systems, IEEE Transactions on*, 21(2):548–558. [15]

[44] Isaac Newton Institute (2013). Energy systems week 2013 – background. `http://www.newton.ac.uk/programmes/SCS/scsw09.shtml`. [91]

[45] Karp, R. M. (1972). Reducibility among combinatorial problems. In Miller, R. E., Thatcher, J. W., and Bohlinger, J. D., editors, *Complexity of Computer Computations*, The IBM Research Symposia Series, pages 85–103. Springer US. [32]

[46] Khaitan, S. and McCalley, J. (2013). Dynamic load balancing and scheduling for parallel power system dynamic contingency analysis. In Khaitan, S. K. and Gupta, A., editors, *High Performance Computing in Power and Energy Systems*, Power Systems, pages 189–209. Springer Berlin Heidelberg. [15]

[47] Khodaei, A. and Shahidehpour, M. (2012). Security-constrained transmission switching with voltage constraints. *International Journal of Electrical Power & Energy Systems*, 35(1):74–82. [42]

[48] Kim, D.-H. and Motter, A. E. (2008). Resource allocation pattern in infrastructure networks. *Journal of Physics A: Mathematical and Theoretical*, 41(22):224019. [21]

[49] Kinney, R., Crucitti, P., Albert, R., and Latora, V. (2005). Modeling cascading failures in the north american power grid. *The European Physical Journal B - Condensed Matter and Complex Systems*, 46:101–107. [16]

[50] Koç, Y., Warnier, M., Kooij, R. E., and Brazier, F. M. (2013). An entropy-based metric to quantify the robustness of power grids against cascading failures. *Safety Science*, 59:126–134. [24]

[51] Lai, Y.-C., Motter, A., and Nishikawa, T. (2004). Attacks and cascades in complex networks. In Ben-Naim, E., Frauenfelder, H., and Toroczkai, Z., editors, *Complex Networks*, volume 650 of *Lecture Notes in Physics*, pages 299–310. Springer Berlin Heidelberg. [16, 17]

[52] Lim, S.-I., Liu, C.-C., Lee, S.-J., Choi, M.-S., and Rim, S.-J. (2008). Blocking of zone 3 relays to prevent cascaded events. *Power Systems, IEEE Transactions on*, 23(2):747–754. [11]

[53] Liu, M. and Gross, G. (2002). Effectiveness of the distribution factor approximations used in congestion modeling. In *Proceedings of the 14th Power Systems Computation Conference, Seville, 24–28 June 2002*. [29]

[54] McCalley, J., Khaitan, S., Dobson, I., Wierzbicki, K., Kim, J., and Ren, H. (2008). Risk of cascading outages. Technical Report 08-04, Power Systems Engineering Research Center. [15]

[55] Mei, S., Zhang, X., and Cao, M. (2011). *Power Grid Complexity*. Springer, Netherlands, Tsinghua University Press, China, 16 edition. [11, 17]

[56] Ministry of Power Enquiry Committee (2012). Report of the enquiry committee on grid disturbance in northern region on 31th july 2012 and in norhern, eastern & north-eastern region on 31th july 2012. [5, 15, 16, 31]

[57] Moreno, Y., Gmez, J. B., and Pacheco, A. F. (2002). Instability of scale-free networks under node-breaking avalanches. *EPL (Europhysics Letters)*, 58(4):630–636. [16]

[58] Moreno, Y., Pastor-Satorras, R., Vzquez, A., and Vespignani, A. (2003). Critical load and congestion instabilities in scale-free networks. *EPL (Europhysics Letters)*, 62(2):292–298. [17]

[59] Motter, A. E. (2004). Cascade control and defense in complex networks. *Phys. Rev. Lett.*, 93:098701. [14, 15, 16]

[60] Motter, A. E. and Lai, Y.-C. (2002). Cascade-based attacks on complex networks. *Phys. Rev. E*, 66:065102. [15, 16, 17]

[61] Nedic, D. P., Dobson, I., Kirschen, D. S., Carreras, B. A., and Lynch, V. E. (2006). Criticality in a cascading failure blackout model. *International Journal of Electrical Power & Energy Systems*, 28(9):627–633. [16]

[62] North American Electric Reliability Corporation (2013). `http://www.nerc.com/page.php?cid=1|15`. [7]

[63] Pahwa, S., Youssef, M., Schumm, P., Scoglio, C., and Schulz, N. (2013). Optimal intentional islanding to enhance the robustness of power grid networks. *Physica A: Statistical Mechanics and its Applications*, 392(17):3741–3754. [14, 15, 33, 34, 37, 39, 93, 94, 98]

[64] Parmer, C., Cotilla-Sanchez, E., Thornquist, H. K., and Hines, P. D. (2011). Developing a dynamic model of cascading failure for high performance computing using trilinos. In *Proceedings of the first international workshop on High performance computing, networking and analytics for the power grid*, HiPCNA-PG '11, pages 25–34, New York, NY, USA. ACM. [15]

[65] Pepyne, D., Panayiotou, C., Cassandras, C., and Ho, Y.-C. (2001). Vulnerability assessment and allocation of protection resources in power systems. In *American Control Conference, 2001. Proceedings of the 2001*, volume 6, pages 4705–4710. [26]

[66] Peterson, N., Tinney, W., and Bree, D. (1972). Iterative linear AC power flow solution for fast approximate outage studies. *Power Apparatus and Systems, IEEE Transactions on*, PAS-91(5):2048–2056. [16, 62]

[67] Press, W. H., Teukolsky, S. A., Vetterling, W. T., and Flannery, B. P. (1992). *Numerical recipes in C: the art of scientific computing*. Cambridge University Press, New York, NY, USA, 2 edition. [23]

[68] Purchala, K., Meeus, L., Van Dommelen, D., and Belmans, R. (2005). Usefulness of DC power flow for active power flow analysis. In *Power Engineering Society General Meeting, 2005. IEEE*, volume 1, pages 454–459. [16, 29]

[69] Relay Work Group (1997). Application of zone 3 distance relays on transmission lines. Technical report, Western Electricity Coordinating Council. [8, 15]

[70] Rios, M., Kirschen, D., Jayaweera, D., Nedic, D., and Allan, R. (2002). Value of security: modeling time-dependent phenomena and weather conditions. *Power Systems, IEEE Transactions on*, 17(3):543–548. [8, 14]

[71] Stott, B., Jardim, J., and Alsac, O. (2009). DC power flow revisited. *Power Systems, IEEE Transactions on*, 24(3):1290–1300. [28]

[72] Talukdar, S. N., Apt, J., Ilic, M., Lave, L. B., and Morgan, M. (2003). Cascading failures: Survival versus prevention. *The Electricity Journal*, 16(9):25–31. [13]

[73] Tamronglak, S. (1994). *Analysis of power system disturbances due to relay hidden failures*. PhD thesis, Virginia Polytechnic Institute and State University. [10]

[74] TechPowerUp (2011). A detailed look into PSUs. `http://www.techpowerup.com/articles//overclocking/psu/160/4`. Written by C. R. Maris. [9]

[75] TenneT (2008). Website of tennet, about tennet, news, press & publications, news. `http://www.tennet.eu/nl/en/news/article/tennet-verantwoord-en-innovatief-ondergronds-in-de-randstad.html`. Dutch article. [27]

[76] TenneT (2013). Website of tennet, about tennet. `http://www.tennet.eu/nl/en/about-tennet.html`. [87]

[77] Tinney, W. F. and Hart, C. (1967). Power flow solution by newton's method. *Power Apparatus and Systems, IEEE Transactions on*, 86(11):1449–1460. [16]

[78] Trodden, P., Bukhsh, W., Grothey, A., and McKinnon, K. (2013). MILP formulation for controlled islanding of power networks. *International Journal of Electrical Power & Energy Systems*, 45(1):501–508. [14, 15, 39, 62]

[79] University of Washington Electrical Engineering (1962). Power systems test case archive. `http://www.ee.washington.edu/research/pstca/`. [20]

[80] U.S.-Canada Power System Outage Task Force (2004). Final report on the august 14, 2003 blackout in the united states and canada: Causes and recommendations. [5, 15, 16]

[81] Wenzhuo, Y. (2010). `http://www.cs.zju.edu.cn/people/zhzhang/papers/note12.pdf`. [78]

[82] Western Area Power Administration (2013). Trees and power lines. `http://ww2.wapa.gov/sites/western/newsroom/Documents/pdf/treesandpowerlines.pdf`. [8]

[83] You, H., Vittal, V., and Wang, X. (2004). Slow coherency-based islanding. *Power Systems, IEEE Transactions on*, 19(1):483–491. [14, 15, 62]

[84] Zhang, Y., Ilic, M., and Tonguz, O. (2011). Mitigating blackouts via smart relays: A machine learning approach. *Proceedings of the IEEE*, 99(1):94–118. [15]

[85] Zhao, L., Park, K., Lai, Y.-C., and Ye, N. (2005). Tolerance of scale-free networks against attack-induced cascades. *Phys. Rev. E*, 72:025104. [14, 15, 16]

[86] Zimmerman, R., Murillo-Sánchez, C., and Thomas, R. (2011). Matpower: Steady-state operations, planning, and analysis tools for power systems research and education. *Power Systems, IEEE Transactions on*, 26(1):12–19. [29, 70]